Float Zone Workshop

*Proceedings of a working group meeting held at
Marshall Space Flight Center, Alabama
September 22-23, 1981*

NASA

CONFERENCE PUBLICATION

NASA CP-2226

FLOAT ZONE WORKSHOP

Edited by E. L. Kern and E. K. Cothran

Space Sciences Laboratory
Science and Engineering Directorate

George C. Marshall Space Flight Center
Marshall Space Flight Center, Alabama   35812

September 1981

1. REPORT NO. NASA CP-2226	2. GOVERNMENT ACCESSION NO.	3. RECIPIENT'S CATALOG NO.
4. TITLE AND SUBTITLE FLOAT ZONE WORKSHOP		5. REPORT DATE September 1981
		6. PERFORMING ORGANIZATION CODE
7. AUTHOR(S) Edited by E. L. Kern* and E. K. Cothran		8. PERFORMING ORGANIZATION REPORT #
9. PERFORMING ORGANIZATION NAME AND ADDRESS George C. Marshall Space Flight Center Marshall Space Flight Center, AL 35812		10. WORK UNIT NO.
		11. CONTRACT OR GRANT NO.
12. SPONSORING AGENCY NAME AND ADDRESS National Aeronautics and Space Administration Washington, D.C. 20546		13. TYPE OF REPORT & PERIOD COVERED Conference Publication
		14. SPONSORING AGENCY CODE

15. SUPPLEMENTARY NOTES
Prepared by Space Sciences Lab, Science and Engineering Directorate *E. L. Kern under United Space Research Associates Contract

16. ABSTRACT

This report summarizes the results of a Float Zone Workshop held at the Marshall Space Flight Center, September 22-23, 1981. The report consists of seven major sections (1) an introduction, (2) crucial material needs for devices and the role of space, (3) power needs in space, (4) Ground Based Research and MEA experiment suggestions, (5) determining the Marangoni effect, (6) modeling and characterizing the silicon float-zone, and (7) a summary of the conclusion from the workshop.

17. KEY WORDS Float-zone Material Materials Processing in Space	18. DISTRIBUTION STATEMENT Unclassified - Unlimited

19. SECURITY CLASSIF. (of this report) Unclassified	20. SECURITY CLASSIF. (of this page) Unclassified	21. NO. OF PAGES 212	22. PRICE

PREFACE

A Float Zone Workshop was held at MSFC on September 22-23, 1981. The purpose of the workshop was to bring together key industrial, academic, and government scientists to (1) Determine the possible advantages from space processing (by float-zoning) and where these improvements are needed by industry and government and (2) Forecast how much power is required for float-zone space processing.

The workshop was structured into two days. The first day consisted of reports from various industrial and government producers and users of float-zone material. The second day was the presentation of present research efforts in the float-zone area.

The list of attendees and an agenda are given in Tables 1 and 2.

TABLE 1. ATTENDANCE LIST FOR FLOAT ZONE WORKSHOP

Dr. Klaus Bachmann
Chemistry Department
North Carolina State University
Raleigh, NC 27607
(919) 737-2538

Mr. Ken E. Benson
Bell Laboratories
555 Union Boulevard
Allentown, PA 18103
(215) 439-7166

Dr. Henry W. Brandhorst, Jr.
Solar & Electrochemistry Div.
Lewis Research Center
21000 Brookpark Road
Cleveland, OH 44135
(216) 433-4000 Ext. 732

Dr. Robert A. Brown
Dept. of Chemical Engineering
RM 6b-468
MIT
Cambridge, MA 02139
(617) 253-5726

Dr. Creed Clayton
Semtec, Inc.
500 Wynn Drive
Huntsville, AL 35805
(205) 830-0430

Dr. Larry M. Foster
Science Applications, Inc.
2019 Clinton, W.
Huntsville, AL 35805
(205) 533-5900

Mr. Gerald Gill
Westech Systems, Inc.
4225 South 37th St.
Phoenix, AZ 85040
(602) 276-4261

Mr. Gordon Griffith
AFWAL/MLP
Wright Patterson Air Force Base
Dayton, OH 45433
(513) 255-4474

Dr. Stephen C. Hardy
Institute of Materials Research
NBS
Washington, DC 20234
(301) 921-2985

Dr. Patrick M. Hemenger
AFWAL/MLP
Wright Patterson Air Force Base
Dayton, OH 45433
(513) 255-6671

Mr. Patrick Hutchings
TRW
One Space Park
Redondo Beach, CA 90278
(213) 536-4745

Dr. Lubek Jastrzebski
RCA/David Sarnoff Research Center
Priceton, NJ 80540
(603) 734-2655

Dr. Gerald Karr
UAH
Mechanical Engineering Dept.
Huntsville, AL 35805
(205) 895-6154

Dr. E. L. Kern
Consultant
13655 Ruette LeParc No. C
Del Mar, CA 92014
(714) 481-2255

Dr. Horst Kramer
Monsanto Company
St. Peters, MO 63376
(314) 272-6281

Dr. John Manning
U.S. Dept. of Commerce
National Bureau of Standards
Washington, DC 20234
(301) 921-3354

Mr. Ogden Marsh
Hughes Research Labs
3011 Malibu Canyon Road
Malibu, CA 90275
(213) 456-6711

TABLE 1. CONCLUDED

Dr. William Oran
Mail Code EM-7
NASA Headquarters
Washington, DC 20546
(202)755-8610

Dr. Guy E. Rindone
201 Steidle Building
Penn State University
University Park, PA 16802
(814)865-6832

Dr. Oscar Stafsudd
U.C.L.A.
Electrical Engineering Department
Los Angeles, CA 90024
(213)825-2214

Dr. David Stroud
Physics Department
Ohio State University
Columbus, OH 43210
(614)422-8140

Dr. R. Noel Thomas
Westinghouse Research Labs
Beulah Road
Pittsburgh, PA 15235
(412)256-3646

Dr. John D. Verhoeven
Professor Metallurgy
Iowa State University
Ames Laboratory
129 Metallurgy Building
Ames, IA 50011
(515)294-9471

Mr. Donald Waltz
TRW
One Space Park
Redondo Beach, CA 90278
(213)536-4745

Mr. Michael J. Wargo
MIT
Room 13-4154
(617)253-6903

Dr. William R. Wilcox
Department of Chemical Engineering
Clarkson College of Technology
Potsdam, NY 13676
(315)268-6650

NASA/MSFC
Marshall Space Flight Center, AL
35812 :

Ms. Wendy Alter, ES72

Ms. Ernestine Cothran, ES72

Mr. Peter A. Curreri, ES74

Dr. Ilmars Dalins, ES71

Dr. Edwin C. Ethridge, ES74

Mr. Sam Lowry, ED14

Mr. Eugene C. McKannan, LA01

Dr. Robert J. Naumann, ES71

Mr. Don Perkinson, PD33

Mr. Charles Schafer, ES82

Mr. John R. Williams, LA11

Mr. I. C. Yates, LA11

Mr. Jim Zwiener, ES72

TABLE 2. AGENDA

FLOAT ZONE WORKSHOP
MARSHALL SPACE FLIGHT CENTER
BUILDING 4200, ROOM P106

September 22, 1981

Introduction	R. Naumann, NASA E. Kern, Consultant	8:00 - 8:30
Materials Processing in Space (MPS) Program	B. Oran, NASA Headquarters	8:30 - 8:50
Past Pertinent Space Experiments	G. McKannan, NASA R. Naumann W. Wilcox, Clarkson	8:50 - 9:50
Break		9:50 - 10:00
Crucial Material Needs for Devices and the Role of Space	E. Kern H. Brandhorst, NASA L. Jastrzebski, R.C.A. K. Bachmann, N. Carolina State	10:00 - 12:00
Lunch		12:00 - 1:00
Crucial Material Needs for Devices and the Role of Space	O. Marsh, Hughes P. Hemenger, Air Force K. Benson, Bell Labs N. Thomas, Westinghouse	1:00 - 2:30
Roundtable Discussion What we should do in space		2:30 - 3:45
Power Needs in Space	E. Kern D. Waltz, TRW H. Kramer, Monsanto	3:45 - 4:45

September 23, 1981

Introduction and Objectives - Goals and Roadmap	E. Kern, Consultant I. C. Yates, NASA R. Naumann, NASA	8:00 - 9:00
MEA Experiment Suggestions	E. Kern J. Verhoeven, Ames O. Staffsud, U.C.L.A.	9:00 - 10:30
Break		10:30 - 10:45
Determining the Marangoni Effect	J. Verhoeven S. Hardy, NBS D. Stroud, Ohio State	10:45 - 12:45
Lunch		12:45 - 1:45
Modeling and Characterizing the Silicon Float-Zone	E. Kern G. Gill, Westec R. Brown, MIT L. Foster, Science App. Inc.	1:45 - 4:45

TABLE OF CONTENTS

TABLE OF CONTENTS (Concluded)

INTRODUCTION

E. L. Kern
Chairman, FZWG
Del Mar, CA

The purpose of the September 1981 Float Zone Workshop was to bring together key industrial, academic, and government scientists to address the questions of:

1) What are the needed improvements in solid crystals?

2) What is the advantage of processing in space?

3) How much power will be needed?

Based upon this rationale, the present (and soon to be) principal investigators presented their recent results and future plans for providing the necessary ground based research.

The set of presentations which addressed the above questions was preceded by a current status of the Material Processing in Space (MPS) program by Dr. Bill Oran, of that program office at NASA Headquarters. A review of past space efforts was provided by a chronology of the types of space vehicles and experiments that were carried out, presented by Gene McKannan of the MPS Project office. Dr. Robert Naumann and Professor Bill Wilcox then reviewed what we have learned from past experiments.

My introductory figures, as Chairman of the Float Zone Working Group (FZWG), follow. Figure I-1 presents my definition and purpose of the FZWG; Figure I-2 defines the purpose of this particular workshop. The need to forecast power needs in the future was outlined in Figure I-3. Past, present, and proposed contractual or grant programs are listed in Figures I-4a and I-4b, with several of these providing results in the papers included in this report. I recently returned from reviewing floar-zone activities in Europe, by attending the 32nd Congress of the International Astronautical Federation and visiting two of the investigators in Germany (Drs. Kolker and Eyre). The efforts are listed in Figures I-6a and I-6b. Figure I-7 gives a proposed program roadmap for the next several years, as a means of defining when our ground-based investigations should be able to lead to a definition of major flight experimentation and hardware.

My impression of the European efforts is that there are several good research programs defining the limits of bouyancy convection and Marangoni flows. These studies are not being integrated into the silicon float-zone experiment of Spacelab 1 and thus a solid ground-based foundation is not being provided for this experiment. In particular, a high thermal gradient will tend to maximize Marangoni flow and the melt-solid system thereby cannot be characterized to the extent of indicating the advantages of space zoning of silicon. Although we will not be zoning silicon in space as soon as Spacelab 1, our ground modeling and characterization will lead to more definitive experiments. We will remain in communication to learn of any of their results which would apply to our studies.

ORGANIZATION:	MARSHALL SPACE FLIGHT CENTER	NAME:
CONSULTANT		E. KERN
		DATE: 9-22-81 I-1

DEFINITION OF FLOAT ZONE WORKING GROUP

A GROUP OF HIGHLY QUALIFIED PROFESSIONALS IN THE FIELDS OF TECHNOLOGY RELATING TO <u>FLOAT ZONING OF SOLIDS</u> WHO WILL <u>ANALYZE THE NEED FOR TECHNOLOGY</u> AND ADVISE NASA ON THE TYPE OF <u>RESEARCH NEEDED</u> AND ON THE POSSIBLE <u>PAY-OFFS</u>. THE MEMBERS SHALL CONSIST OF SCIENTISTS IN THE FIELD, REPRESENTATIVES FROM <u>INDUSTRY</u>, FROM NASA AND FROM OTHER APPROPRIATE GOVERNMENT AGENCIES AND MAY INCLUDE PRINCIPAL INVESTIGATORS OF CURRENT RESEARCH PROGRAMS.

CHAIRMAN (ACTING): E. L. KERN
NASA REPRESENTATIVE: R. J. NAUMANN

Figure I-1.

ORGANIZATION:

CONSULTANT

NAME:

E. KERN

DATE:

9-22-81   I-2

PURPOSE OF FLOAT ZONE WORKSHOP

● DETERMINE THE ADVANTAGES POSSIBLE FROM SPACE PROCESSING (BY FLOAT-ZONING) OF SOLIDS (SEMICONDUCTOR CRYSTALS AND OTHERS), WHERE THESE IMPROVEMENTS ARE NEEDED BY INDUSTRY AND THE GOVERNMENT, AND WHAT THE POSSIBLE PAY-OFF IS.

● FORECAST HOW MUCH POWER WILL BE NEEDED TO SEE THE RECOMMENDED SPACE PROCESSING THROUGH TO FRUITION.

Figure I-2.

MARSHALL SPACE FLIGHT CENTER	
ORGANIZATION:	NAME:
CONSULTANT	E. KERN
	DATE:
	9-22-81 I-3

POWER REQUIREMENTS FOR SPACE PROCESSING

NEED TO FORECAST POWER REQUIREMENTS FOR DOING RESEARCH, DEVELOPMENT AND
POSSIBLE "PRODUCTION" OF FLOAT ZONED CRYSTALS IN SPACE FOR THE NEXT 10 - 15
YEARS AND ADVISE NASA. (LEAD-TIME = 2 - 10 YRS.)

BACKGROUND:

THE SPACE SHUTTLE IS LIMITED TO 7-8 KW OF AVAILABLE POWER. THE MEC (MATERIALS
EXPERIMENT CARRIER) IS SCHEDULED FOR 12.5 KW IN THE TIME FRAME OF 1988 (LAUNCH)
TO MID 90'S.

Figure I-3.

ORGANIZATION:	MARSHALL SPACE FLIGHT CENTER	NAME:
CONSULTANT		E. KERN
		DATE: 9-22-81 I-4

PRESENT RESEARCH EFFORTS IN FLOAT ZONE AREA

DAVIS/HOMSY — MARANGONI EFFECT OF FLUIDS ANALYSIS

BROWN — NUMERICAL SOLUTION OF ZONE MELT HEAT & MASS FLOW

KERN-GILL — GROUND-BASED SILICON ZONING (BREAD-BOARD ZONER)

(PAST)
FOWLE — MARANGONI EFFECT/DESIGN OF SPACE-LAB ZONER UNIT

MANN — LASER DOPPLER ANALYSIS OF MELT SURFACES

OSTRACH — MARANGONI EFFECT OF FLUIDS

Figure I-4a.

Figure I-4b.

THE SPACE EXPERIMENTATION CYCLE

JOHN PADDAY - EASTMAN KODAK (ENG.)

OBSERVED PHENOMENOLOGY

CONTROLLED EXPERIMENTS

ANALYSIS (THEORY)

PREDICTIONS

Figure I-5.

ORGANIZATION:	MARSHALL SPACE FLIGHT CENTER	NAME: E. KERN
CONSULTANT		DATE: 9-22-81 I-6

EUROPEAN ASTRONAUTICAL MEETING - SEPTEMBER 1981

32ND CONGRESS OF THE INTERNATIONAL ASTRONAUTICAL FEDERATION

UNIVERSITY OF ROME   SEPTEMBER 6-12, 1981

3 - HALF DAY SESSIONS ON MATERIAL PROCESSING IN SPACE

- MARANGONI EFFECT (NAPOLITANO, DA-RIVA, CHUN, SCHWABE)

- FLUID PHYSICS FLIGHT HARDWARE

- METAL SOLIDIFICATION (AG, CU, AL/CU, SN/PB, GD$_3$CO, AL/1N)

Figure I-6a.

EUROPEAN SPACE PROCESSING RESEARCH EFFORTS

GERMAN

SPACE-LAB (1 & 2) EXPERIMENTS IN THE MIRROR FURNACE:

SILICON ZONING (NITSCHE & EYER)

SILICON DROP MELT FLOWS (KOLKER)

CdTe GROWTH (VAPOR TRANSPORT & TRAVELING HEATER ZONING)   (FREIBURG)

ZnS VAPOR GROWTH (FREIBURG)

GaSb

PbSnTe

PLUS FLUID ANALYSIS BY SCHWABE (NaNO$_3$), CHUN & WUEST (SILICONES).

OERTEL (CELLULAR CONVECTION - SILICONES)

Figure I-6b.

ORGANIZATION:	MARSHALL SPACE FLIGHT CENTER	NAME:
CONSULTANT		E. KERN
		DATE: 9-22-81 I-7

FLOAT ZONE PROCESSING IN SPACE - PROPOSED ROAD MAP

FLY MEC 1991 ⟶

ψ A/B ψ C/D

GROUND BASED
RESEARCH ⟶

DEFINITION
STUDIES ⟶

DES, BUILD, QUILFY SPACE
HARDWARE

MEC HARDWARE
DES., BUILD,
QUALIFY

FLY SHUTTLE ⟶

81	82	83	84	85	86	87	88	89	90	91

MEA | GROUND RESEARCH | FLY ⟶

"GET AWAY| GROUND RESEARCH| FLY ⟶
SPECIAL"
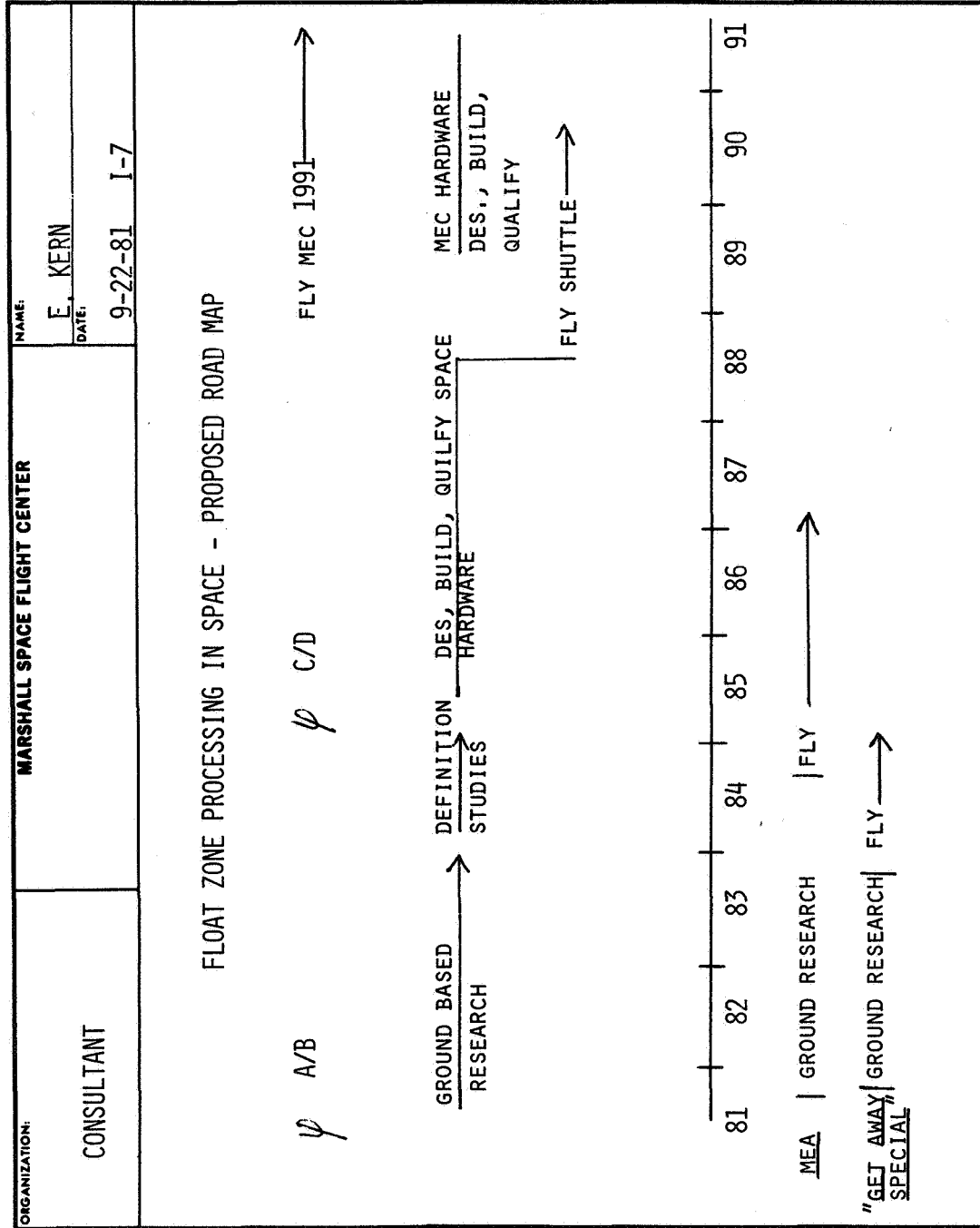
Figure I-7.

A. NASA: MATERIALS PROCESSING IN SPACE OVERVIEW

William Oran
NASA Headquarters
Washington, DC

Dr. William Oran, from the Materials Processing in Space (MPS) Program Office at NASA Headquarters, welcomed the workshop attendees. He presented a general overview of the MPS program, as outlined in Table I-1. Because of the present budget reviews and possible reductions in the MPS budget, Dr. Oran indicated that the size and speed of progress on the float-zone program could not be predicted at this time (September 1981).

TABLE I-1. MATERIALS PROCESSING IN SPACE

Research Area	Research Task	Space Hardware
Current Program in Physical and Chemical Sciences		
Containerless Science	Glass Fining Studies	Acoustic Containerless Experiments System
	Positioning Force Interaction Studies	Acoustic Containerless System
		Electromagnetic Containerless Experiments System
Fluid Behavior	Crystal Growth Kinetic Studies and Fluid Dynamics Influences	Fluid Experiments System
	Low Gravity Fluid Behavior	
Combustion Science	Gravity Influences on Flame Initiation, Spreading, Kinetics, and Two-Phase Combustion	Planned
Cloud Physics	Cloud Formation Processes, Ice/Water Role, Charging Phenomena, Chemistry	Planned
Vacuum Science	Characterization of Gas Molecular Density and Distribution Behind Orbiting Shield Configurations	Planned
Current Program in Materials Processing		
Crystal Growth	Semiconductor Crystals Grown from the Melt with Uniform Compositions	Solidification Experiment System
	Semiconductor Crystals Grown from the Vapor with Controlled Morphologies and Low Defect Densities	Vapor Crystal Growth Furnace
Solidification	Metal Alloys with Aligned Phase Structures	Solidification Experiment System
	Composite Variable Density Solids with Uniform Distribution of Second Phase	Solidification Experiment System
Containerless Processing	Glass Shell Formation and Uniformity Studies	Acoustic Containerless Experiments System and Drop Dynamics Module
	Glass Formation in New Materials Systems	Acoustic Containerless Experiments Systems
Chemical Processing	Formation of Monodisperse Polymer Latex Spheres Kinetics, and Two-Phase Combustion	Polymer Latex Reactor and Experiment Kinetic Chambers

B. REVIEW OF PAST FLIGHT EXPERIMENTS PERTINENT TO FLOAT-ZONE

Gene McKannan
NASA-MSFC
Huntsville, AL

Mr. Gene McKannan from the Materials Processing in Space Project Office provided a review of relevant material processing experiments that were done in space since 1973. These included experiments carried out in Skylab, in the Apollo-Soyuz mission, and on SPAR sounding rockets. The lists of experiments discussed are shown in Tables I-2 and I-3.

TABLE I-2. MATERIALS PROCESSING IN SPACE
1973 FLIGHT EXPERIMENTS PERTINENT TO FLOAT-ZONE

Skylab No.	Title	Principal Investigator	Institution/ Organization	Material
M551	Metals Melting	McKannan	MSFC	2219 Al + 304 SS
M553	Sphere Forming	Larson	Grumman	Ni_3Sn + Ni-1 Ag
M556	Vapor Growth	Wiedemeier	RPI	GeSe + GeTe
M557	Immiscible Alloy	Reger	TRW	Au-Ge + Pb-Sn-In
M558	Radioactive Tracer Diffusion	Ukanwa	Howard Univ.	65_{Zn}
M559	Microsegregation in Ge	Yue	TI	Ga doped Ge
M560	Spherical Crystals	Walter	UAH	Se doped In-Sb
M562	In-Sb Crystals	Witt	MIT	Sn doped in-Sb + Te doped In-Sb
M563	III-V Crystals	Wilcox	USC	$In_xGa_{1-x}Sb$
M564	Halide Eutectic	Yue	UCLA	Al 33 Cu
M565	Silver Grids	Aernoudt	Leuven	Porous Ag
M566	Cu-Al Eutectic	Hasemeyer	MSFC	
TV101	Liq Float Zone	Carruthers	Bell Labs	Water

TABLE I-3. MATERIALS PROCESSING IN SPACE
1975 FLIGHT EXPERIMENTS PERTINENT TO FLOAT-ZONE

Apollo Soyuz No.	Title	Principal Investigator	Institution/ Organization	Material
MA041	Surface Tension Convection	Reed	Oak Ridge	Pb-0.05 Au
MA060	Interface Marking in Crystals	Gatos/Witt	MIT	Ga doped Ge
MA070	Processing of Magnets	Larson	Grumman	Mn-Bi
MA085	Vapor Growth	Wiedemeier	RPI	Te doped Ge-Se + Se doped Ge-S
MA131	Halide Eutectic	Yue	UCLA	NaF/NcCl
SPAR				
74-21	Dendritic Solidification	Johnston	MSFC	NH_4Cl/H_2O
74-48	Electromagnetic Processing	Frost	GE	Be
76-22	Directional Solidification of Eutectics	Pirich	Grumman	Mn-Bi
76-51	Immiscible Alloys	Potard	Grenoble	Al-In

C. THE NATURE OF MELT PROCESS CHANGES IN MICROGRAVITY

William Wilcox
Dept. of Chemical Engineering
Clarkson College
Potsdam, NY

The lack of bouyancy-driven convection in melts and the gas phase microgravity will have pronounced effects on impurities within the melts, such as the case for doped silicon crystals. The change in growth characteristics could be complicated and significant and are difficult to predict. The first change is that a very thin adsorbed impurity layer could retard convective flow because of surface tension gradients (Marangoni flow), whereas the addition of bulk melt convection at g = 1 would not allow such easy flow retardation.

The second effect is the lack of convective flow on the transport of volatile impurities to the melt surface, thus reducing evaporation as compared to g = 1 processing. Normally volatile impurities (such as As or In in silicon) need much lower overpressures to prevent evaporative losses.

The third effect is the lack of convective flow in the gas next to the melt. This will change the dependence of evaporation rates on pressure and could change the heat loss magnitudes significantly.

These process changes can only be observed in space experiments and point to the need for precusory space experiments to be made soon.

Thermocapillary Convection

Surface film or layer - stops all convection.

Impurity adsorption (monolayer or less)

Retards flow increasingly as:

1. Solubilities in bulk phases decreases.

2. Amount of impurity increases.

3. Impurity dependence of surface tension increases.

How to observe:

1. Rate of bubble rise decreased.

2. Do not have rapid movement of surface, as determined by flowing particles on surface.

REDUCED EVAPORATION

No convective transport of volatile species. Diffusion only. Consider 1 dimensional transport through inert gas layer of thickness X at total pressure P condensing on surface so cold that vapor pressure is zero. Vapor pressure p at melt surface. Evaporation flux is:

$$N = -\frac{DP}{RTX} LN \left(1 - \frac{p}{P}\right) \quad MOL/M^2S$$

If zone contains n moles and has free surface area A, then in time t fraction evaporating is:

$$F = -\frac{DPAt}{RTXn} LN \left(1 - \frac{p}{P}\right)$$

EXAMPLE

DP = 0.1 cm^2 atm/s

Zone: 2 cm diameter, 2 cm long, containing 0.5 mol

T = 1600 k

X = 1 cm

p/P	Evaporation
0.5	5%/hr
0.1	0.7%/hr
0.01	0.07%/hr
0.001	0.007%/hr

To hold losses below 0.1%, need overpressure about 100 x larger than vapor pressure.

On Earth, evaporation rates are much larger and much less pressure dependent --
more like $\propto 1/P^{1/2}$ (laminer) or $1/P^{1/3}$ (turbulent).

May have condensation in vapor to form mist or fog.

Would increase evaporation rate and reduce radiation losses from zone. Re-evaporation.

<u>Complicated</u>

II. CRUCIAL MATERIAL NEEDS FOR
DEVICES AND THE ROLE OF SPACE

A. THE NEED FOR GROWING CRYSTALS IN SPACE

E. L. Kern
Consultant
Del Mar, CA

I have summarized some of the areas of growth understanding and some of the payoffs to microgravity crystal growth in Figures II-1, II-2, and II-3. Comparison of the real zone shape at $g = 1$ (Fig. II-4) to the ideal shapes possible in microgravity (Fig. II-5) shows the flexibility to be gained by processing in space. The possible heating methods are reviewed (Fig. II-6). Figure II-7 lists critical devices which need the uniformity and lower defect density which might be obtained by growth in space. Another payoff is to grow crystals which are difficult or impossible to grow on Earth, such as Silicon-germanium alloys and III-V and II-VI compounds (Figs. II-8 and II-9).

ORGANIZATION:	MARSHALL SPACE FLIGHT CENTER
CONSULTANT	NAME: E. KERN
	DATE: 9-22-81 II-1

THE NEED FOR GROWING CRYSTALS IN SPACE

1. NEED TO UNDERSTAND CRYSTAL GROWTH & MELT FLOW MECHANISMS.

   - ROLE OF BUOYANCY DRIVEN CONVECTION

   - ROLE OF SURFACE TENSION FLOWS

2. ABILITY TO GROW CRYSTALS WITH MORE UNIFORMITY & LOWER DEFECT DENSITIES.

   - NO BUOYANCY CONVECTION

   - REDUCE OR ELIMINATE INSTABILITIES (TRANSIENT)

   - FLATTEN GROWTH INTERFACE SHAPE

   - CONTROL SURFACE TENSION DRIVEN FLOWS (?)

3. ABILITY TO GROW CRYSTALS OF COMPOSITION DIFFICULT TO GROW AT G=1.

   - SEMICONDUCTORS (SI-GE, III-V)

   - METALS

Figure II-1.

ORGANIZATION:

MARSHALL SPACE FLIGHT CENTER

NAME:

E. KERN

CONSULTANT

DATE: 9-22-81   II-2

PROPOSED PAYOFFS

1. UNDERSTANDING OF CRYSTAL GROWTH TO AID IN IMPROVING PROCESSES AT $G=1$.

   - BASIC RESEARCH FOR LARGE CRYSTAL GROWTH INDUSTRY

2. MAKE UNIFORM CRYSTALS FOR CRUCIAL ELECTRONIC, ELECTRO-OPTICAL OR OPTICAL CIRCUITS & DEVICES.

   - UNIFORM DOPING & COMPOSITION

   - UNIFORM (LOWER) DEFECT DENSITY

   - NO CRUCIBLE CONTAMINATION

3. GROWTH OF NEW CRYSTALS FOR NEW DEVICES.

Figure II-2.

ORGANIZATION:	MARSHALL SPACE FLIGHT CENTER	NAME:
CONSULTANT		E. KERN
		DATE: 9-22-81 II-3

EUROPEAN EXPERIMENTAL EFFORTS

1. SILICON ZONING (NITSCHE & EYER) IN MIRROR FURNACE

    SHOW: SINGLE CRYSTAL GROWTH (DISLOCATION FREE)
           MELT LENGTH
           LACK OF STRIATIONS (?)

2. SILICON MOLTEN DROP FLUID DYNAMICS (KOLKER)

    SHOW: CRITICAL RAYLEIGH NO. FOR NO CONVECTION (BUOYANCY DRIVEN)
           CRITICAL CONDITIONS FOR MARANGONI FLOW

3. CdTe GROWTH BY TRAVELING HEATER METHOD (FREIBURG)

    SHOW: STOICHIOMETRY & RESISTIVITY
           SUITABILITY AS DETECTOR

Figure II-3.

MODEL OF SILICON GROWTH
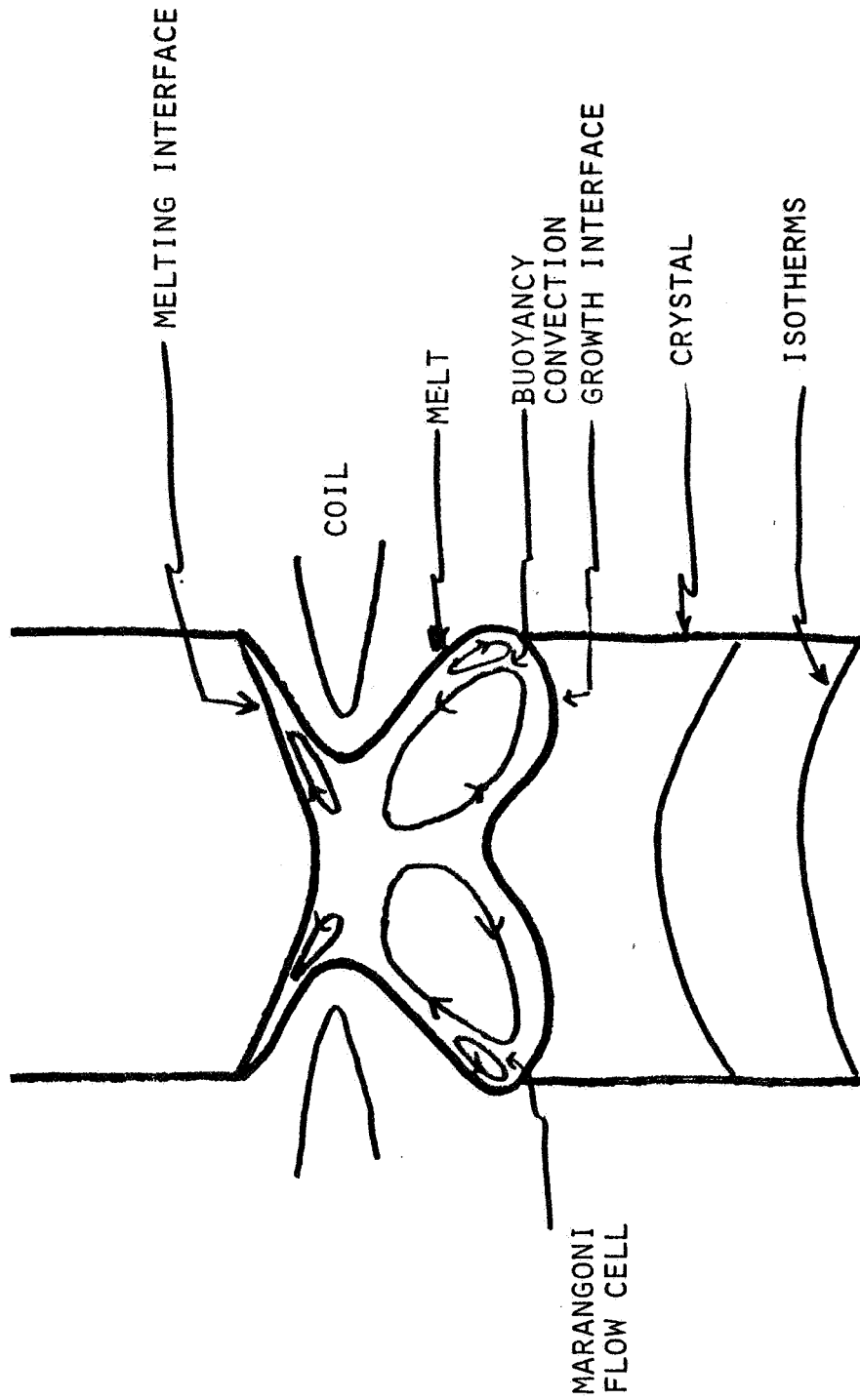

MELTING INTERFACE

COIL

MELT

BUOYANCY
CONVECTION
GROWTH INTERFACE

CRYSTAL

ISOTHERMS

MARANGONI
FLOW CELL

Figure II-4.

27

Figure II-5.

ORGANIZATION:

CONSULTANT

MARSHALL SPACE FLIGHT CENTER

NAME:
E. KERN

DATE:
9-22-81   II-7

POSSIBLE METHODS OF HEATING

1. R.F. COIL: - COLD SPOT FROM SPLIT COIL (REDUCE)

   - HIGH THERMAL GRADIENT IN MELT

   - MAGNETIC LEVITATION & PINCHING

   - FAST RESPONSE TIME

2. RADIANT HEATING: TAILOR FLUX BY OPTICAL SURFACES
   GAS ZONING MEANS ENCLOSING FILAMENT
   EFFICIENT
   ELLIPTICAL MIRRORS/TOROIDAL-ELLIPSOIDAL

3. RESISTANCE FURNACE: TAILOR FLUX BY WINDING CONFIGURATION
   OBSERVATION FOR CONTROL NOT EASY

Figure II-6.

ORGANIZATION:	MARSHALL SPACE FLIGHT CENTER	NAME:
CONSULTANT		E. KERN
		DATE: 9-22-81 II-8

DEFINING NEEDS FOR SPECIAL PROPERTIES IN SILICON

DEVICE	IMPROVEMENTS NEEDED
1. INTRINSIC, DEPLETED DETECTORS	VERY FLAT RADIAL RESTIVITY GRADIENT
2. LARGE Si APD ARRAYS	VERY FLAT RADIAL RESISTIVITY GRADIENT PLUS LOW DEFECT DENSITY
3. VERY HIGH POWER RECTIFIERS & SCR's	UNIFORM RESTIVITY & LOW DEFECT DENSITY
4. SPACE SOLAR CELLS	LOW IMPURITIES & DEFECTS, UNIFORM (GA)
5. I.R. DETECTOR ARRAYS	LOW IMPURITIES, HIGH DOPANT (TL)
6. VERY HIGH DENSITY I.C.'s	LOW DEFECTS, NO STRIATION FLUCTUATIONS(?)

Figure II-7.

SI-GE ALLOYS

NEED: Si_x-Ge_{1-x} ALLOYS WITH $(1-x) > 10\%$
NEED ABSORPTION EDGE $> 1.06 \mu$ (OR HIGHER EFF. AT 1.06μ)
$1.3-1.5 \mu$ (FIBER OPTIC DETECTORS,
POSSIBLY APD'S)
(POSSIBLE APD ARRAYS)

PROBLEM: GROWTH INSTABILITIES (DENDRITIC SI FORMATION)
DIFFICULT TO OVERCOME IN CZOCHRALSKI $>10\%$ GE
CAN'T ZONE MORE THAN A FEW % OF GE (FAST INSTANTANEOUS GROWTH RATES)
& CAN'T KEEP PURE.

POSSIBILITY: SPACE ZONING
VERY UNIFORM & LOW GROWTH RATES
HIGH PURITY
NO BUOYANCY CONVECTION
HIGHER % OF GE

Figure II-8.

31

ORGANIZATION:	MARSHALL SPACE FLIGHT CENTER	NAME:
CONSULTANT		E. KERN
		DATE: 9-22-81 II-10

COMPOUND SEMICONDUCTOR PROCESSING IN SPACE

ADVANTAGE: LOW INSTANTANEOUS GROWTH RATES

NO BUOYANCY CONVECTION

NO IMPURITY OR ABSORPTION OF COMPONENT PROBLEM

DISADVANTAGE: HARD TO MAINTAIN VOLATILE COMPONENT OVER PRESSURE (?)

POSSIBLE CANDIDATES: III-V's WITH GROWTH NUCLEATION PROBLEMS (?)

GA As (?)

CdTe BETTER CRYSTALLOGRAPHY & STOICHIOMETRY
THAN SOLUTION GROWN

FASTER THAN VAPOR TRANSPORT

CHALCOGENIDES (?) - NO CRUCIBLE WALL

Figure II-9.

B. MATERIAL AND PROCESSING NEEDS FOR SILICON SOLAR CELLS IN SPACE

Henry W. Brandhorst, Jr.
NASA-Lewis Research Center
Cleveland, OH

Dr. Brandhorst presented the NASA technical concerns on space grade solar cells. His first figure projects the rather low and constant solar power needs, until space platforms (PEP) increase the need to 50 kW new production/year in the later 1980's.

The main technical concerns are cell efficiency and radiation performance reduction (Figs. II-11 and II-12). The main causes for radiation degradation are complexes of impurities and crystal defects (Fig. II-13). Vacancy-oxygen-carbon complexes form the largest concentration of centers which dissapated carriers within the solar cells. Boron-oxygen-vacancy complexes and Boron-oxygen complexes also degrade the cell performance.

Float-zone silicon is superior to the normally used silicon made by the Czochralski process. Figure II-14 shows a direct correlation, with the very low oxygen leading to the improved float-zone silicon performance. Figure II-15 shows that reducing oxygen and carbon (as float-zoning does) allows for much faster low temperature annealing of the defects. Figure II-16 shows a marked improvement using gallium as the dopant in float-zone, as opposed to boron.

The advantages of improved crystal purity and perfection upon cell properties are summarized in Figure II-17.
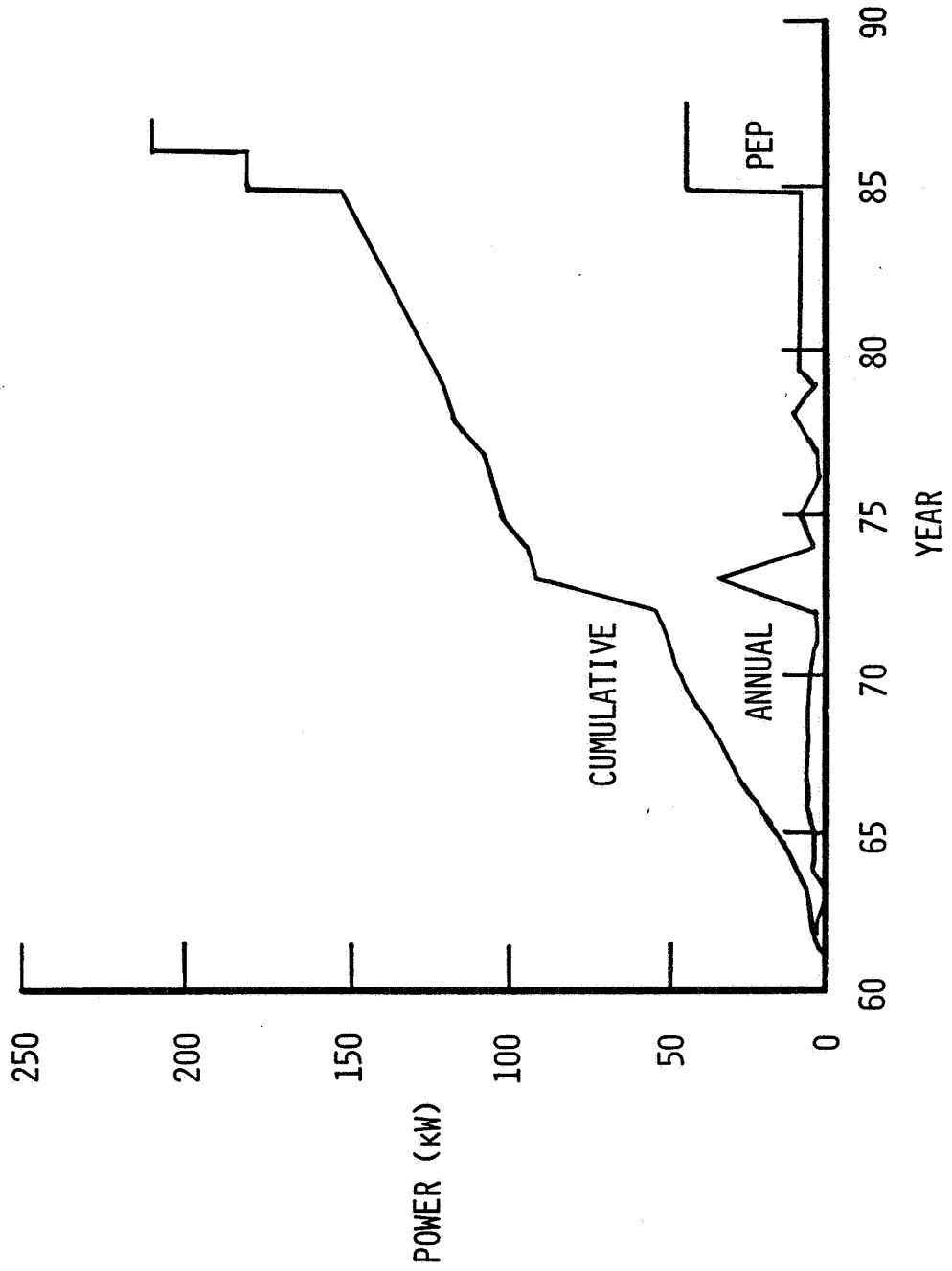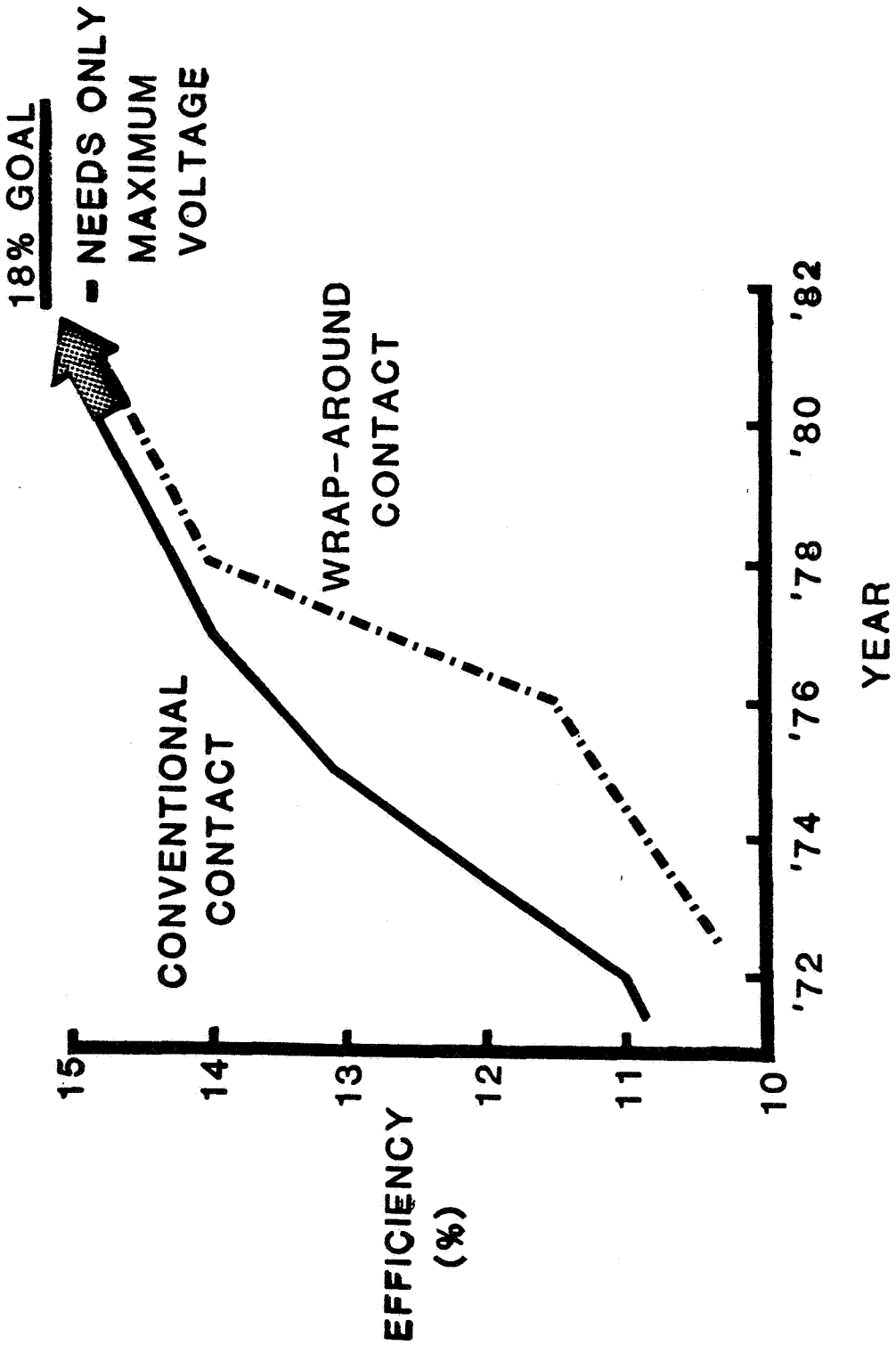
Figure II-10.

Figure II-11.

EFFECT OF SPACE RADIATION ON
SILICON SOLAR CELL PERFORMANCE

1982 GOAL

FLIGHT AND
GROUND TEST
DATA

NORMALIZED
MAX.
POWER

1.0
0.9
0.8
0.7
0.6

1   5   10 15 20

YEARS IN GEO ORBIT

Figure II-12.

36

Figure II-13.

37
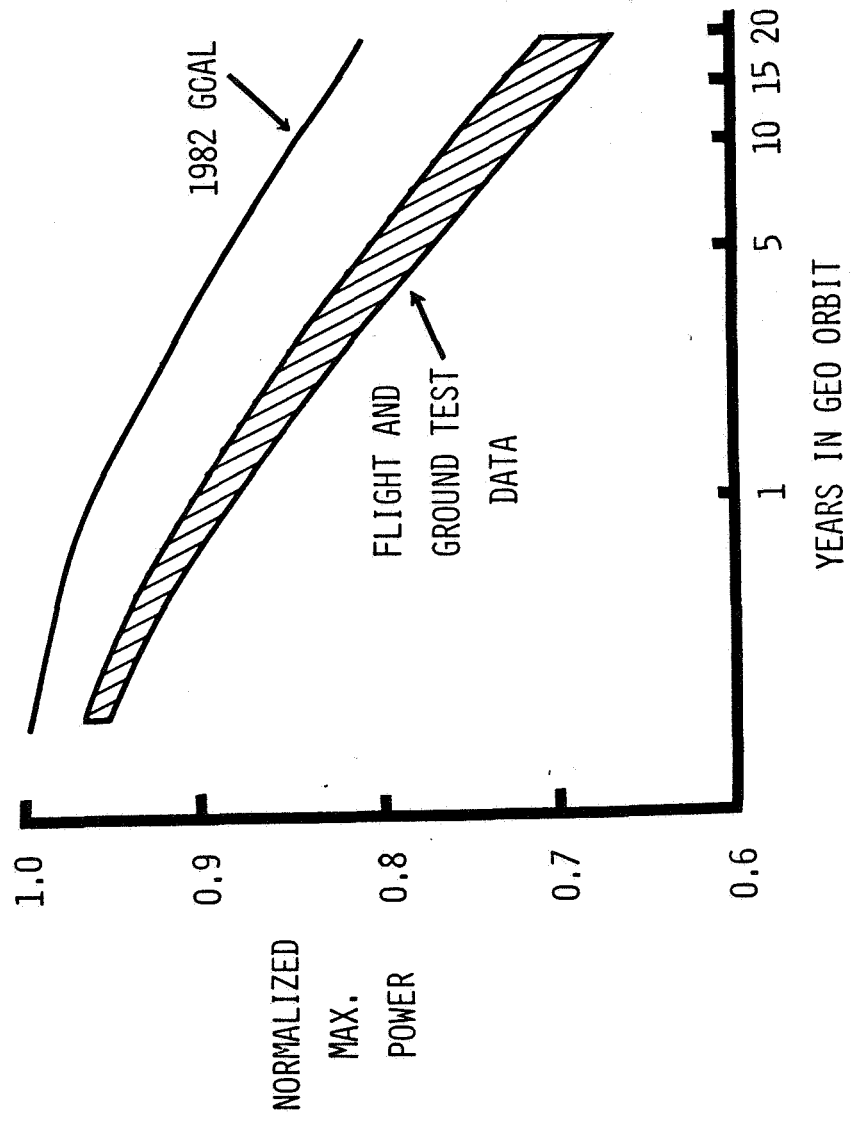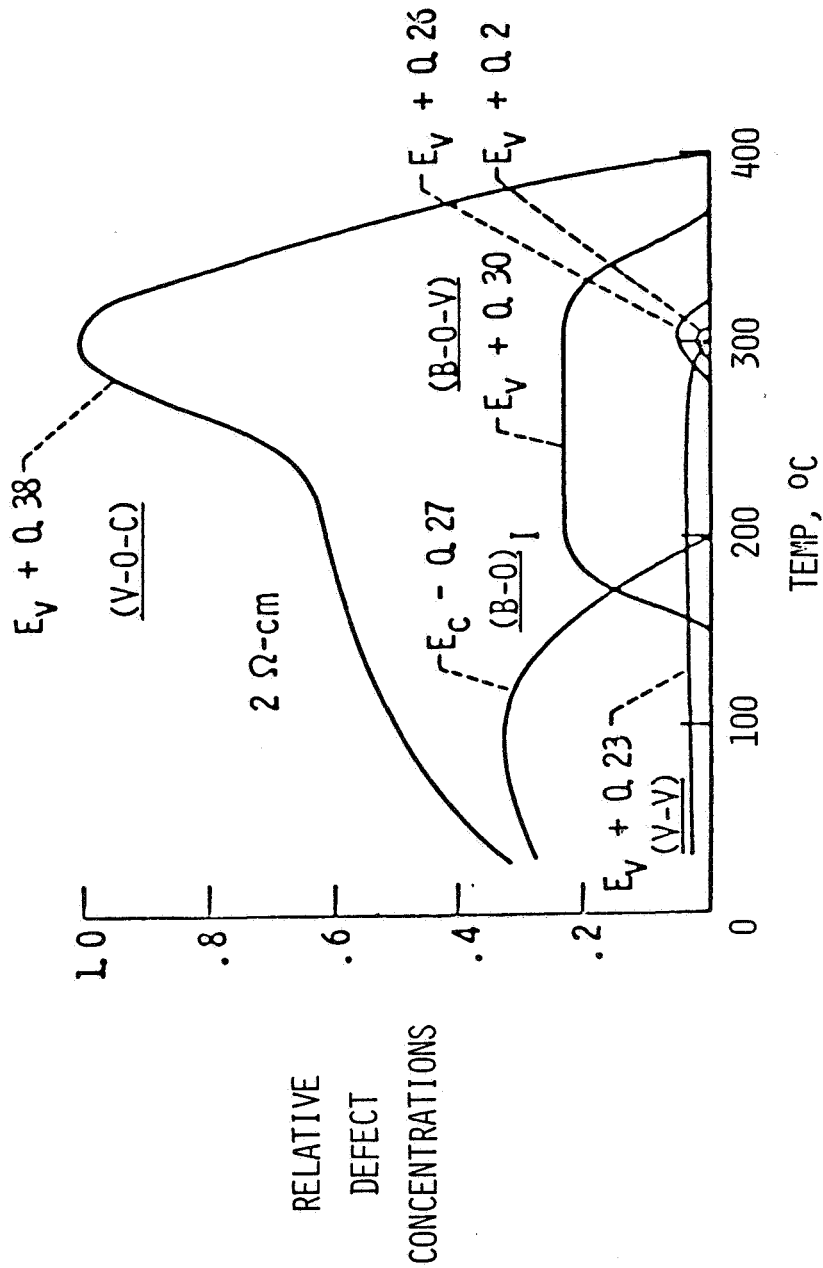
EFFECT OF MATERIAL ON SILICON SOLAR CELL PERFORMANCE

Figure II-14.

38
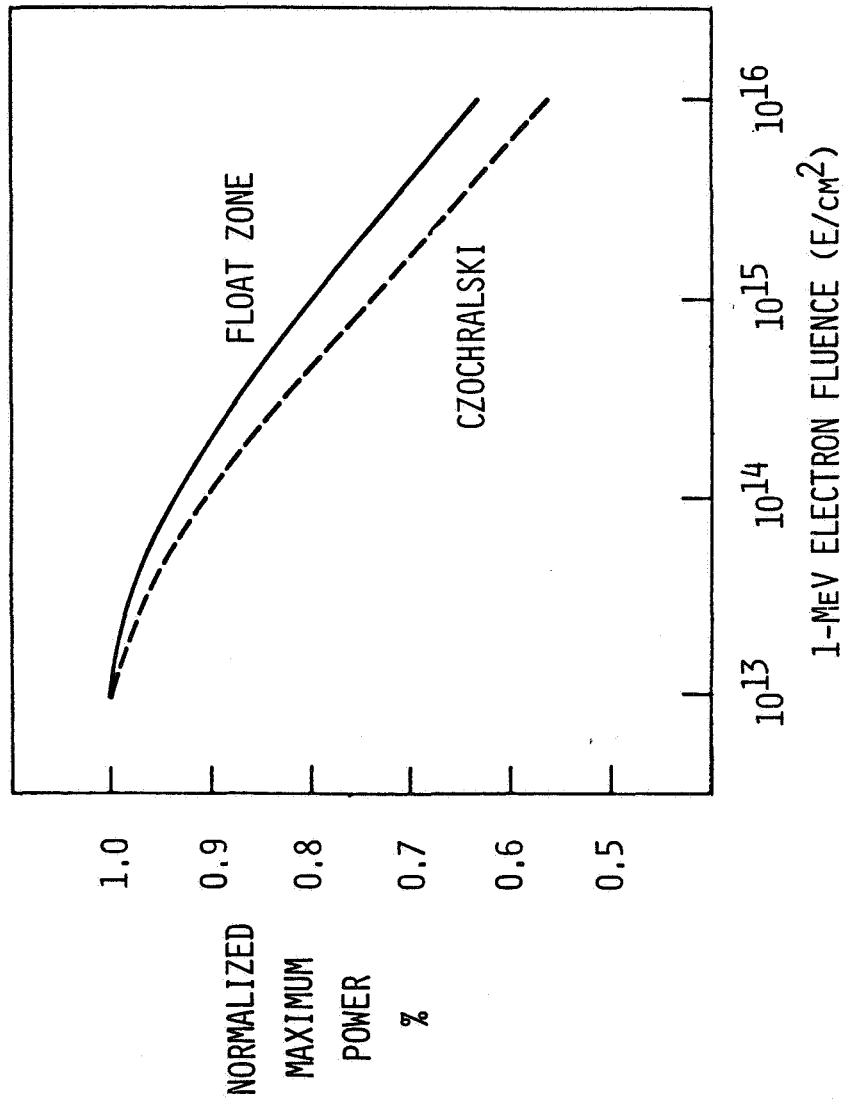
EFFECT OF REDUCED OXYGEN AND CARBON ON

SILICON SOLAR CELL ANNEALING TEMPERATURE

Figure II-15.

39
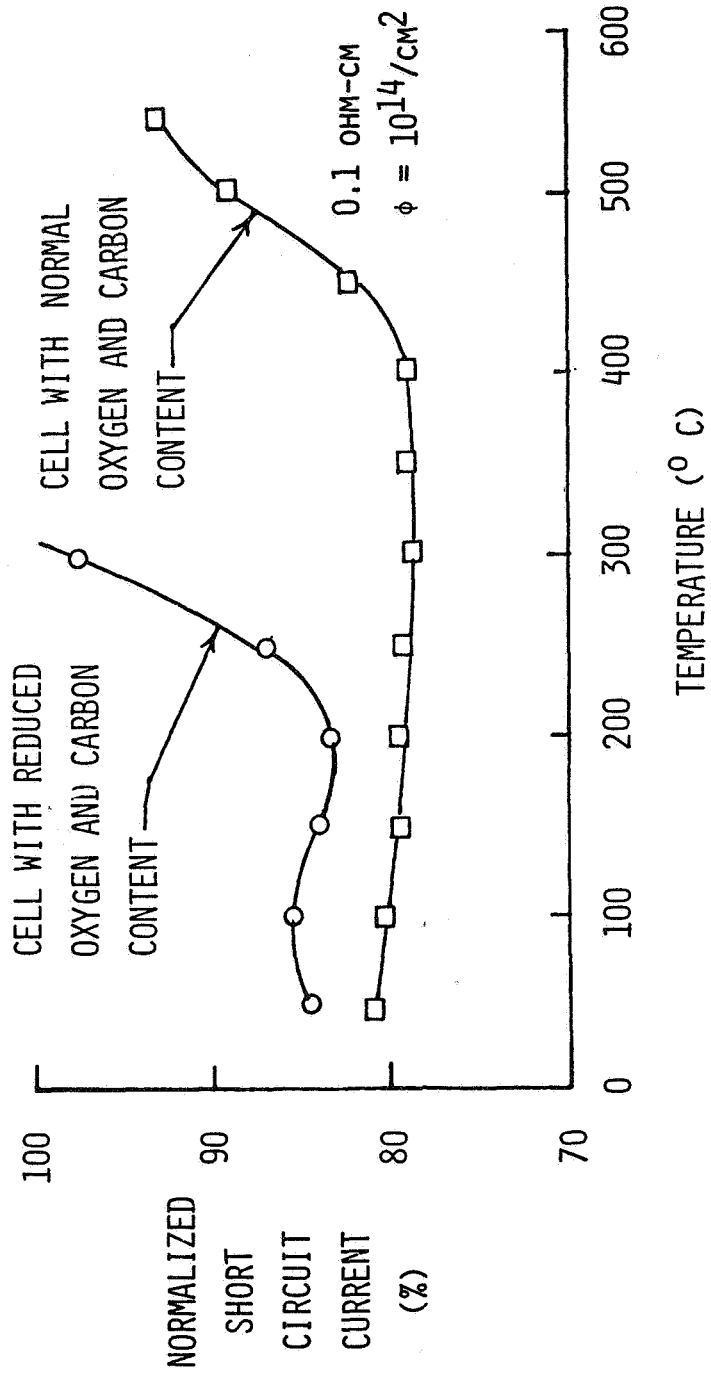
EFFECT OF DOPANTS ON CELL DEGRADATION AND ANNEALING

Figure II-16.

40
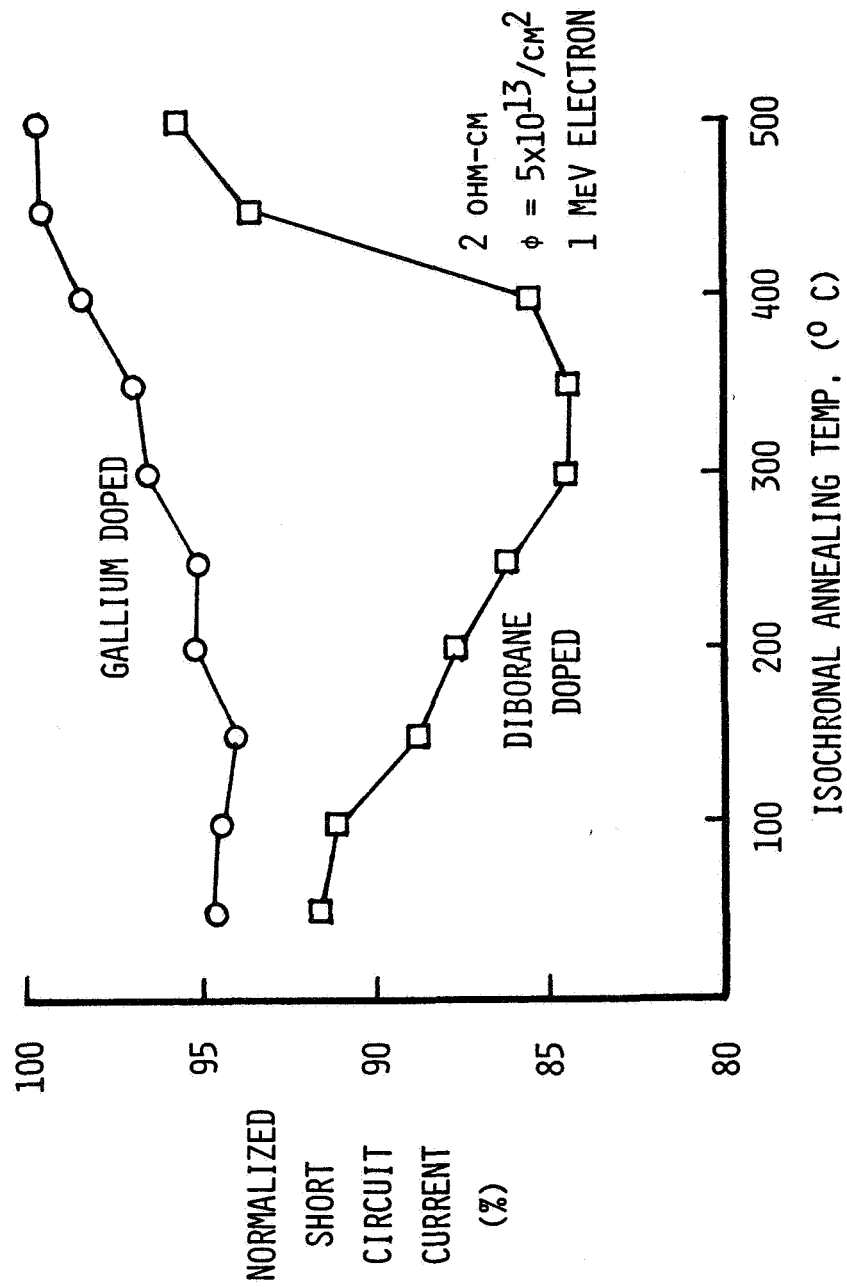
SILICON MATERIAL AND PROCESSING REQUIREMENTS FOR INCREASED

END-OF-LIFE EFFICIENCIES IN SPACE

REQUIREMENT

ADVANTAGE

- FLOAT ZONE

- OXYGEN AND CARBON < $10^{15}/CM^3$

⎫
⎬ • DECREASED DEGRADATION DUE TO
⎭   PARTICULATE RADIATION.

- JUNCTION FORMATION BY ION IMPLANTATION

• REDUCED ANNEALING TEMPERATURES.

- GALLIUM DOPING

• DECREASED DEGRADATION DUE TO PARTICU-
  LATE RADIATION AND PHOTONS.

• ABSENCE OF REVERSE ANNEAL.

• POTENTIAL FOR REDUCED ANNEAL TEMP.

- REDUCED DIVANCANCY CONTENT AFTER
  IRRADIATION

• REDUCED ANNEALING TEMPERATURES
  (POTENTIAL TO ATTAIN < 200^0 C).

Figure II-17.

41

C. FLOAT-ZONE SPACE PROCESSING RATIONALE

Lubek Jastrzebski
RCA
Princeton, NJ

Because float-zone growth in space is considered for commercial applications, there is a tendency to first establish which devices or circuits will feasibly be made from space grown float-zone silicon from an economical point of view. I believe that this is not totally justified. The majority of material problems which affect the performance of the circuits can presently be eliminated by adjustment of processing or changes in circuit design. The best example is striations observed in CCD imagers, which one and a half years ago were considered to be an insurmountable problem caused by materials. They have recently been eliminated by changes of processing and circuit design. This indicates that any material problems which right now seems to be an obstacle could be solved by future developments in processing or circuit design in the period of a few years, and it will take this long before float-zone crystals of at least 3-in. diameter will be grown in space. Therefore, focusing of research effort in space right now on any particular problem could be a little premature.

It seems that the first objective of the present program should be to demonstrate that growth in space will result in an improvement of silicon crystal properties. It is difficult to predict requirements for silicon of the future, because they depend on the directions in which technology will evolve and only some guesses on this subject can be made. It seems that future ICs will not need to interface with TTL logic, and therefore high resistivity material will be used for processing. In this material, the problem of oxygen thermal donors, and especially their inhomogeneous distribution, could become a critical issue (Fig. II-19). It has to be pointed out that this problem cannot be simply solved by elimination of oxygen from silicon crystals because oxygen in silicon also plays a beneficial role (Fig. II-18). In this case float-zone silicon crystals doped with oxygen and grown in space can be of interest.

THE ROLE OF FLOAT-ZONED SILICON IN ICs

Material (Silicon) for IC's

	(+)	(–)
CZ - Majority -	Oxygen pinning (mechanical strength)	- Defects (crystal growth)
	- Oxygen gettering (decontamination)	- Low resistivity - problem
		- Large change of resistivity possible.
FZ - Special Applications (CCD imagers)	- Easy dislocations movement	- No crystal growth related defects
	- Lack of gettering	- High resistivity
	- Inhomogeneity	- Small changes of resistivity

Present silicon for IC's: Resistivity, few Ωcm ($\sim 10^{16}$cm^{-3})

reason: circuits are designed for 5V to interface with TTL logic.

future: computer on a chip (e.g., 32 bit microproc.) interfacing with TTL

logic will no longer be required $\longrightarrow$ lower voltages (speed) $\longrightarrow$

higher resistivity material 100-1000 Ωcm range.

Possible problem: Nonuniform oxygen distribution.

Figure II-18.

CRITICALITY OF OXYGEN AND DOPANT RADIAL
PROFILES IN MOS DEVICES
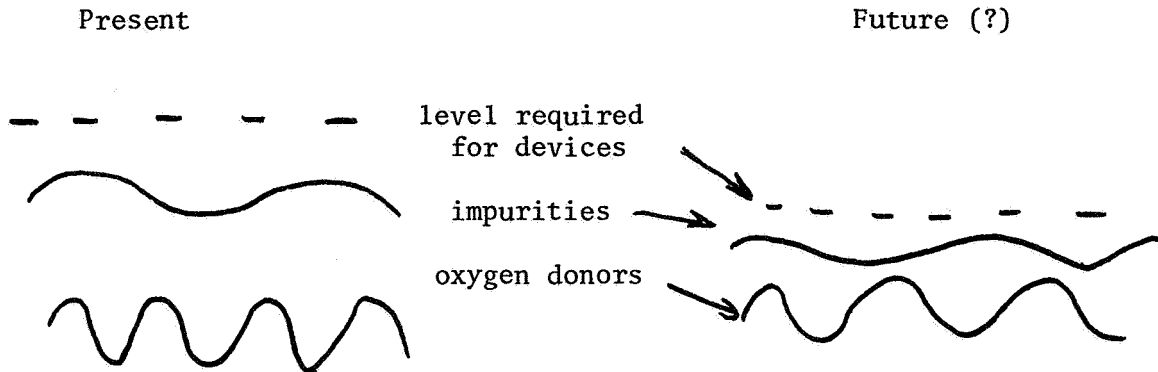
Present   Future (?)

- CMOS, latch up, threshold voltage

- NMOS, dynamic, threshold control
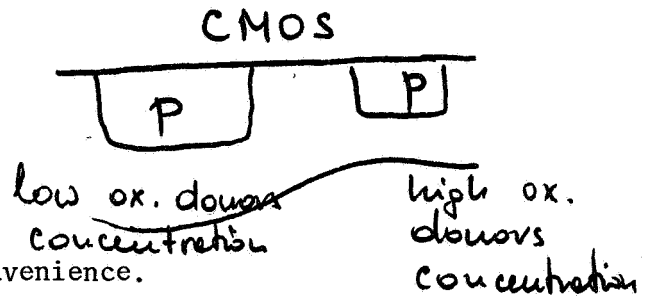
Present: inhomogeneities can be overcome - inconvenience.

Future: possible problem with oxygen, uniformity--problem of point defects

and their nonequilibrium trapping (their effect on initial stage of

oxygen precipitation kinetics (?))

Silicon requirements in the future--depends on direction in which system

development will go.

Flat Radial Profile of dopant required.

For mass production space advantages:

crystal growth - size of the grown crystals

processing - wafer thickness

Figure II-19.

FLOAT-ZONED SILICON FOR BULK DEVICES

Float Zone Silicon - Power Devices - High Resistivity

For very deep junctions - bulk silicon required.

Nonuniformity of resistivity on micro scale - junction depth variations - breakdown - (due to electric field nonuniformity).

Question: cost

Power devices require a large amount of silicon material (compared with IC's) - cost low (IC's) - material cost is a large contributor to device cost.

Will improvement in device performance pay for additional cost?

IR Detectors $\longleftrightarrow$ supporting IC's speed.

Figure II-20.

D. GROWTH OF III-V AND II-VI ALLOY CRYSTALS IN SPACE BY VERTICAL ZONE LEVELING

Klaus J. Bachmann
North Carolina State University
Raleigh, North Carolina

Because of the change in density of zincblende structure compounds, e.g., InP, upon melting, a vertical zone melting process proceeds in outer space without contact of the molten zone with the container walls providing thus the advantages of float-zoning and confinement of high decomposition pressures which cannot be obtained under the conditions of ground based research (compare Figs. II-21 through II-28). This advantage is expected to result in substantial improvements in the perfection of important electronic materials, e.g., CdTe and InP, when grown by vertical zone leveling in space and promises, in addition, to provide unique and essential conditions for the growth of III-V and II-VI alloy crystals, e.g., $Cd_xHg_{1-x}Te$ and InP_yAs_{1-y}. An evaluation of various ternary and quaternary III-V alloy systems in terms of their suitability for experiments of very limited duration, and we suggest some work on InP_yAs_{1-y} and $Cd_xHg_{1-x}Te$ that are of interest in the context of near infared devices for optical communications and of far infrared detectors for mosaic focal plane sensors, respectively. For details we refer to a recent review: K. J. Bachmann, H. Schreiber, Jr., and F. A. Thiel, Progr. in Crystal Growth and Characterization, Vol. 2, pp. 171-206 (1979).

Figure II-21.

0.55 μm
Ga P
1438°C

Ga0.516 In0.484 P/
GaAs

Ga0.505 In0.495 P/
Ge

0.92 μm
In P
1062°C

0.6 μm

0.8 μm

1.2 μm

2.0 μm

0.87 μm
Ga As
1243°C

Ga0.468 In0.532 As/
InP

3.44 μm
In As
942°C

Figure II-22.

48

Figure II-23.

49

Figure II-24.

50
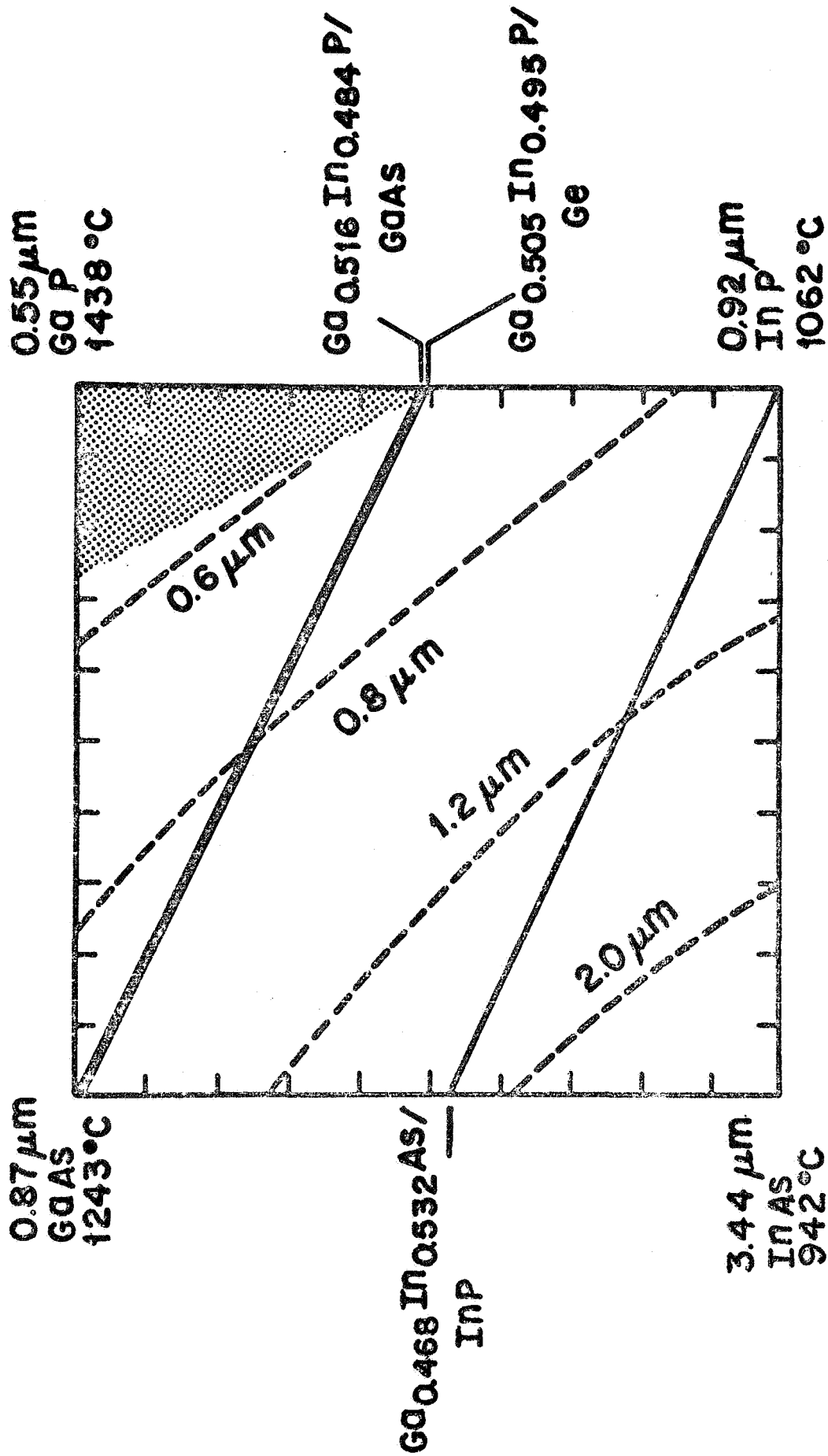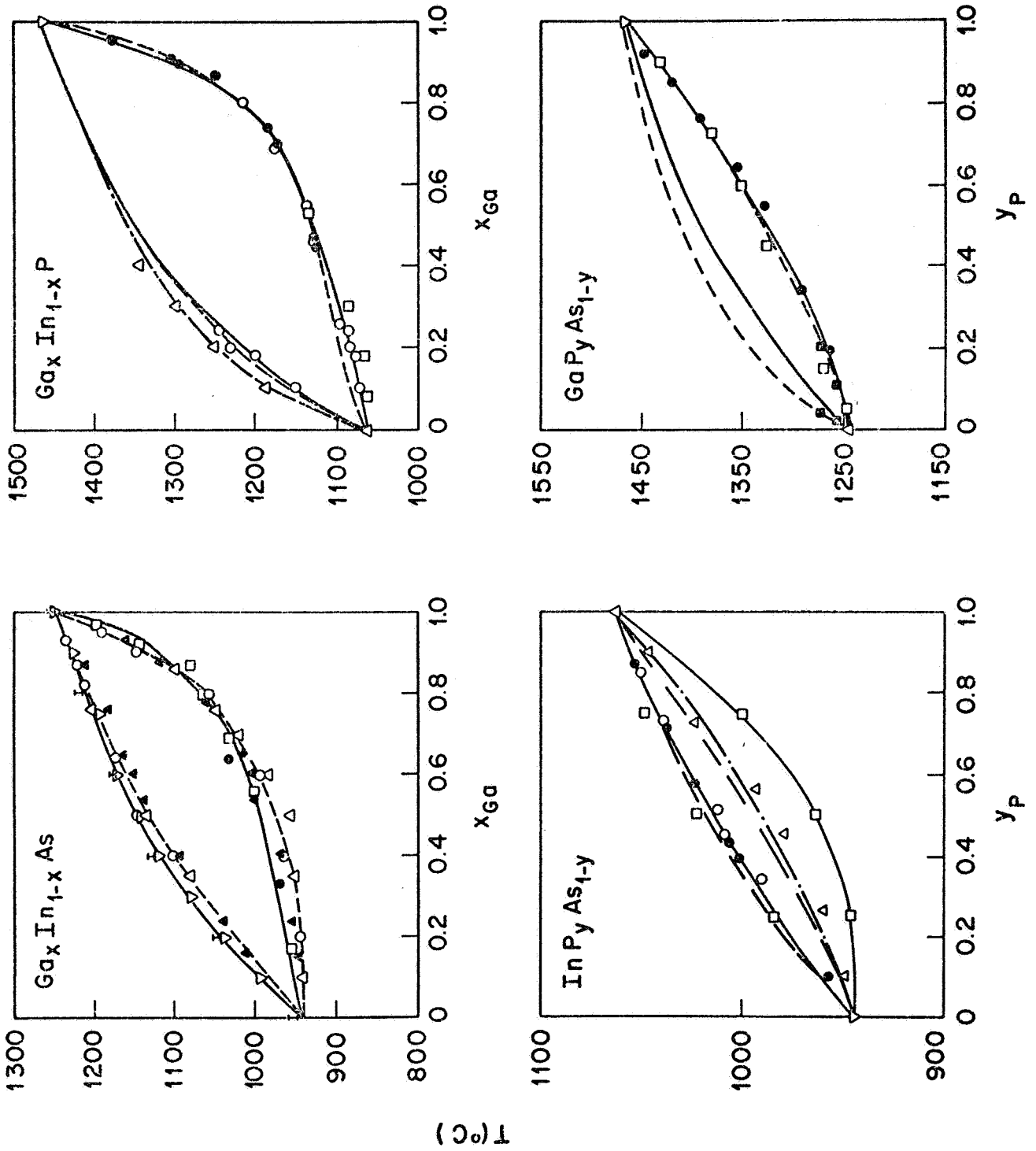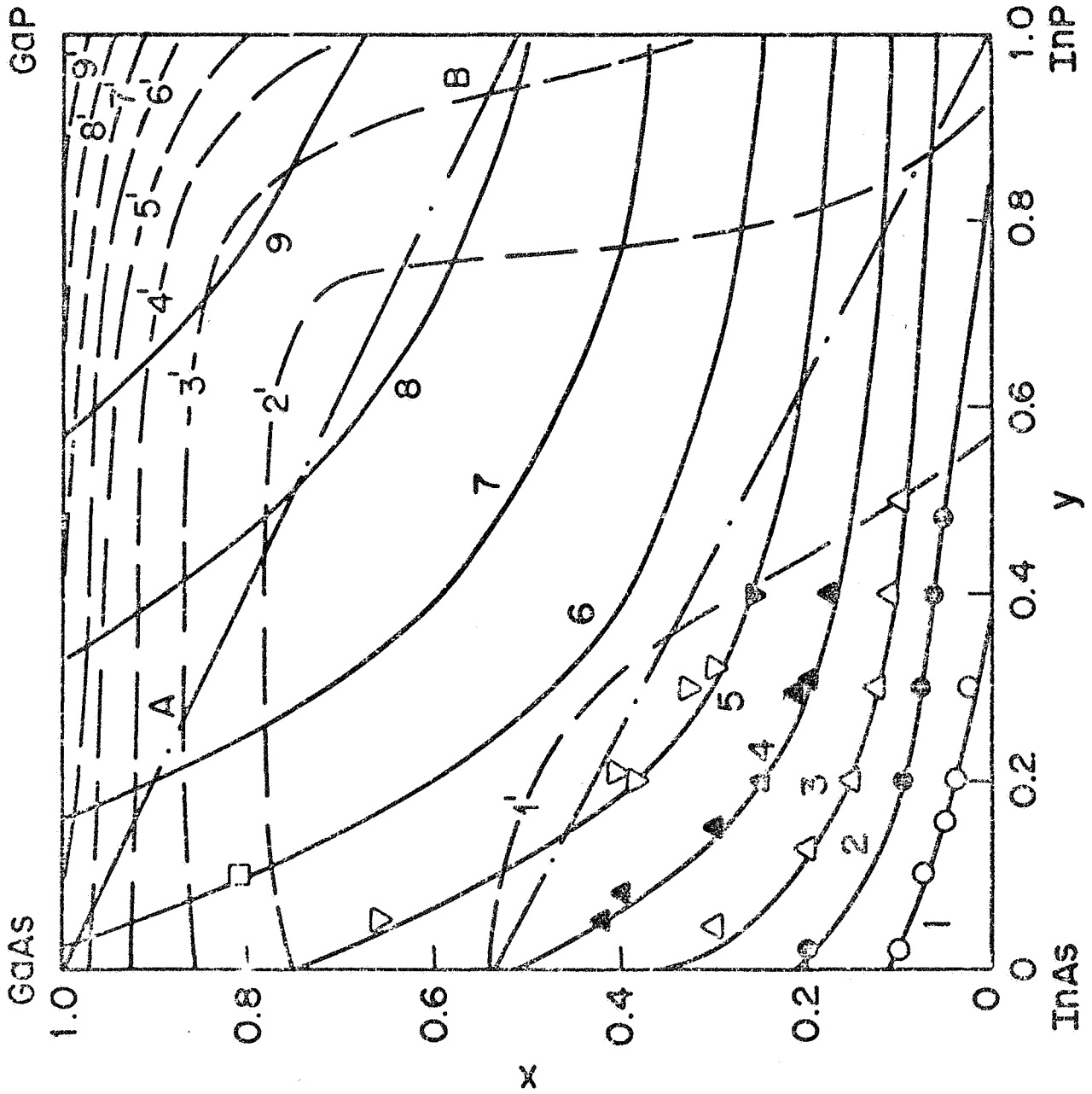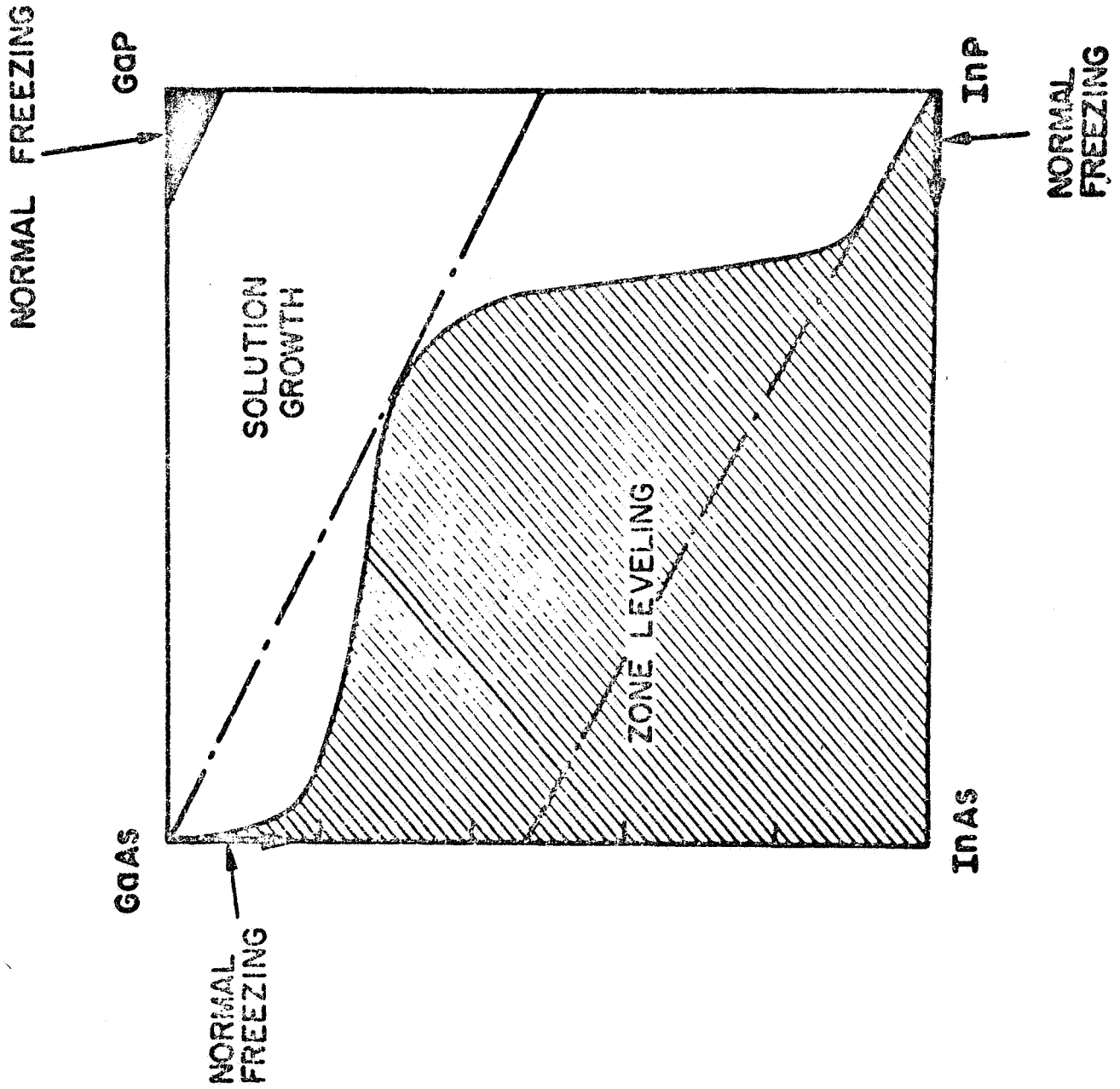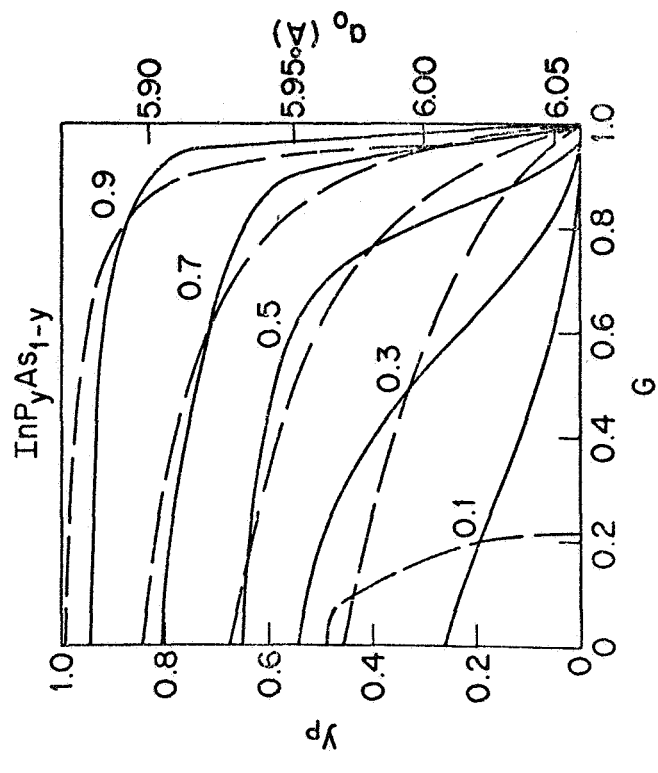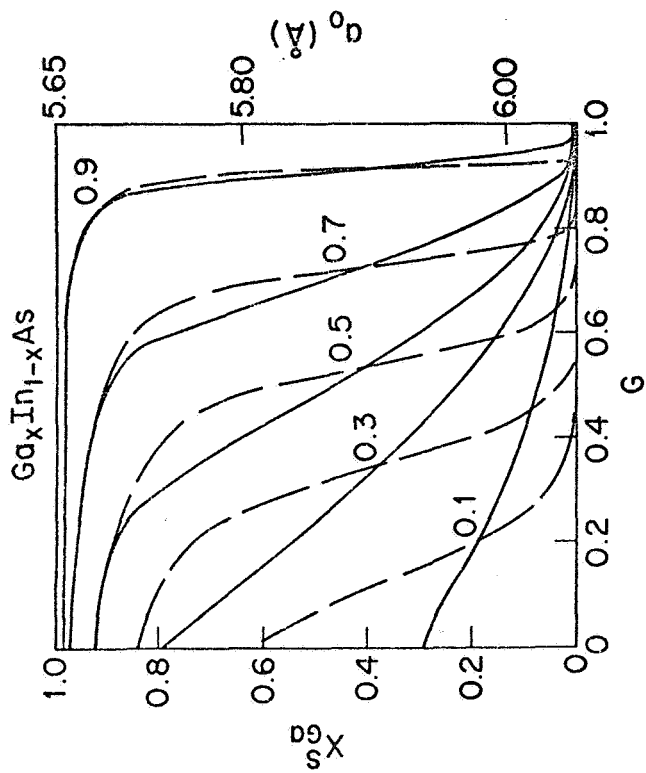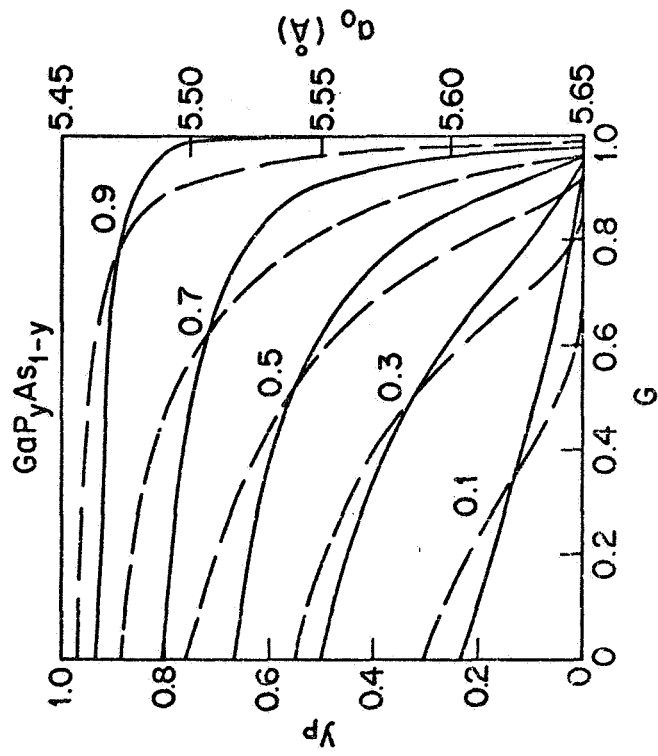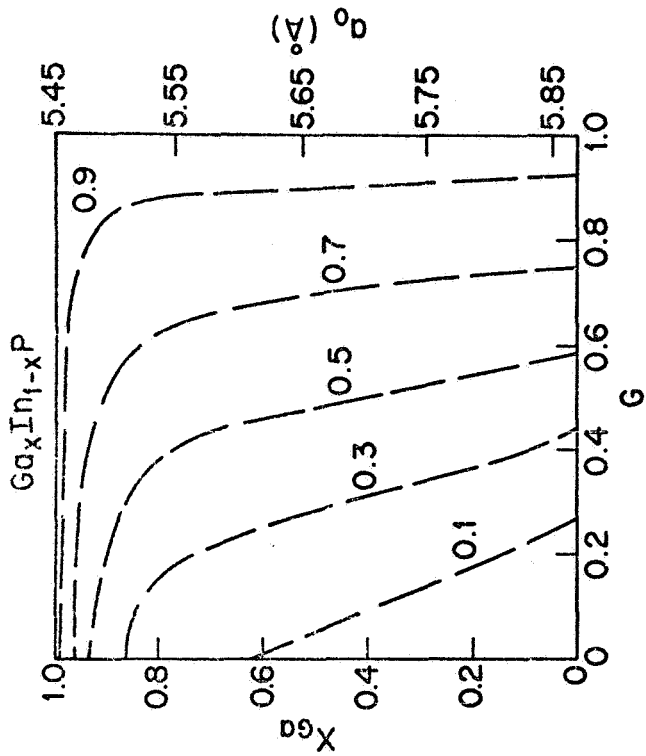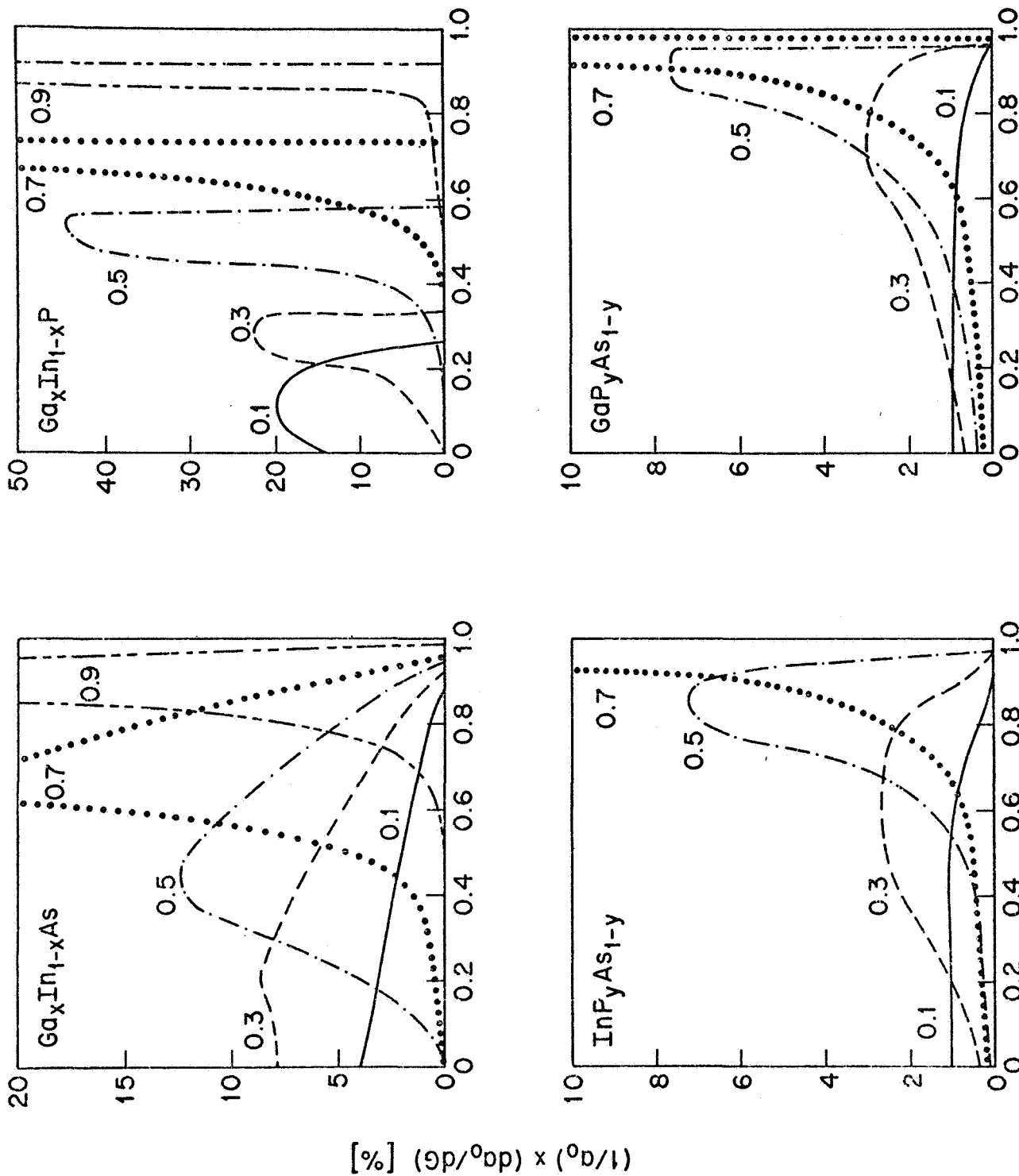
Figure II-25.
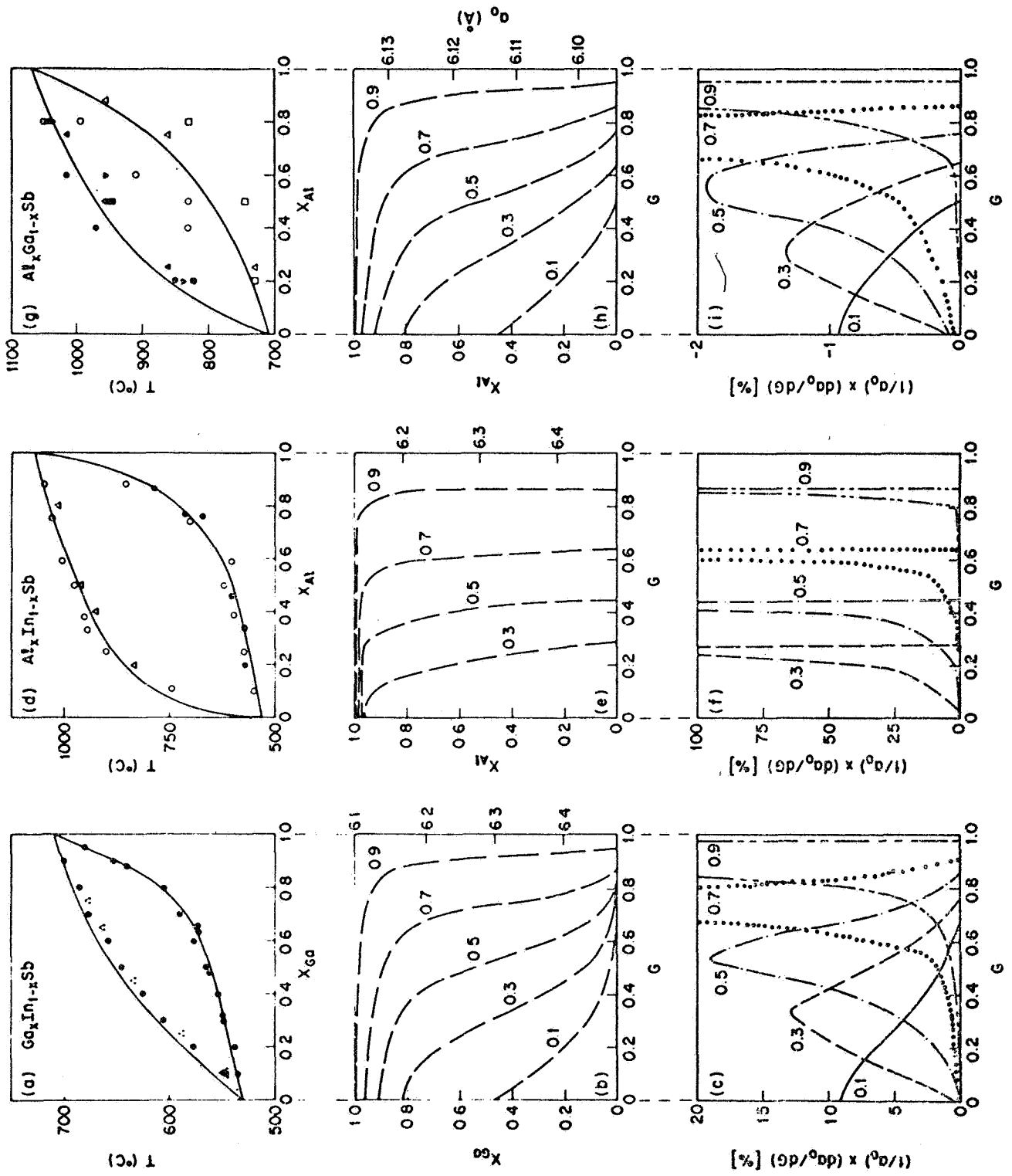
Figure II-26.
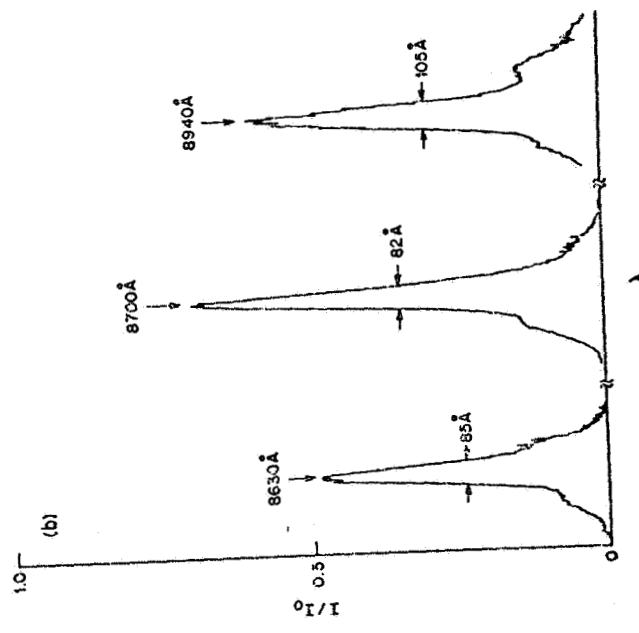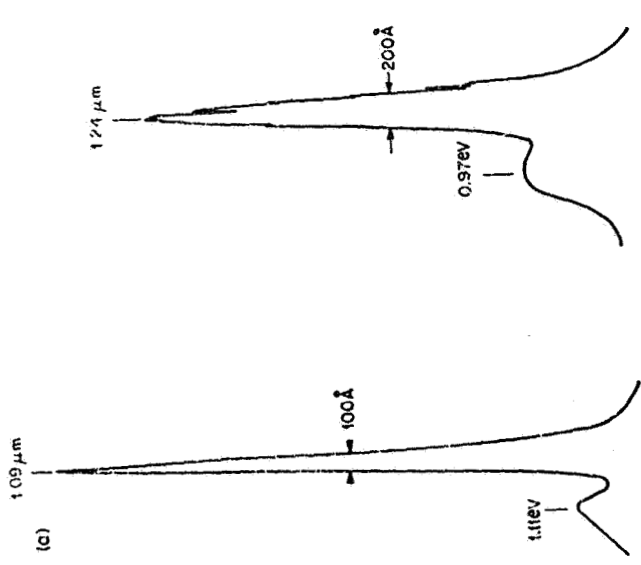
Figure II-27.

Figure II-28.

E. AIR FORCE FUTURE TECHNICAL REQUIREMENTS
FOR SILICON

Patrick M. Hemenger
Wright-Patterson Air Force Base
Wright-Patterson AFB, OH

The Materials Laboratory (ML) is presently supporting materials improvement programs that include a range of semiconductors (e.g., Si, GaAs, HgCdTe, InAs) in both bulk and thin layer forms which are aimed at solving a spectrum of problems ranging from impurity control to radiation hardening of integrated circuits. This presentation emphasizes the Si based bulk materials because they are more directly related to this meeting. However, closely related work on other materials and on thin-layer Si are summarized for completeness. Figures II-29, II-30, and II-31 summarize the three topics covered:

1) Si based materials requirements

2) ML supported programs

3) ML inhouse characterization facility.

Several general thoughts and questions come to mind when considering the growth of crystals in space:

1) Some of the desired improvements for bulk Si should be realized directly, namely higher purity, greater uniformity, and better overall control of defects and dopants.

2) Can the Si-Ge system (Si-rich) be grown with the quality necessary for use in wavelength tuned detectors, both intrinsic and extrinsic?

3) Will magnetic field growth retain any advantages?

4) Can the solution growth process be improved in the zero gravity environment if it allows a larger solution zone while maintaining stability?

The Air Force and the ML plan to participate actively in this project. This participation will include, on a continuing basis, characterization of the space grown crystals and evaluation of their applicability to Air Force systems. The complete inhouse characterization facility which is outlined on the attached sheet will be made available for this project.

REQUIREMENTS/BACKGROUND

HIGHER QUALITY DOPED SILICON IS REQUIRED SUITABLE FOR
FABRICATING MONOLITHIC FOCAL PLANE ARRAYS WITH ON CHIP CCD
SIGNAL PROCESSING.

- Gallium Doped Silicon with Greater Uniformity of
  Responsivity and Higher Responsivity is Required
  for the Next Generation Tactical FLIR.

- Indium Doped Silicon with Higher Operating Temperature
  and Greater Uniformity of Responsivity and Higher
  Responsivity is Required for Very Large Focal Planes of
  the HALO Type for Space Surveillance.

- Ultra-high Purity Silicon Required for Laser Guided
  Weapons Systems.

- Very Long Wavelength Doped Silicon Material Such as
  Si:As is Required for Space Missions.

OTHER SILICON BASED AIR FORCE MATERIALS REQUIREMENTS

- Bulk Silicon with Larger Minority Carrier Lifetime and
  Thin Silicon Films (2000$\overset{o}{A}$) on Sapphire with Higher
  Mobilities Required for VLSI Applications. Air Force
  Program all Silicon Based.

- Long Lifetime Si-based Microwave Sources and Detectors
  are Required for Phased-array Radars (Over the Horizon
  and Spaceborne) In Early Warning Systems.

Figure II-29

56

Si-Ge ALLOY INFRARED DETECTORS

OBJECTIVE

- DEVELOP A DETECTOR MATERIAL SYSTEM TO EXACTLY "TUNE" THE SPECTRAL RESPONSE TO NECESSARY OPERATIONAL CONDITIONS

APPROACH

- MANUFACTURE IR DETECTORS FROM SILICON-RICH Si-Ge ALLOYS

PAYOFF

- FOR EXTRINSIC DETECTORS (FLIRS) A HIGHER OPERATING TEMPERATURE FOR ANY SPECIFIED ATMOSPHERIC WINDOW, THEREBY REDUCING POWER REQUIREMENTS, COOLER COST AND WEIGHT

- FOR INTRINSIC DETECTORS (RANGEFINDERS), A FACTOR OF 2 INCREASED SENSITIVITY AT 1.06 MICRONS, WHICH PRODUCES AN EVEN LARGER FACTOR IN TARGET ACQUISITION RANGE

Figure II-30.

FACILITIES/CAPABILITIES

● **ELECTRICAL AND OPTICAL**

  -HIGH RESISTIVITY HALL FACILITY

  -PHOTO-HALL FACILITY

  -LASER ANNEALING FACILITY

  -IR ABSORPTION SPECTROMETRY

  -PHOTOLUMINESCENCE FACILITY

  -PHOTOCONDUCTIVITY/PHOTOTHERMAL
   IONIZATION

  -THEORETICAL CAPABILITY

● **SURFACE/CHEMISTRY**

  -SCANNING AUGER MICRO-
   SCOPY

  -X-RAY PHOTOELECTRON
   SPECTROMETER

  -ION SCATTERING SPECT-
   ROMETER

  -SECONDARY ION MASS
   SPECTROSCOPY

  -SCANNING ELECTRON
   MICROSCOPE

  -AUGER DEPTH PROFILE
   INSTRUMENT

  -ELLIPSOMETER

  -LASER-RAMON SPECTRO-
   METER

  -LOW ENERGY ELECTRON
   DIFFRACTION

PLANNED

  -CDLTS & C-V MEASUREMENTS FOR FILMS

  -AC TECHNIQUE FOR CHARACTERIZING WAFERS/FILMS

  -UPGRADE OF EXISTING FACILITIES/CAPABILITIES

Figure II-31.

F. INDUSTRY NEEDS FOR SILICON CRYSTALS AND STANDARDS

Kenneth E. Benson
Bell Laboratories
Allentown, PA
(Chairman ASTM F-1 Committee on Electronics)

The trend of the device fabrication industry requiring larger crystals is reviewed. The standard Czochralski wafer size is now 100 mm (4 in.) and going to 125 mm (5 in.) within 2 or 3 years, with 5-in. wafer device lines now coming "on-stream" (Fig. II-32). The mass of Czochralski crystals has steadily increased over the past years and crystals of 30 kgm mass are now standard (Fig. II-33).

A real need of the device industry, which cannot be met by the nonuniformity in production crystals, is for measurement standards. This is an area where the NASA crystal growth program could make an important contribution to industry and government needs. Standards are needed for resistivity (four-point probe and spreading resistance) and for chemical composition of oxygen and carbon impurities. The ranges of properties and uniformities for these standards are given in the following figures.

STANDARD REFERENCE SILICON MATERIALS NEEDS

ASTM Committee F-1 on Electronics

- Resistivity Standards
  Four-Point Probe
  Spreading Resistance
- Oxygen Standards
- Carbon Standards

RESISTIVITY STANDARDS

Nominal Doping Ranges — for N and P Type Material,
<100> and <111> Orientations 5×10^{17}, 1×10^{16},
1×10^{15}, and $1 \times 10^{14}/cm^3$

Uniformity $\leq 0.5\%$

OXYGEN STANDARDS

Nominal Concentration — 0.1, 1, 40 ppm

Uniformity ±5%

CARBON STANDARDS

Nominal Concentration — 0.1, 1, 10 ppm

Uniformity ±5%
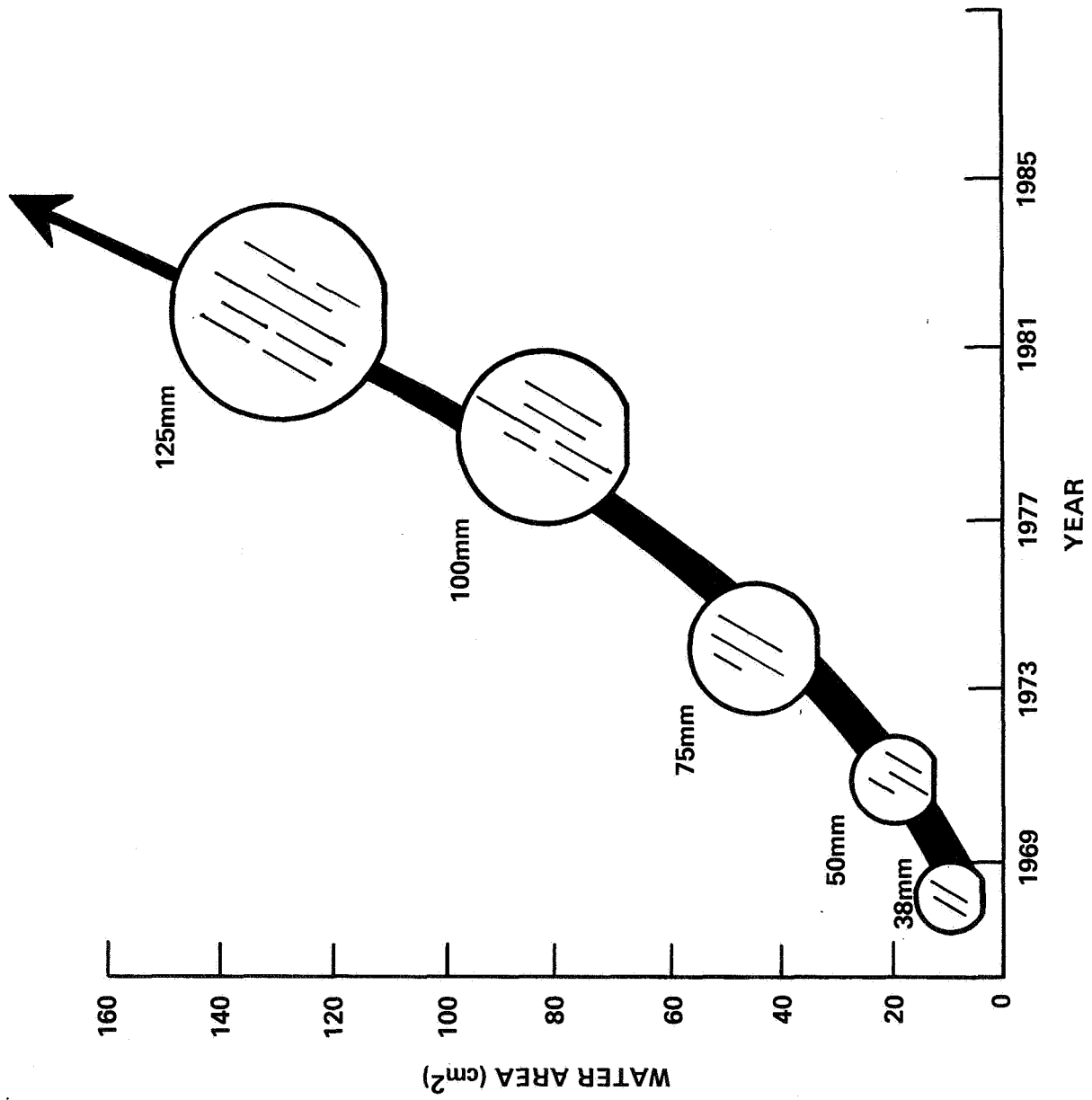
Figure II-32.
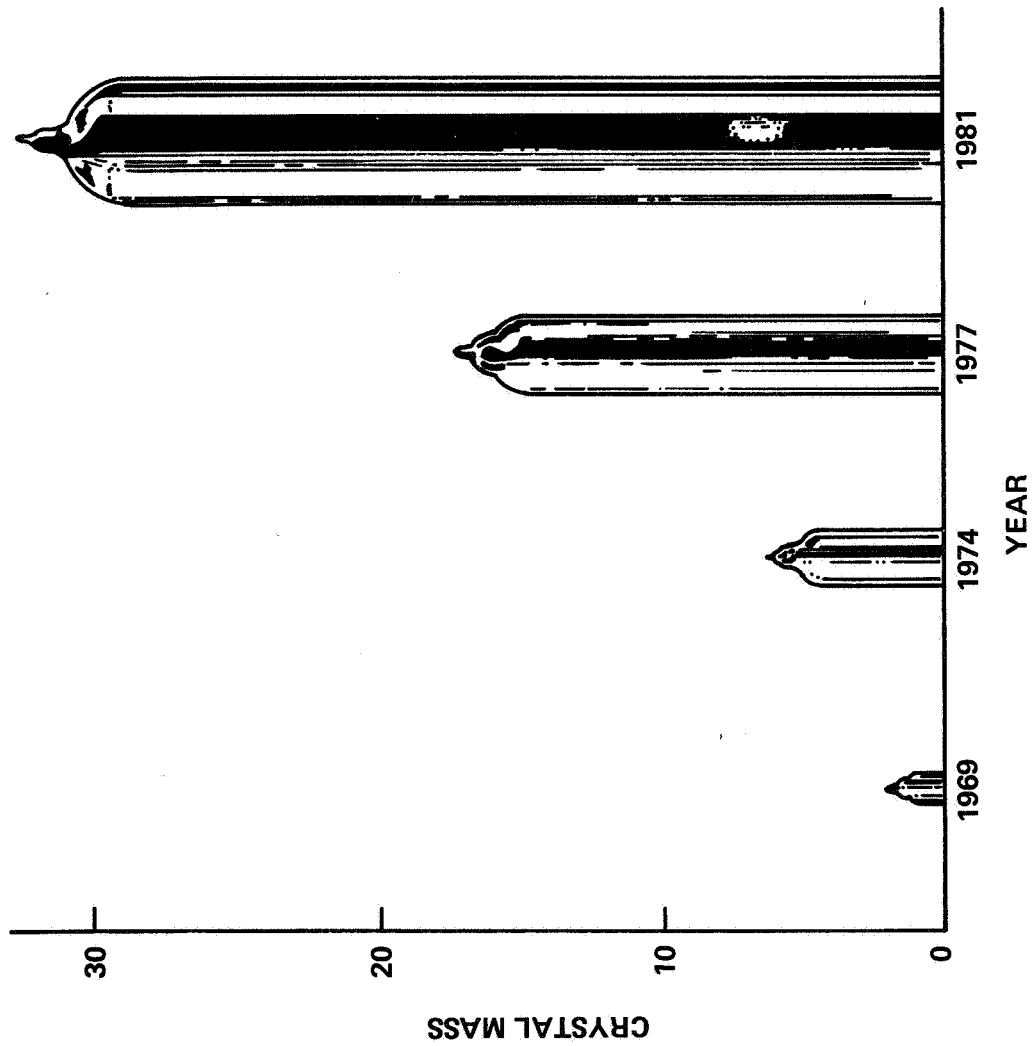
Figure II-33.

FOUR POINT PROBE.

WAFER RESISTIVITY

$S = 1.6mm$

$0.5mm = t$
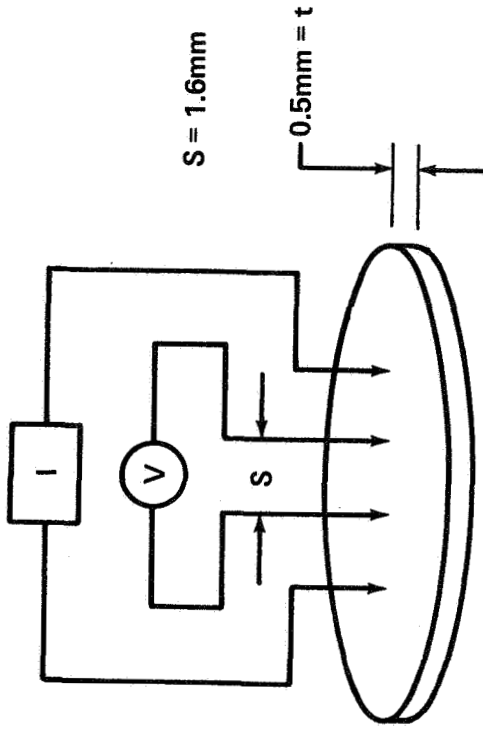
$\rho = \dfrac{V}{I} \bullet t \bullet F_T \bullet F \, (^t/_s) \bullet F_2 \bullet F_{sp}$

$V =$ VOLTAGE (5 — 50 mV)

$I =$ CURRENT (0.1μA TO 1.0A)

$t =$ WAFER THICKNESS

$F_T =$ TEMPERATURE CORRECTION

$F(t/s) =$ FINITE THICKNESS CORRECTION

$F_2 =$ FINITE LATERAL GEOMETRY CORRECTION

$F_{sp} =$ UNEQUAL PROBE SPACING CORRECTION

A)   RANGE — 0.0008 TO 5,000 Ω—cm

B)   VOLUME SAMPLED — 0.02 cm³

C)   PRECISION ±1%

Figure II-34.

SPREADING RESISTANCE PROBE

WAFER AND IN–DEPTH RESISTIVITY

I) SURFACE

a = RADIUS
OF CONTACT

$\rho = 2aRC$

a = RADIUS OF CONTACT

R = RESISTANCE (1 TO 10^8 OHMS)

C = CORRECTION FACTOR

S = PROBE SPACING

II) IN–DEPTH (PROFILE)

θ = 0.2 TO 10°

LAYER

SUBSTRATE

PIECE CUT FROM WAFER AND BEVELED
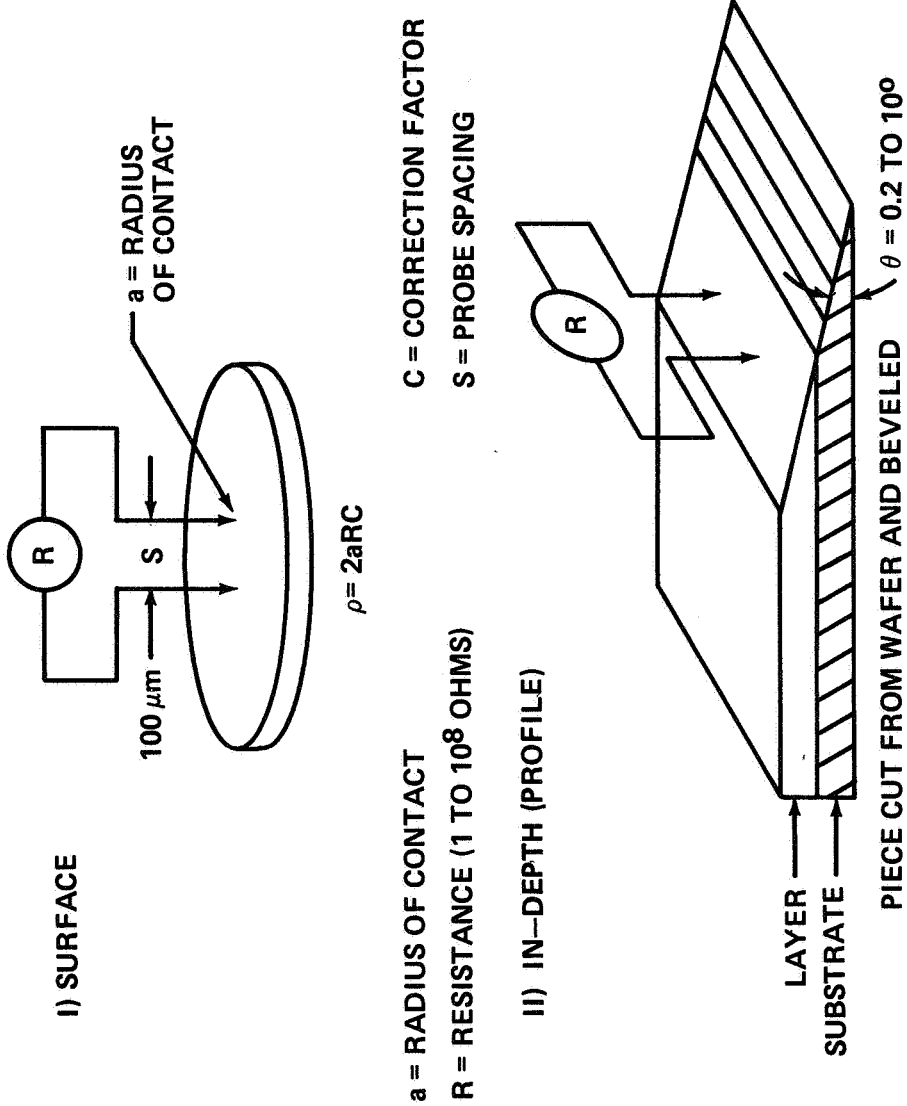
A)   RANGE – 0.0008 TO 10^6 Ω – cm

B)   VOLUME SAMPLED – 6 x 10^{-10} cm³

C)   PRECISION ±10%

Figure II-35.

G. ROLE OF SUBSTRATE QUALITY ON IC PERFORMANCE AND YIELDS

R. N. Thomas
Westinghouse R&D Center
Pittsburgh, PA

The dramatic progress made in silicon device and IC technology in recent years is derived in part from the availability of high quality, large-area silicon substrates. The widespread acceptance of the Czochralski growth process by the IC manufacturers arises from the relative ease with which large, doped single crystalline material can be produced by crystal pulling from a silicon melt contained in a quartz crucible. Over the past decade, engineering efforts have focused almost exclusively upon the scaling of crystal growth equipment to larger and larger crystal diameters until today; 100-mm diameter crystals have become commonplace. Crystals up to 150-mm diameter are anticipated in the next few years due to the favorable economics of large-area wafer processing (Fig. II-36).

Device performance is, however, often limited by the basic substrate properties, and there is considerable concern at the present time that the quality of commercially available silicon will impose severe limitations as device features are scaled down to the micron and sub-micron VLSI range. The adverse effects of crucible dissolution on compositional purity combined with micro-segregation effects and crystalline imperfections resulting from uncontrolled thermal convection in large volume melts are major problems. In silicon LSI, these chemical and structural defects are found to interfere with device processing with deleterious consequences to performance and yields.

An even more crucial need for improved materials quality exists in high-speed GaAs FETs and the newly emerging monolithic microwave GaAs ICs, which are expected to have a broad impact on future microwave signal processing and power amplification. In the past, the variable and often inferior quality of commercial horizontal Bridgeman or gradient freeze substrates has been a major deterrent to the emergence of a reproducible, low-cost GaAs manufacturing technology. Recent advances in liquid encapsulated Czochralski equipment offer a capability for producing large-area, cassette-compatible GaAs slices of improved quality.

At the Westinghouse R&D Center, these problems are being addressed through crystal growth research of large diameter crystals directed at developing improved Si and GaAs by the Czochralski crystal growth process for high performance IC processing.

SILICON

Infrared Focal Plane Arrays

Infrared CCD imagers based on extrinsically-doped silicon form an important family of ICs, where performance is strongly influenced by the silicon purity. For 3 to 5 μm infrared imaging, high photosensitivity depends on indium-doped silicon substrates of high indium content and high background purity. Unfortunately, dissolution of the quartz crucible in the silicon melt contributes, in addition to large amounts of oxygen, boron, and aluminum impurities which are particularly harmful to p-extrinsic silicon detectors.

The use of high purity synthetic fused silica crucibles in place of the industry-standard quartz crucibles in the Czochralski process offers considerable advantage. Figure II-37 illustrates the effectiveness of these synthetic fused silica crucibles. An order of magnitude reduction in the boron content is observed. When high purity Si:In crystals are compensated by precise neutron transmutation doping techniques, extrinsic indium-doped silicon of exceptionally high IR sensitivity is produced (Fig. II-38). Undoped silicon crystals produced by high purity Czochralski pulling exhibit p-type resistivities in the 3000 to 5000 Ω-cm range.

LSI Silicon

Oxygen and, to a lesser extent, carbon impurities have a profound influence on defect nucleation and precipitate formation in large-area Czochralski silicon. Oxygen is present at concentrations in excess of the solid solubility at the temperatures normally employed in device processing. An oxidation step leads to SiO_2 precipitation and the generation of oxidation-induced stacking faults (OSF). Carbon impurities occur in striated distributions (as do all strongly segregating impurities) forming nucleation sites for point defects and interstitial oxygen. These micro-defects are sinks to electrically-active impurities introduced inadvertently during processing with major consequences to LSI processing.

Although occurrence of these defects in active junction regions is harmful, causing high leakage currents, it is now common practice in complex LSI cycles to develop a denuded, low oxygen content surface layer and encourage SiO_2 precipitate formation in the bulk for intrinsic gettering (Fig. II-39).

Crystal growth studies of large, 100-mm diameter silicon crystals are being carried out because of the anticipated need for substrates of very low microdefect content in future very high speed integrated circuit (VHSIC) fabrication. Improved purity and uniform incorporation of oxygen are prime goals. The axial and radial oxygen distribution in 100-mm diameter silicon crystals pulled in a HAMCO CG200RC is shown in Figure II-40.

Exploratory studies of magnetic field effects in Czochralski silicon crystal growth are also being undertaken. Transverse magnetic fields are found to suppress unwanted melt convection (Fig. II-41) and offer a unique means of controlling the oxygen in silicon (Fig. II-42).

GALLIUM ARSENIDE

Monolithic Microwave GaAs Circuits

The recent emergence of high performance monolithic GaAs circuits for digital logic and analog high gain/low noise and power amplification at microwave frequencies has caused renewed interest in semi-insulating GaAs crystal growth.

The use of high purity semi-insulating GaAs prepared by LEC growth for selective direct ion-implantation processing has been a major factor in the improved performance and reproducibility of monolithic GaAs ICs which are currently undergoing development at different laboratories. Figure II-43 illustrates round, 50- and 100-mm diameter GaAs slices cut from <100>-crystals grown in a high pressure liquid encapsulated Czochralski (LEC) Melbourn puller. Recent investigations emphasizing in-situ synthesis of the GaAs melt in silicon-free pryoltyic boron nitride crucibles to

preserve purity, yield reproducible growths of thermally stable, semi-insulting <100>-GaAs crystals without resorting to conventional chromium doping. Residual silicon, Group VI, chromium and iron impurities are maintained below the 10^{15} cm^{-3} range in undoped LEC crystals (Fig. II-44).

Improvements in the compositional purity of undoped GaAs crystals pulled from PBN crucibles are also indicated by the high measured carrier mobility. Mobilities of about 6000 cm^2/Vsec are observed and correspond to a total ionized impurity content in the low 10^{16} cm^{-3} range (Fig. II-45). Indirect evidence of the substrate purity is also obtained from the transport properties of n-layers formed by Si ion implantation of undoped GaAs/PBN substrates. The electron mobility in n-implanted layers with doping levels between 1×10^{16} cm^{-3} and 5×10^{17} cm^{-3} is found to be limited only by impurity scattering and comparison with theoretical predictions again indicated about 1×10^{16} cm^{-3} residual impurity concentration in the substrate.

The microscopic inhomogeneity of dopant and residual impurities in GaAs substrates is cause for concern in large-area substrate processing of microwave devices and monolithic circuits. Impurity striation behavior is observed in large diameter LEC GaAs crystals as shown in longitudinal sections of Figure II-46. In the case of semi-insulating GaAs/PBN where the impurity content is low, the observed striations are probably the result of local fluctuations in stoichiometry brought about by variations in the microscopic growth rate. Measurement of temperature fluctuations in a 6-in. diameter, 3 kg B$_2$O$_3$-encapsulated GaAs melt in the high-pressure Melbourn system are shown in Figure II-47. Temperature excursions approaching 10°C are observed at the center of the encapsulated GaAs melt, which are significantly higher than those generally observed in unencapsulated Czochralski melts of silicon.

The improved quality of round, large-area LEC substrates, which are compatible with modern semiconductor processing equipment, is source of considerable optimism that a reproducible, low-breakage GaAs IC processing technology will be realized in the near future.

<div align="center">SUMMARY</div>

Industrial research and development in silicon and gallium arsenide crystal growth are directed towards producing large diameter substrates (because of the cost leverage advantages), which satisfy the specific needs of today's complex electronic devices through the "tailoring" of substrate quality for optimum device processing. As the IC technologies are driven more and more towards high operating speeds, by scaling of device features to micron and sub-micron geometries, it is anticipated that large-area substrates of significantly improved compositional purity, dopant distribution and structural perfection on a microscopic as well as macroscopic scale will become increasingly important requirements. These needs are currently being addressed through the exploratory use of, for example, magnetic fields to suppress convection effects in Czochralski crystal growth. Although the growth of large crystals in space appears impractical at present, the current efforts to improve substrate quality could obviously benefit from the experiences gained in smaller-scale growth experiments conducted in the zero-gravity environment of space.

ACKNOWLEDGMENTS

Favorable Economics of Large Area
Wafer Processing

Figure II-36.

$N_{In} \approx 2.5 \times 10^{17}$ cm^{-3}

△ CZ
Natural Quartz
$N_B = 1.5 \times 10^{14}$ cm^{-3}
$N_P = 5.8 \times 10^{13}$

□ CZ
Synthetic
$N_B = 1.5 \times 10^{13}$ cm^{-3}
$N_{Al} = 2.7 \times 10^{12}$
$N_P = 2.2 \times 10^{13}$

○ FZ
$N_B = 2.7 \times 10^{12}$ cm^{-3}
$N_{Al} = 5.6 \times 10^{11}$
$N_P = 2.2 \times 10^{12}$
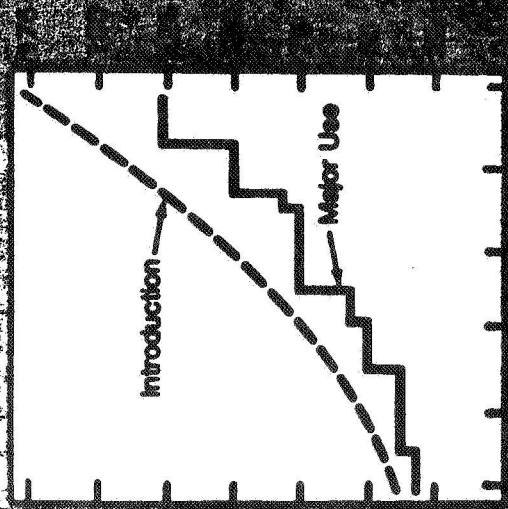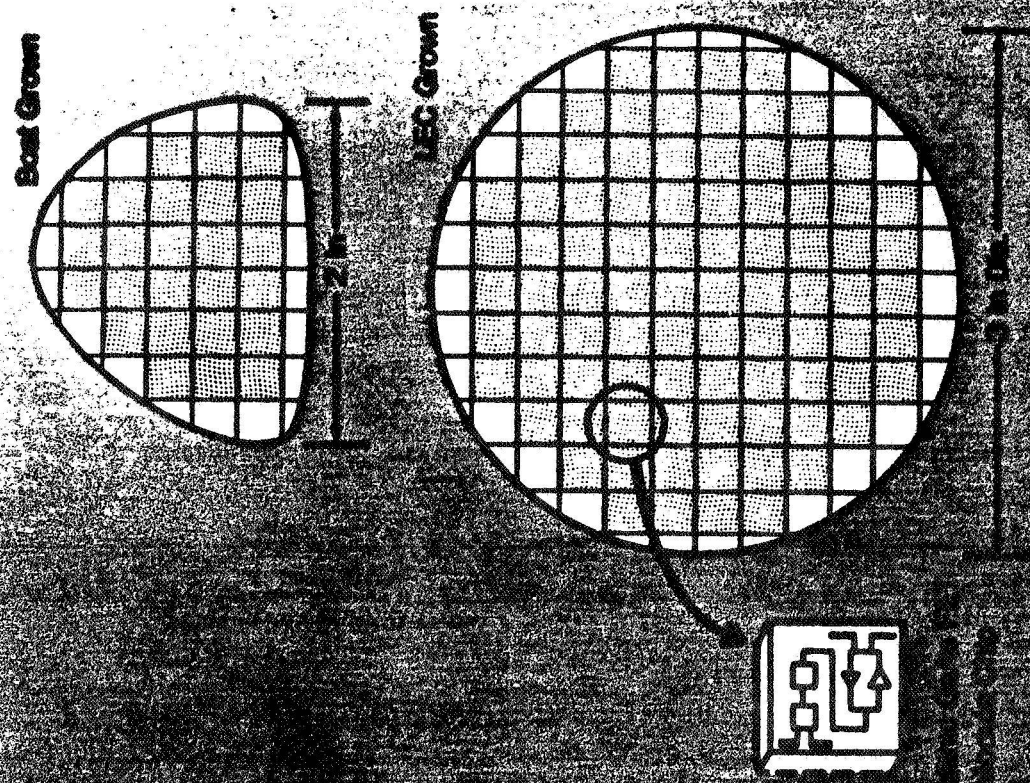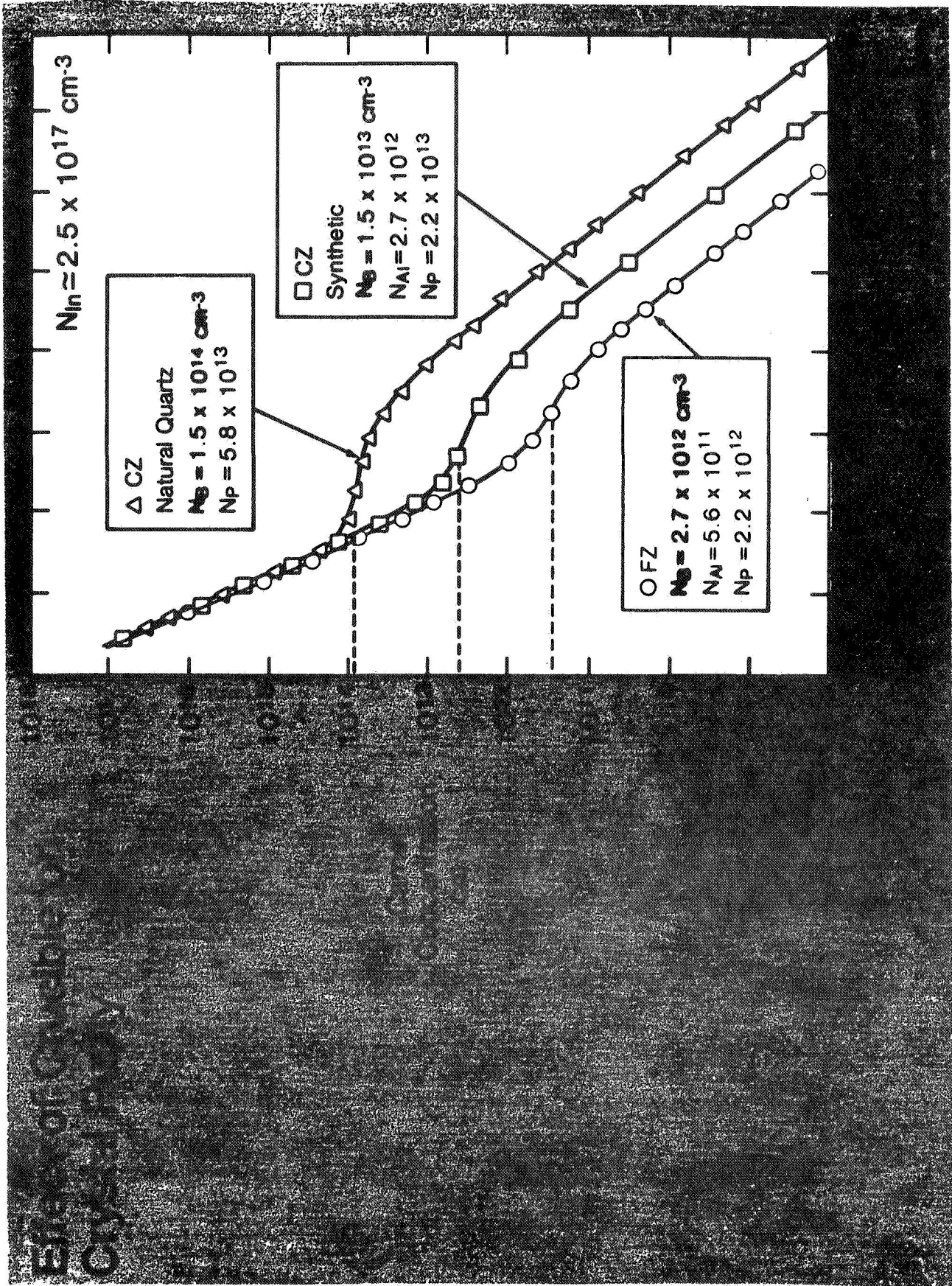
Figure II-37.
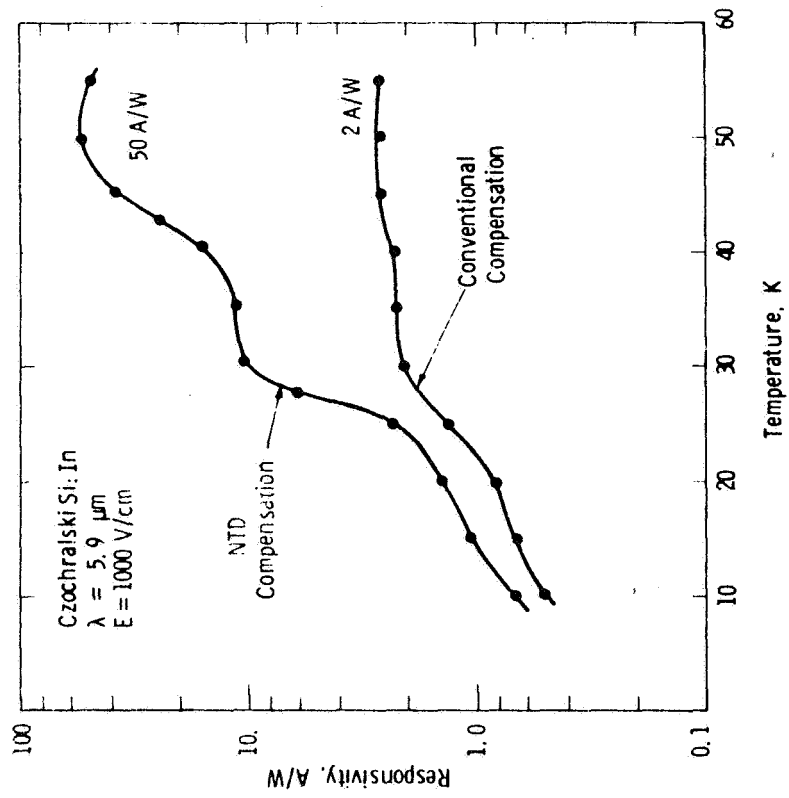
Figure II-38.

Comparison of responsivity for neutron compensated and conventionally compensated Czochralski Si:In.

Intrinsic Gettering by Oxygen Related Defects

(a) Microdefects After Thermal Treatment

(110) - Cleavage Plane Cross-Section

(b) Intrinsic Gettering

Surface: Denuded Zone

n+

Bulk: Microdefects Act as Self-Gettering Sites

Oxygen Related Defects
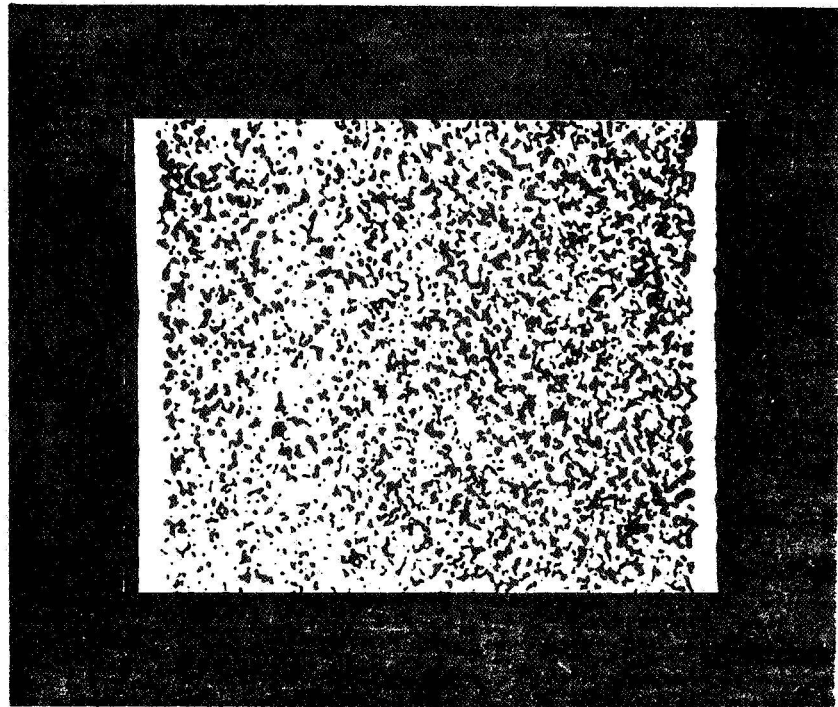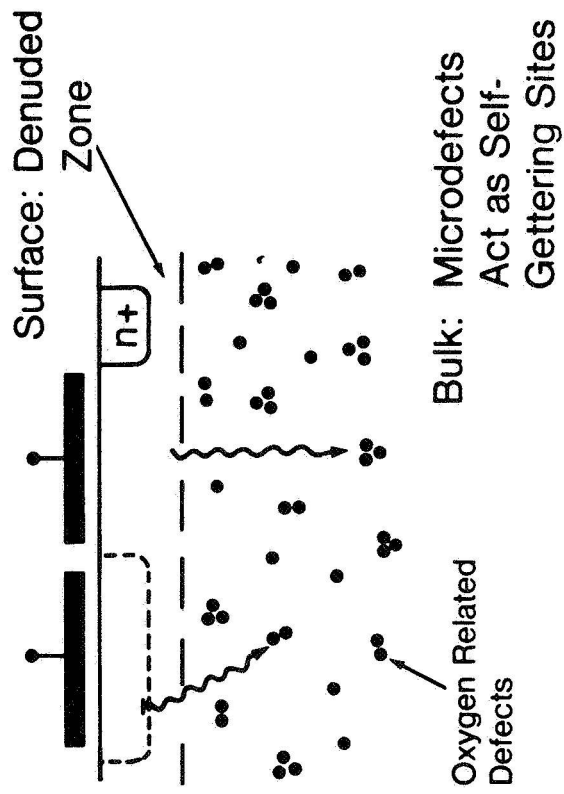
Figure II-39.

AXIAL & RADIAL DISTRIBUTION OF OXYGEN
IN LARGE DIAMETER CZOCHRALSKI SILICON
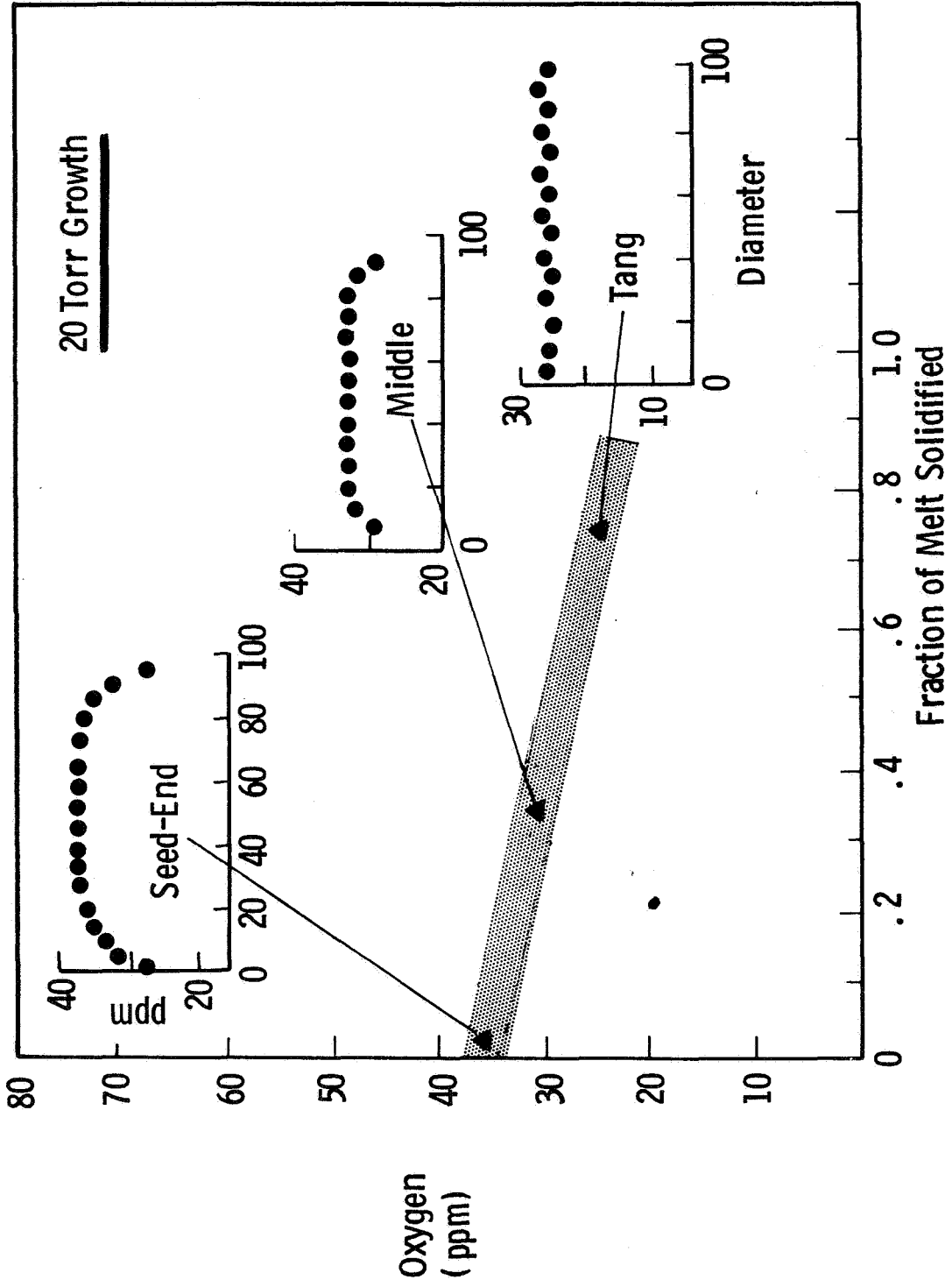
Figure II-40.

Effect Of Magnetic Field On Temperature Fluctuations In Czochralski Si Growth
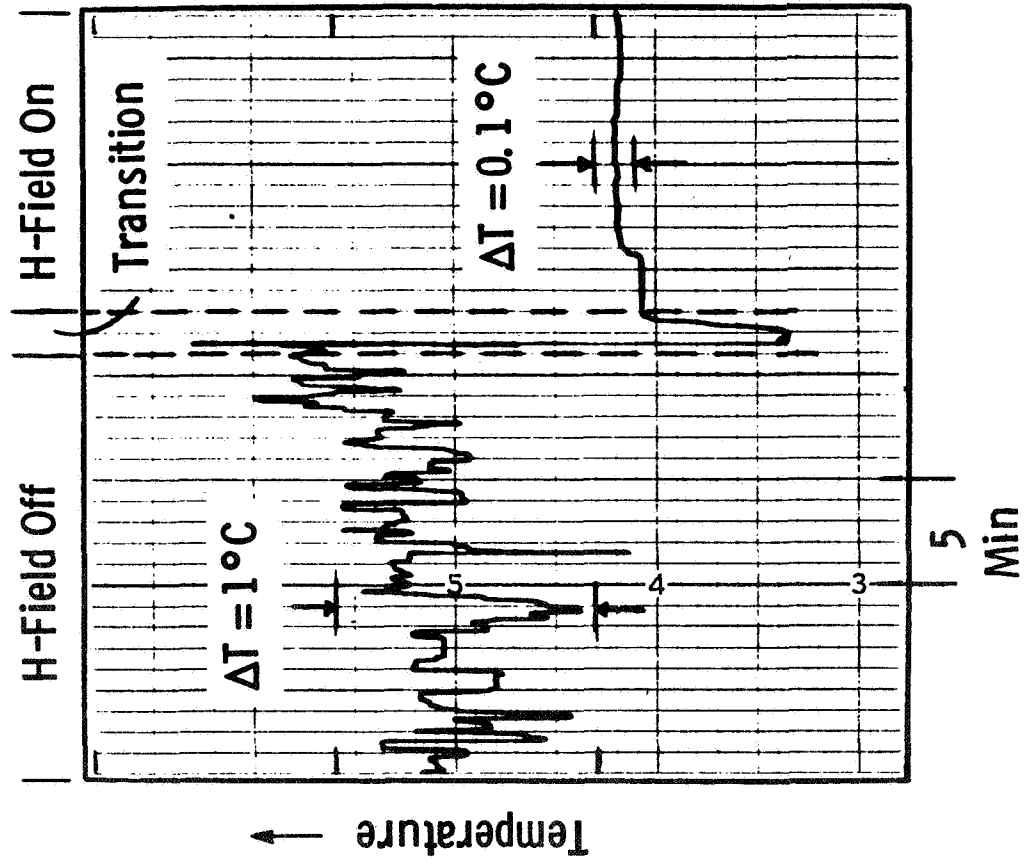
Figure II-41.

EFFECT OF TRANSVERSE MAGNETIC FIELD ON OXYGEN CONTENT
IN CZOCHRALSKI SILICON

Curve 728461-A

<100> - Silicon
45 mm Diameter
Seed 20 rpm
Crucible 0 rpm

Magnetic Field 700 Gauss

Figure II-42.

75
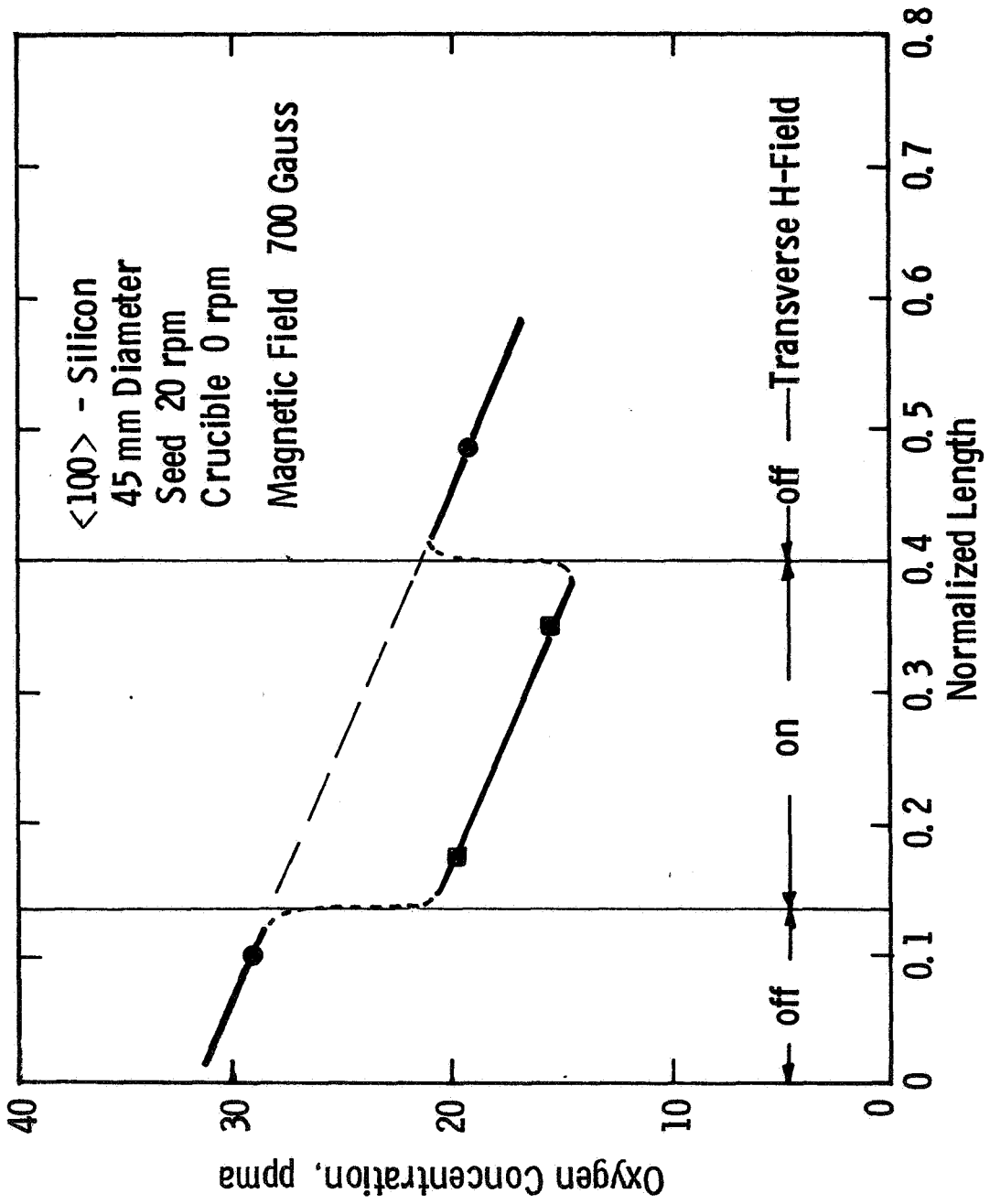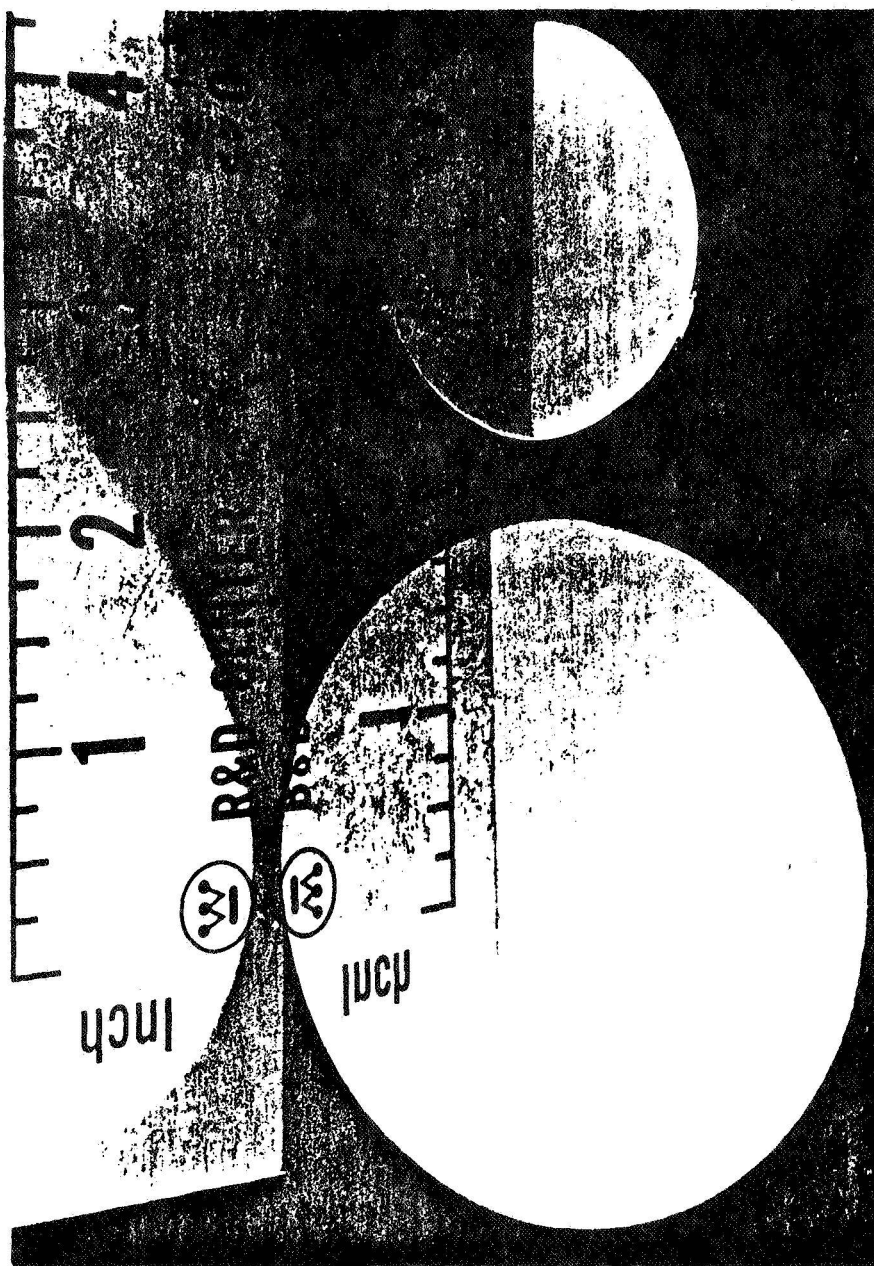
Two- and three-inch diameter GaAs wafers cut from <100>-axially oriented crystals pulled in a Melbourn liquid encapsulated Czochralski puller.

Figure II-43.
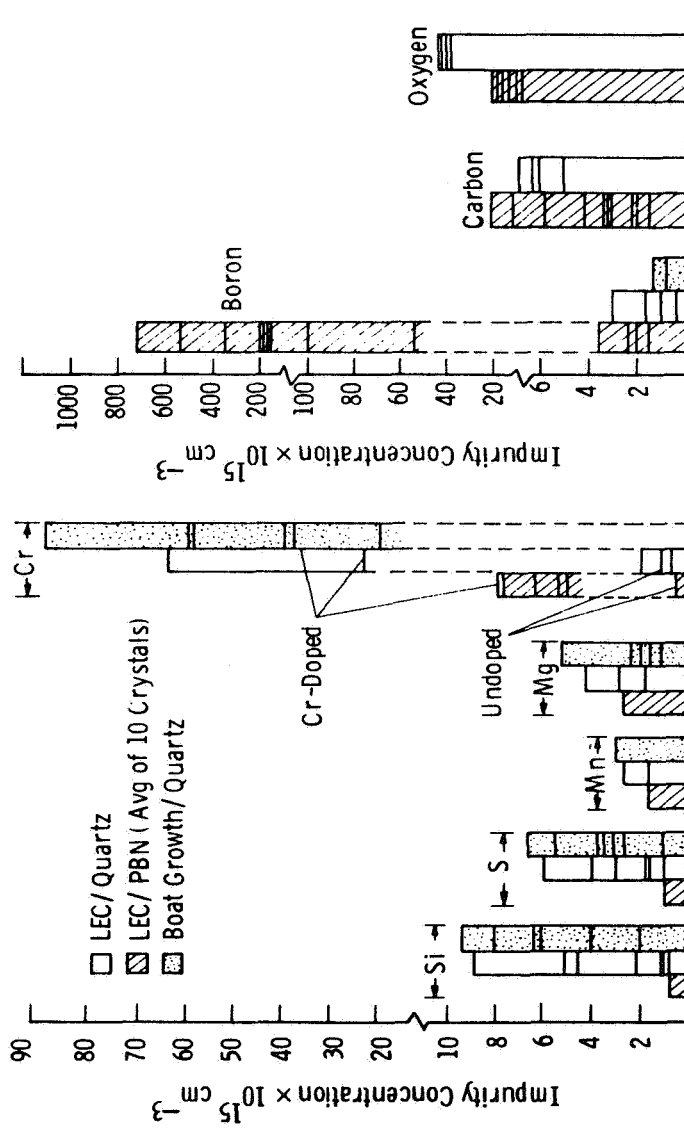
Bulk SIMS analysis of semi-insulating GaAs prepared by LEC and horizontal Bridgeman growth. Note marked reduction of Cr and Si in PBN growth runs. (Note scale discontinuity.)

Figure II-44.

APPARENT MOBILITY VS TOTAL IMPURITY CONTENT FOR N-TYPE SEMI-INSULATING GaAs

Figure II-45.

10 μm

(111)
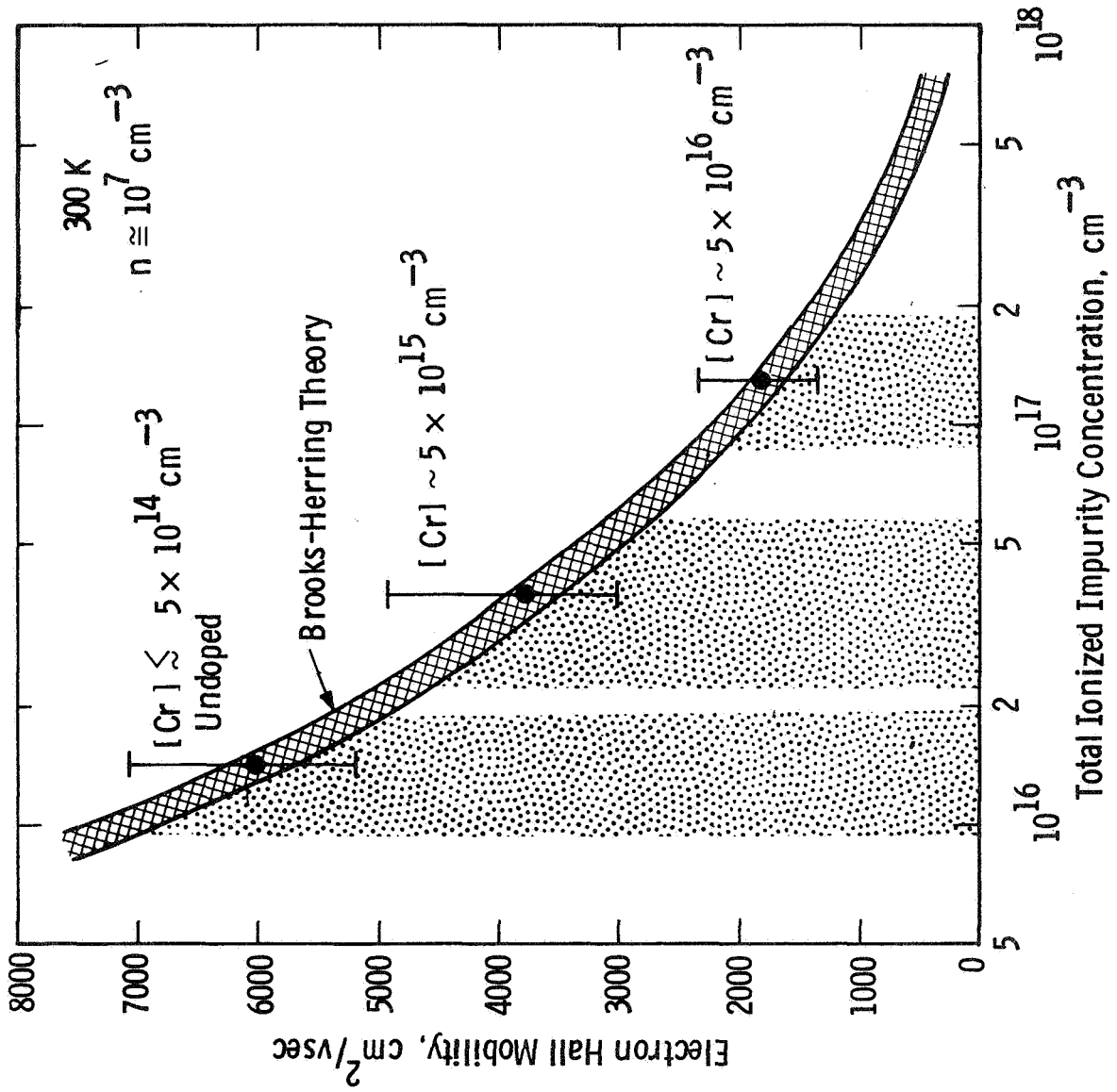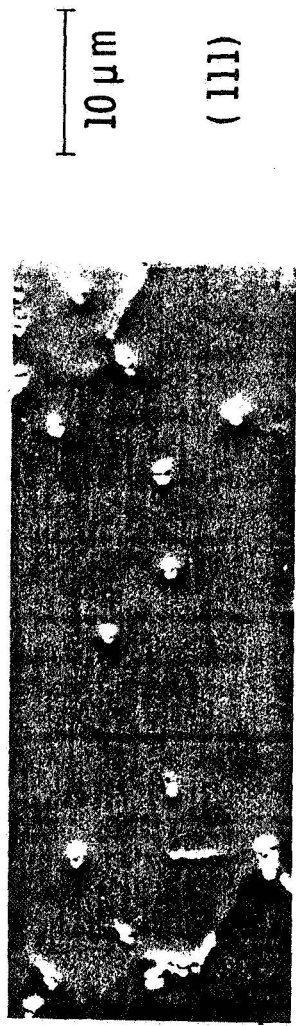
Striations in Semi-Insulating GaAs/PBN.
$\rho \sim 10^7 \, \Omega \, cm.$

(a)

10 μm

(111)
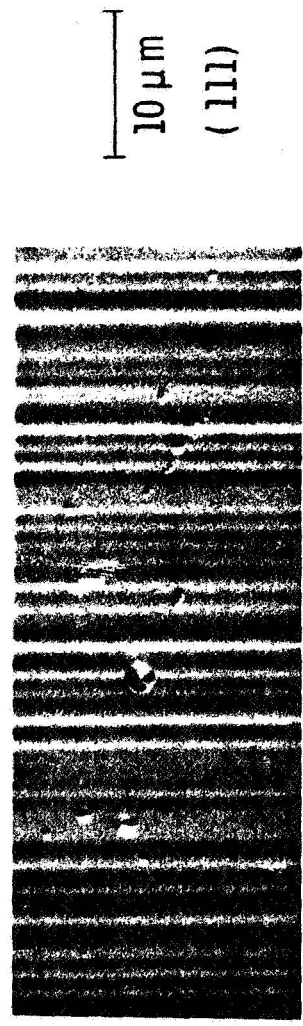
Striations in Si-Doped GaAs/SiO$_2$.
$\rho \sim 0.04 \, \Omega \, cm$

(b)

Longitudinal striations in (100) LEC GaAs crystals.

Figure II-46.

Curve 728667-A
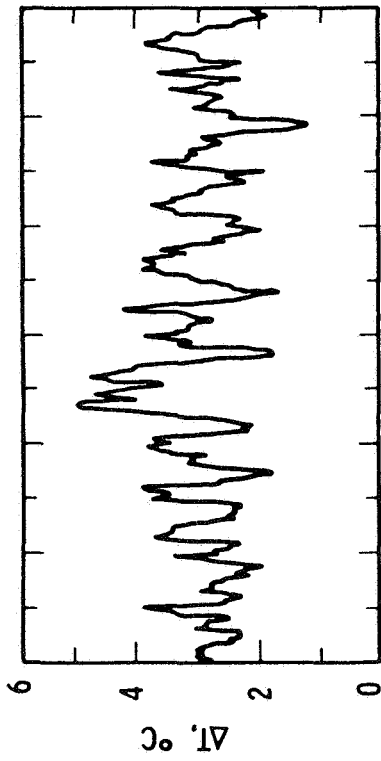
(a) B_2O_3/GaAs
Interface
$\langle \Delta T \rangle = 0.9 \pm 0.7°C$
$f = 10.5$ min^{-1}
$\Delta T_{max} \simeq 3°C$
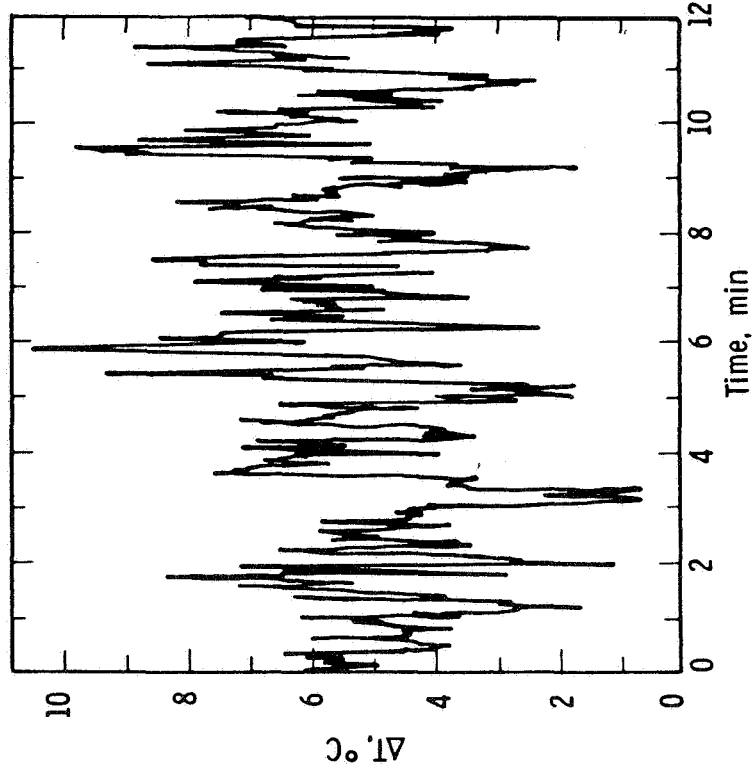
(b) Within GaAs Melt
$\langle \Delta T \rangle = 1.4 \pm 1.2$ °C
$f = 19.7$ min^{-1}
$\Delta T_{max} \simeq 6.0°C$

$^+ B_2O_3$: 600 g
GaAs: 3 Kg
Cruc. Dia: 6-inches

Temperature fluctuations in liquid-encapculated GaAs melt.

Figure II-47.

III. POWER NEEDS IN SPACE

A. POWER REQUIREMENTS FOR SPACE CRYSTAL GROWTH

E. L. Kern
Consultant
Del Mar, CA

The need for power to grow silicon of a size suitable to test and to eventually make into devices must be addressed, so that expected results are tied to power which is available. Of particular interest is the projection of size of float-zone crystals as a function of time. The accompanying graph (from the book "Floating Zone Silicon" by Keller and Muhlbauer) shows that 4 in. (107 mm on graph) will be the normally used diameter by 1985 and 5 in. (125 mm) by 1990. Material to be tested in device lines in this time frame should be 4 in. or more. By analyzing the various power losses, this translated into 25 kW with a 50 percent power efficiency, which is much improved over present RF heating efficiencies. Further development is therefore needed to provide this improvement – a prerequisite to processing in space.

FLOAT-ZONE CRYSTAL DIAMETERS, 1954 TO 1995

Figure III-3.

FLOATING-ZONE SILICON

86

MARSHALL SPACE FLIGHT CENTER	NAME: E. KERN
ORGANIZATION: CONSULTANT	DATE: 9-22-81 III-2

SEQUENCE OF EVENTS LEADING TO SPACE PROCESSING

1. SHOW INITIAL FEASIBILITY IN MEA
   GROUND-BASED RESEARCH + 1 YR. FOR FLIGHT

2. DO GROUND-BASED EXPERIMENTS, ANALYSIS & PREDICTIONS (2 YRS.)

3. DEFINE PHASE C/D (FLIGHT HARDWARE) & FUND (1 YR.)

4. PHASE C/D (FLIGHT HARDWARE DESIGN, BUILDING & QUALIFYING) (2-3 YRS.)

5. INITIAL FLIGHTS & CONFIRMATION ON SHUTTLE OR MEC (1-2 YRS.)

SILICON:
  #2 - 1984
  #3 - 1985
  #4 - 1988 (SHUTTLE)   1991 (MEC)
  #5 - 1989 (SHUTTLE)   1992 (MEC)

Figure III-2.

FLOAT-ZONE CRYSTAL DIAMETERS, 1954 TO 1995

Figure III-3.

FLOAT–ZONE APPARATUS
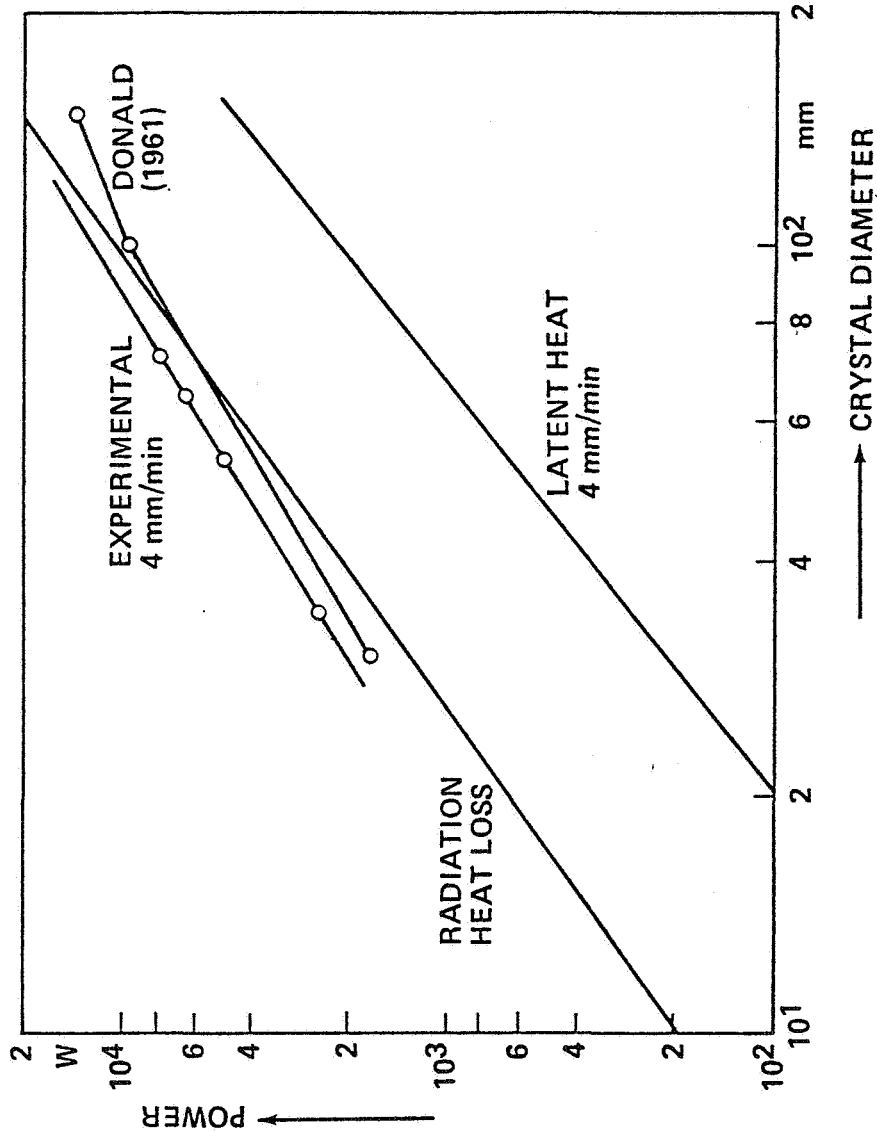
POWER REQUIREMENTS AS CALCULATED AND MEASURED, COMPARED WITH
RATE OF LIBERATION OF LATENT HEAT OF FUSION AT FREEZING INTERFACE

Figure III-4.

ORGANIZATION: CONSULTANT	MARSHALL SPACE FLIGHT CENTER	NAME: E. KERN	
		DATE: 9-22-81	III-6

R.F. ZONING POWER EFFICIENCY

FROM: KELLER & MUHLBAUER "FLOATING ZONE SILICON"

SI DIA.	LATENT HEAT LOSS	RADIATION HEAT LOSS	TOTAL CRYSTAL POWER KW	COIL LOSS	CAPACITOR LOSS	INPUT POWER	% EFF.
1"	.15	.8	.95	~.35	~.15	~3.1	~32%
2"	.6	2.5	4(EXP.)	1.7	.5	12	33%
3"	1.5	6	7.5			22.5	33%
4"	2.2	10.5	13			26	50%*
5"	3	15	18			36	50%

*ASSUMES 50% EFFICIENCY IMPROVEMENT THROUGH DEVELOPMENT EFFORTS.

Figure III-5.

B. ELECTRIC POWER NEEDS IN SPACE

Donald M. Waltz
TRW
Redondo Beach, CA

Mr. Don Waltz of TRW's Defense and Space Group presented the power requirements for some specific float-zone experiments in space. He also gave the present available power figures for the Space Shuttle and some projected available power for advanced vehicles. The details are shown in the following figures.

FLOAT ZONE ELECTRIC POWER NEEDS IN SPACE

TOPICS

I. POWER REQUIREMENTS

- SILICON
- CADMIUM TELLURIDE

II. POWER AVAILABLE

- SPACE SHUTTLE
- ADVANCED VEHICLES

III. CONCLUSIONS

Figure III-6.

FLOAT ZONE PROCESSING ELECTRIC POWER

INPUT ELECTRIC POWER FOR FZ (P_{el})

n_p

ELECTRIC POWER CONDITIONING

loss=$P(1-n_p)$

n_c

ELECTRICAL ENERGY CONVERSION TO HEAT ENERGY

loss=$Pn_p(1-n_c)$

$n_a = n_f \times n_e$

FOR RADIANT HEATING METHODS

ABSORPTION OF HEAT ENERGY BY FZ SAMPLE

loss=$Pn_pn_c(1-n_a)$

CONDUCTION LOSS FROM ENDS OF MOLTEN ZONE

RADIATION LOSS FROM CIRCUMFER-ANCE OF MOLTEN ZONE

HEAT LOAD REQUIRED FOR PROCESSING FZ SAMPLE (P)

$$P_{el} = \frac{P}{n_{Total}}$$

$$n_{Total} = n_p \times n_c \times n_a$$
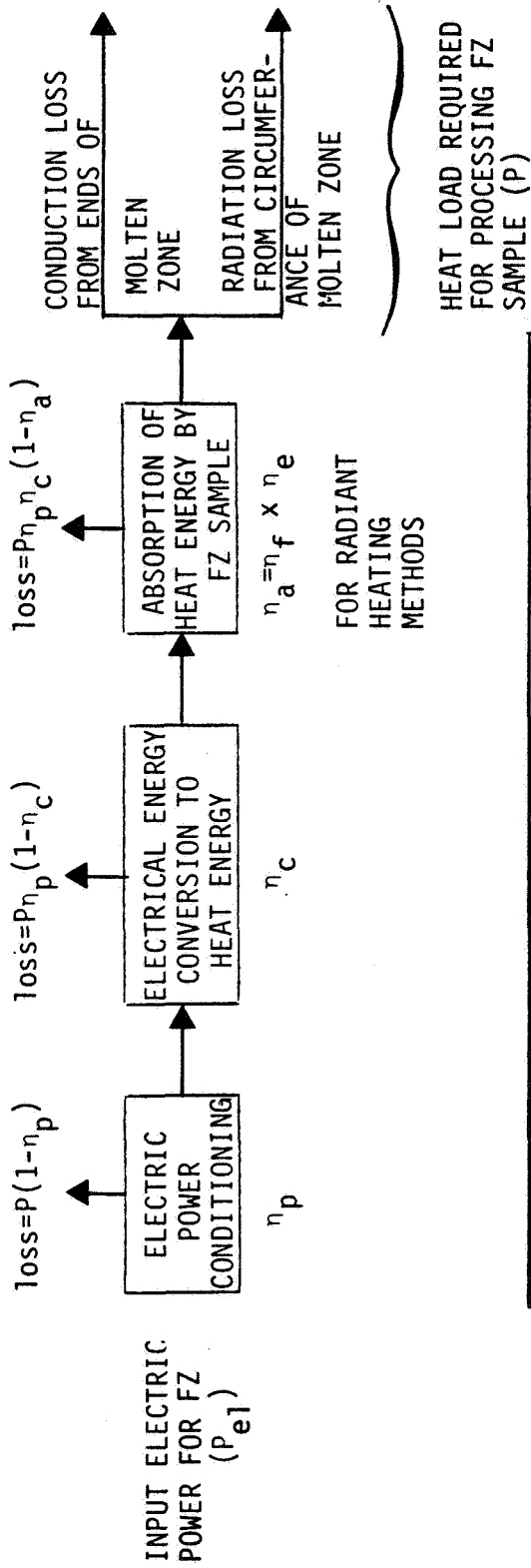
$$P = \frac{2K\pi d^2}{4}\frac{\partial T}{\partial x} + \epsilon\pi dl\sigma T_o^4$$

K = THERMAL CONDUCTIVITY
d = SAMPLE DIAMETER
ϵ = EMISSIVITY
l = MOLTEN ZONE LENGTH
σ = BOLTZMANN'S CONSTANT
T = PROCESS TEMPERATURE

$\frac{\partial T}{\partial x}$ = TEMPERATURE GRADIENT AT ZONE BOUNDARY

Figure III-7.

POWER CONVERSION EFFICIENCIES

FOR A Ge SAMPLE, 2.54 cm dia, 1/d OF THE MOLTEN ZONE=1, AND THE SHUTTLE-SPACELAB POWER SUPPLY

HEATING METHOD	TYPE OF POWER REQUIRED	ELECTRIC POWER CONDITIONING η_p	ELECTRICAL ENERGY CONVERSION TO HEAT ENERGY η_c	ABSORPTION OF HEAT ENERGY BY SAMPLE η_a	η_{total}
1) RADIANT HEATING FROM AN INCANDESCENT SOURCE	28 VOLTS DC	1.0	0.88	$\eta_f=0.68; \eta_e=0.25$ 0.17	0.15
2) INDUCTION HEATING	200-400 VOLTS AC 400 Hz TO 10 KHz	FOR FREQUENCY OF 400 Hz $\eta_p=0.9$	0.31	0.95	0.28
		FOR FREQUENCY OF 10 KHz $\eta_p=0.8$	0.88		0.70
3) ELECTRON BOMARDMENT HEATING	10,000 VOLTS DC	0.5 max		$\eta_c \times \eta_a = 0.80$	0.4
4) RADIANT HEATING FROM A LASER SOURCE	DEPENDS ON TYPE OF LASER CHOSEN	DEPENDS ON TYPE OF LASER CHOSEN <1	~ 0.05 (EXCEPT FOR CHEMICAL LASER)	$\eta_f=0.9; \eta_e=0.2$ 0.18	<0.01

Figure III-8.

DATA USED FOR POWER VS. SAMPLE DIAMETER CALCULATIONS

—————— MATERIAL PROCESSED ——————

PARAMETER	SILICON	GERMANIUM	CADMIUM TELLURIDE
1. MELTING POINT	1410°C (1683°K)	937°C (1205°K)	1098°C (1371°K)
2. TEMPERATURE OF MOLTEN ZONE	1725°K	1250°K	1425°K
3. EMISSIVITY OF LIQUID	0.3	0.2	0.05
4. THERMAL CONDUCTIVITY	0.25 watts/cm$^\circ$C	0.16 watts/cm$^\circ$C	0.02 watts/cm$^\circ$C
5. TEMPERATURE GRADIENT ZONE BOUNDARY	-250°C/cm	250°C/cm	250°C/cm
6. ZONE LENGTH/DIAMETER RATIO	1 FOR d LESS THAN 2 cm; THEN FOR d GREATER THAN 2 cm, l=2 cm CONSTANT	1	1

Figure III-9.

HOST VEHICLE FLOAT ZONE POWER BUDGETS

VEHICLE	POWER AVAILABLE TO FZ PAYLOAD WATTS	—	PAYLOAD SUBSYSTEMS POWER TO SUPPORT THE PROCESSING WATTS	=	POWER AVAILABLE TO HEAT SAMPLE WATTS
CURRENT					
Space Shuttle Mid Deck	300 to 400		200		100 to 200
Space Shuttle Spacelab	1350 to 1750		750		600 to 1000
Space Shuttle Pallet	3750 to 5250		750		3000 to 4500
IN DEFINITION					
Initial Materials Experiment Carrier (MEC) Attached to the Early Space Platform (SP) (1987)	6750 to 13000		1500		5250 to 11500
Growth MEC/SP (Early 1990's)	6750 to 25000		1500		5250 to 23500
Evolutionary MEC Vehicles and Space Platforms (> 2000)	?		?		?

Figure III-10.

Figure III-11.

95
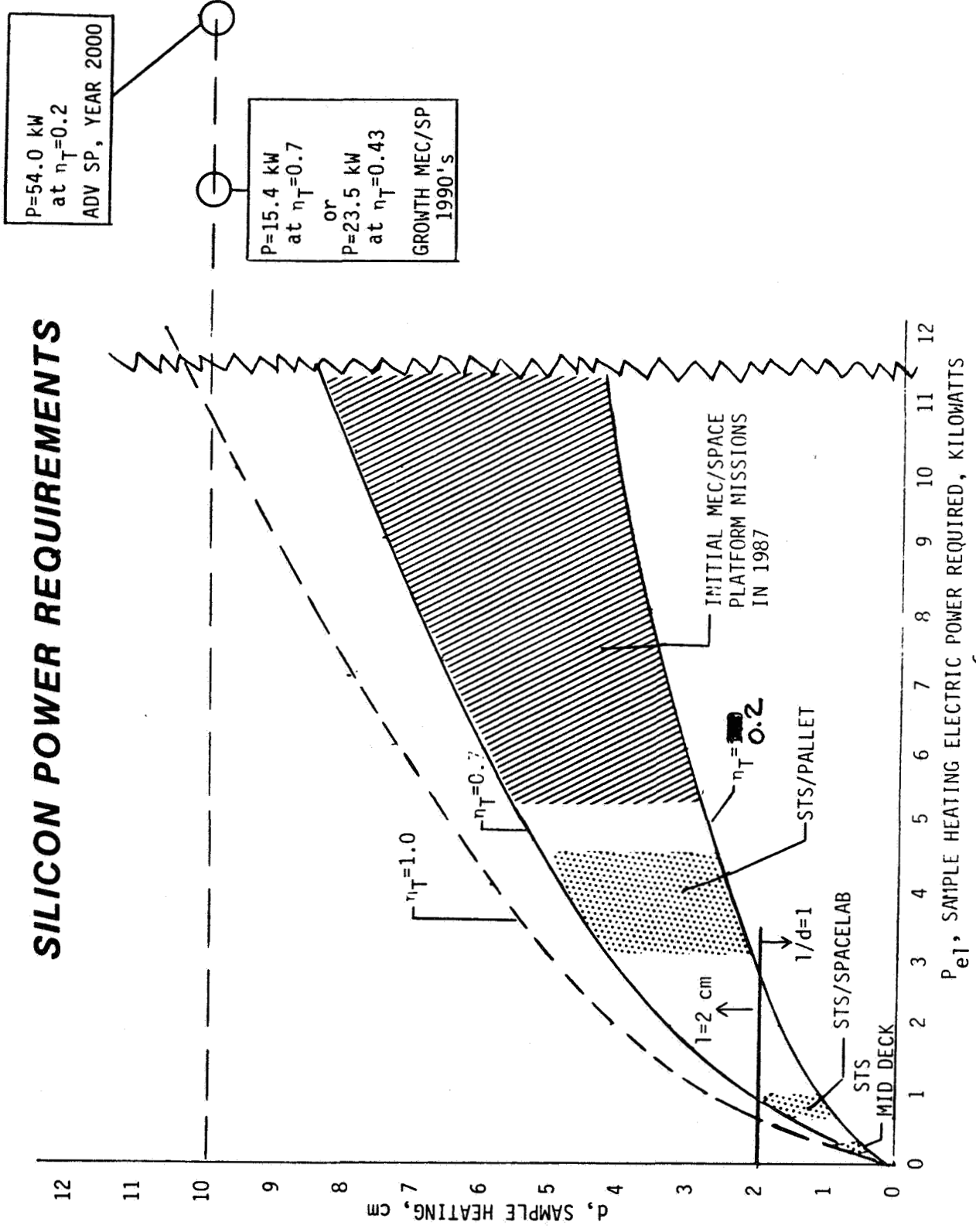
GERMANIUM POWER REQUIREMENTS
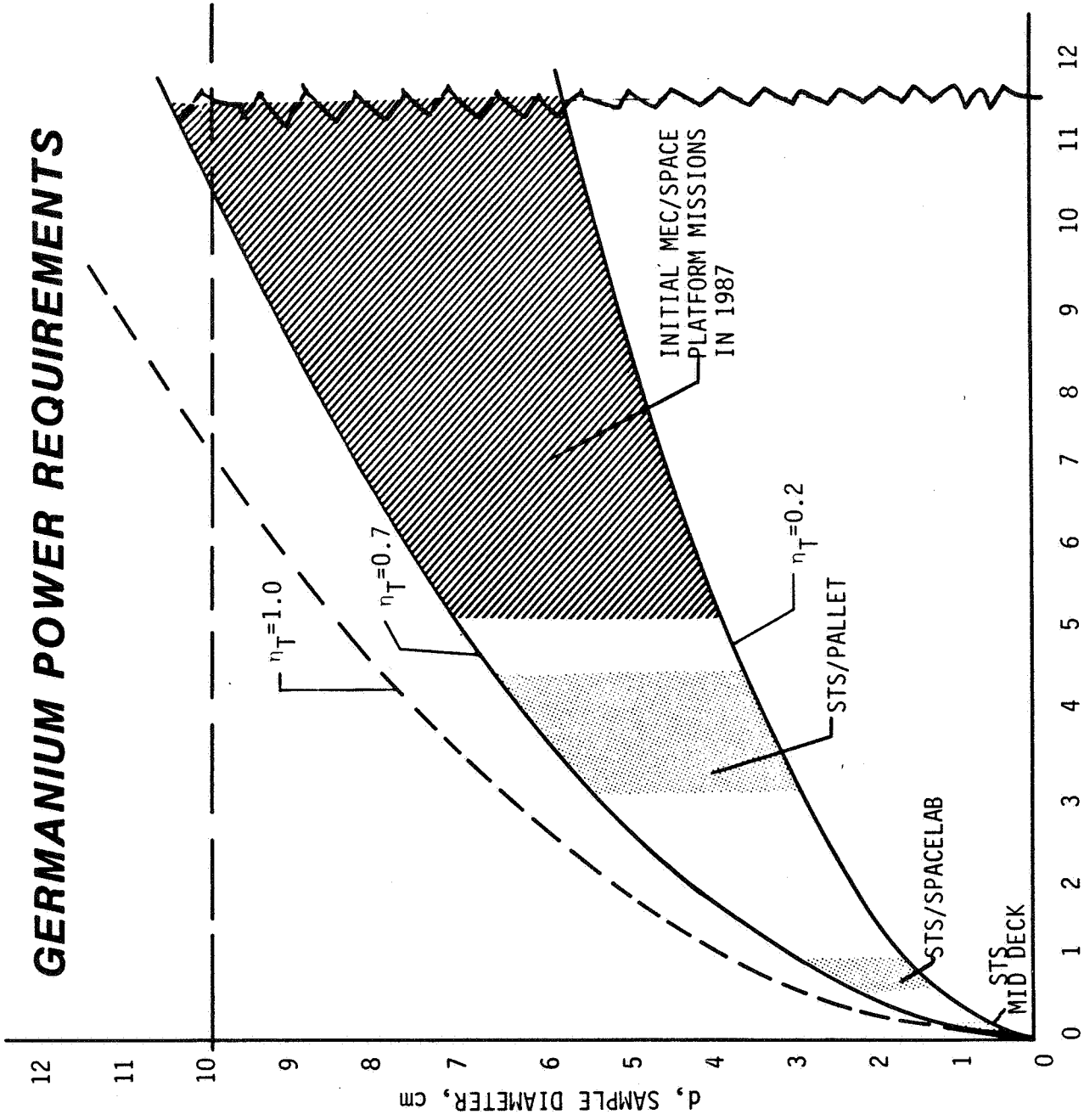
Figure III-12.

P_{el}, SAMPLE HEATING ELECTRIC POWER REQUIRED, KILOWATTS

d, SAMPLE DIAMETER, cm

$\eta_T = 1.0$

$\eta_T = 0.7$

$\eta_T = 0.2$

INITIAL MEC/SPACE PLATFORM MISSIONS IN 1987

STS/PALLET

STS/SPACELAB

STS MID DECK

CADMIUM TELLURIDE POWER REQUIREMENTS

Figure III-13.

SUMMARY

-----THE FOLLOWING POWER RELATED TRENDS WERE DERIVED FROM THIS BRIEF ANALYSIS------

1. FLOAT ZONE PROCESSING OF UP TO 5 CENTIMETERS DIAMETER SILICON AND 16.0 CENTIMETERS DIAMETER CADMIUM TELLURIDE CAN BE CONDUCTED ON SHUTTLE PALLET MISSIONS, ASSUMING A TOTAL HEATING EFFICIENCY OF 70%.

2. FLOAT ZONE PROCESSING OF UP TO 8.5 CENTIMETERS DIAMETER SILICON FOR 70% TOTAL HEATING EFFICIENCY CAN BE CONDUCTED ON THE PLANNED INITIAL MEC/SPACE PLATFORM. SILICON PROCESSING AT 10 CENTIMETERS DIAMETERS FOR 70% MUST BE PROGRAMMED FOR THE GROWTH MEC/SPACE PLATFORM VEHICLE.

3. HOST VEHICLE POWER AVAILABLE FOR FLOAT ZONE SAMPLE HEATING:

   - UP TO 4.5 kW FOR SHUTTLE - PRESENT
   - UP TO 11.5 kW FOR INITIAL MEC/EARLY SPACE PLATFORM - PLANNED FOR LATE 1980's
   - UP TO 23.5 kW FOR ALL-UP MEC/GROWTH SPACE PLATFORM - MAYBE EARLY 1990's

4. INDUCTION HEATING LOOKS TO BE THE MOST PROMISING CANDIDATE HEATING METHOD, BUT THE HEATING COIL MUST BE DESIGNED MATCHED TO MATERIAL TYPE AND DIAM-ETER AND TO HOST VEHILCE POWER SUPPLY CHARACTERISTICS.

5. OTHER FACTORS THAT WILL INFLUENCE HEATING METHOD SELECTION ARE PROCESS CONTROL AND EASE OF EQUIPMENT INTEGRATION INTO THE HOST VEHICLE

Figure III-14.

C. THE HISTORICAL TREND IN FLOAT-ZONE CRYSTAL DIAMETERS AND POWER REQUIREMENTS FOR FLOAT-ZONED SILICON CRYSTALS

Horst G. Kramer
Monsanto Industrial Chemicals Co.
St. Peters, MO

Mr. Kramer presented an alaysis of the power needed to zone silicon crystals by RF heating. The heat loss mechanisms are analyzed in the following figures. Curves are then given for power as a function of crystal diameter for commercial silicon zoning.
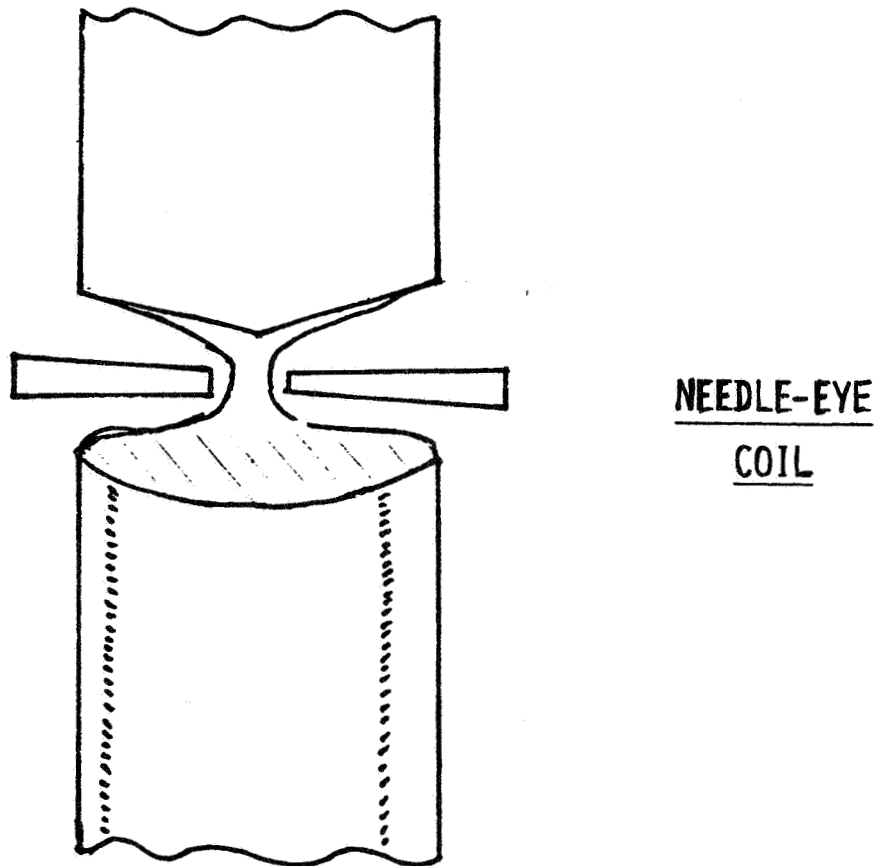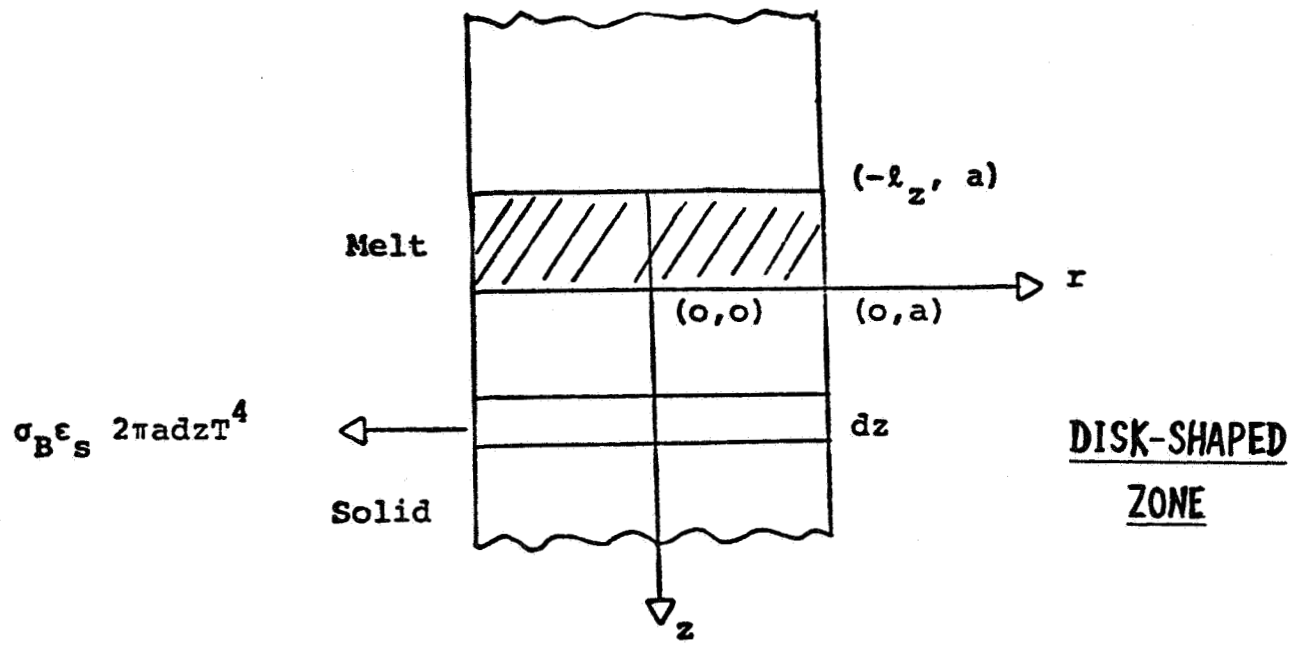
Figure III-15.

Conduction Losses

The power into the solid over the surface $z = o$ (solid-melt interface) is:

$$P_{cond} = \int_{o}^{a} -k_s \left(\frac{\partial T}{\partial z}\right)_{z = o} 2\pi r dr \qquad (II-1)$$

This is the heat loss from the melt via conduction through the solid.

Neglecting radial temperature gradients, the one-dimensional steady state heat conduction equation is:

$$\frac{d}{dz}\left(k_s \frac{dT}{dz}\right) + q''' = 0 \qquad (II-2)$$

The heat loss per unit volume due to radiation from the surface is:

$$q''' = - \frac{\sigma_B \epsilon_s 2\pi a dz T^4}{\pi a^2 dz} \qquad (II-3)$$

Thus,

$$\frac{d}{dz}\left(\frac{1}{T}\frac{dT}{dz}\right) = \frac{2 \sigma_B \epsilon_s}{k_m T_m a} T^4$$

where the expression $k_s = \frac{k_m T_m}{T}$ has been used for silicon.

Assuming $T = T_m$ at $z = o$

$$\frac{dT}{dz} = T = o \quad \text{at } z = \infty$$

Then,

$$\frac{dT}{dz} = -\left(\frac{\sigma_B \epsilon_s}{k_m T_m a}\right)^{\frac{1}{2}} T^3 \qquad (II-4a)$$

$$\frac{dT}{dz} = -\left(\frac{\sigma_B \epsilon_s}{k_m T_m a}\right)^{\frac{1}{2}} \left[2\left(\frac{\sigma_B \epsilon_s}{k_m T_m a}\right)^{\frac{1}{2}} z + T_m^{-2}\right]^{-3/2} \qquad (II-4b)$$

$$T = \left[2\left(\frac{\sigma_B \epsilon_s}{k_m T_m a}\right)^{\frac{1}{2}} z + T_m^{-2}\right]^{-\frac{1}{2}} \qquad (II-5)$$

The power by conduction is found from eqs. (II-1) and (II-4a)

$$\boxed{P_{cond} = \pi \left(\sigma_B \epsilon_s k_m T_m^5\right)^{\frac{1}{2}} a^{3/2}} \qquad (II-6)$$

Figure III-16.

Radiation Losses from the Liquid

For the vertical surface:

$$P_{rad}(V) = 2\pi \ \ell_z \ (\sigma_B \ \epsilon_\ell \ T_m^4) \ a \qquad\qquad \text{II-7}$$

where ℓ_z = zone length, cm

For the horizontal surface:

$$P_{rad}(H) = \pi(\sigma_B \ \epsilon_\ell \ T_m^4) \ a^2 \qquad\qquad \text{II-8}$$

Contribution of Latent and Specific Heats

$$P_L = 4.18 \ \pi dLva^2 \qquad\qquad \text{II-9}$$

$$P_H = 4.18 \ \pi dC_p \Delta Tva^2 \qquad\qquad \text{II-10}$$

where v = zone travel in cm/sec.

Total Power Requirements

For disk-shaped zone

$$P(disk) = 2P_{cond} + P_{rad} \ (V) + P_L + P_H \qquad\qquad \text{II-11}$$

and for zone formed by needle-eye coil

$$P(needle\text{-}eye) = P(disk) + 2P_{rad} \ (H) \qquad\qquad \text{II-12}$$

Figure III-16. Concluded.

102

THE VALUES OF THE CONSTANTS USED

Emissivity, solid: $\qquad\qquad\qquad\qquad$ $\varepsilon_s = 0.46$

Emissivity, liquid: $\qquad\qquad\qquad\quad$ $\varepsilon_\ell = 0.3$

Melting temperature: $\qquad\qquad\qquad$ $T_m = 1685°K$

Thermal conductivity, solid: $\qquad\quad$ $k_s = \dfrac{k_m T_m}{T}$

Thermal conductivity, solid, at T_m: $\quad$ $k_m = 0.216 \ w/cm°K$

Latent heat of fusion: $\qquad\qquad\qquad$ $338 \ cal/g$

Specific heat, average: $\qquad\qquad\quad$ $C_p = 0.23 \ cal/g°K$

Stefan-Boltzman constant: $\qquad\quad$ $\sigma_B = 5.729 \times 10^{-12} \ w/cm^2°K^4$

Figure III-17.

Figure III-18.

POWER REQUIRED FOR
NEEDLE-EYE COIL,
ZONE TRAVELLING AT
4 MM/MINUTE.

o SIEMENS

△ MONSANTO

POWER, KW

ZONE
LENGTH = A

LATENT HEAT OF
FUSION, AT
4 MM/MINUTE

CRYSTAL DIAMETER, CM

Figure III-19.

THE TREND IN FLOAT-ZONE CRYSTAL DIAMETERS

CRYSTAL DIAMETER, MM

SOURCES: MONSANTO
SHIN-ETSU

SIEMENS
WACKER
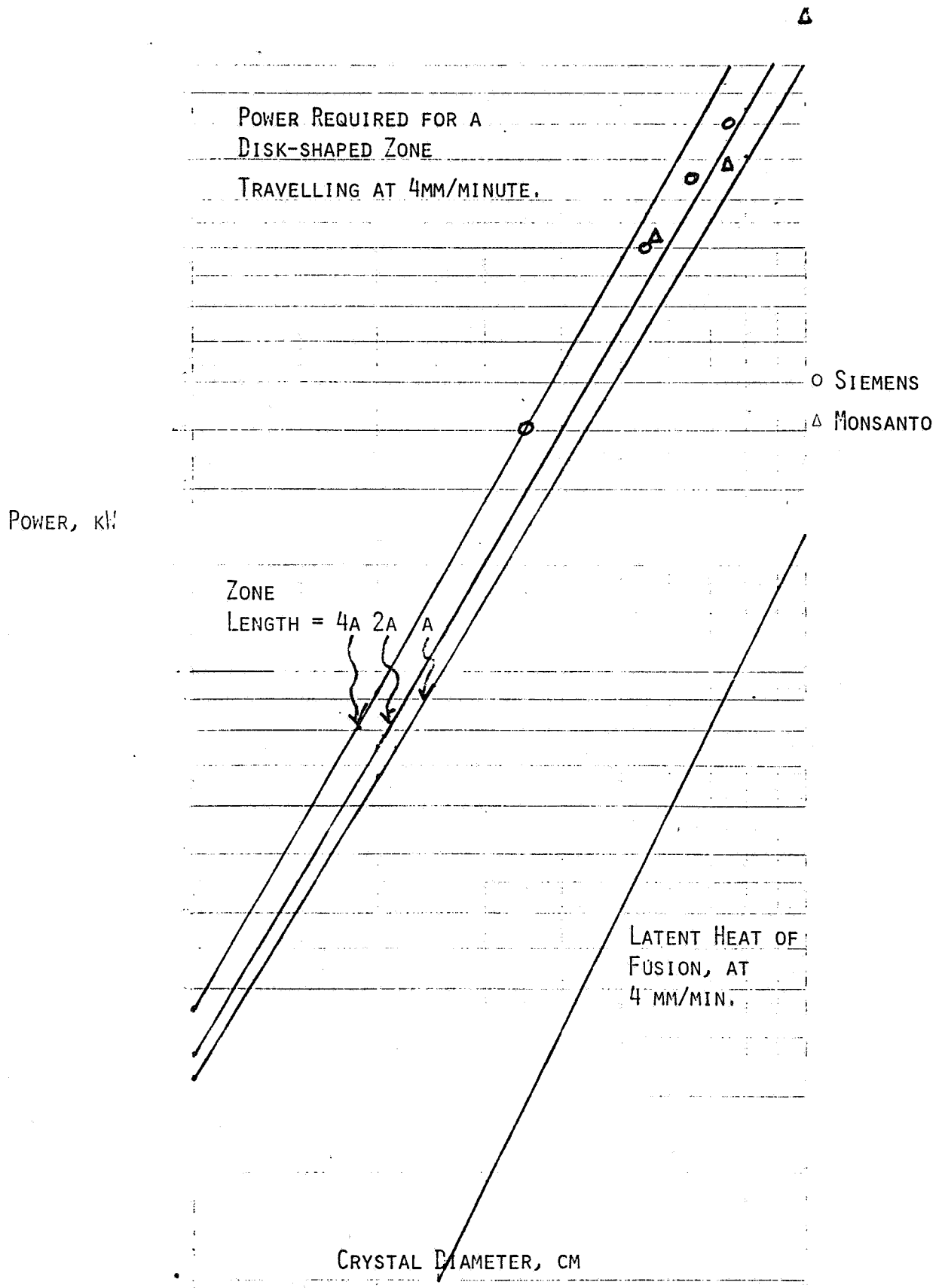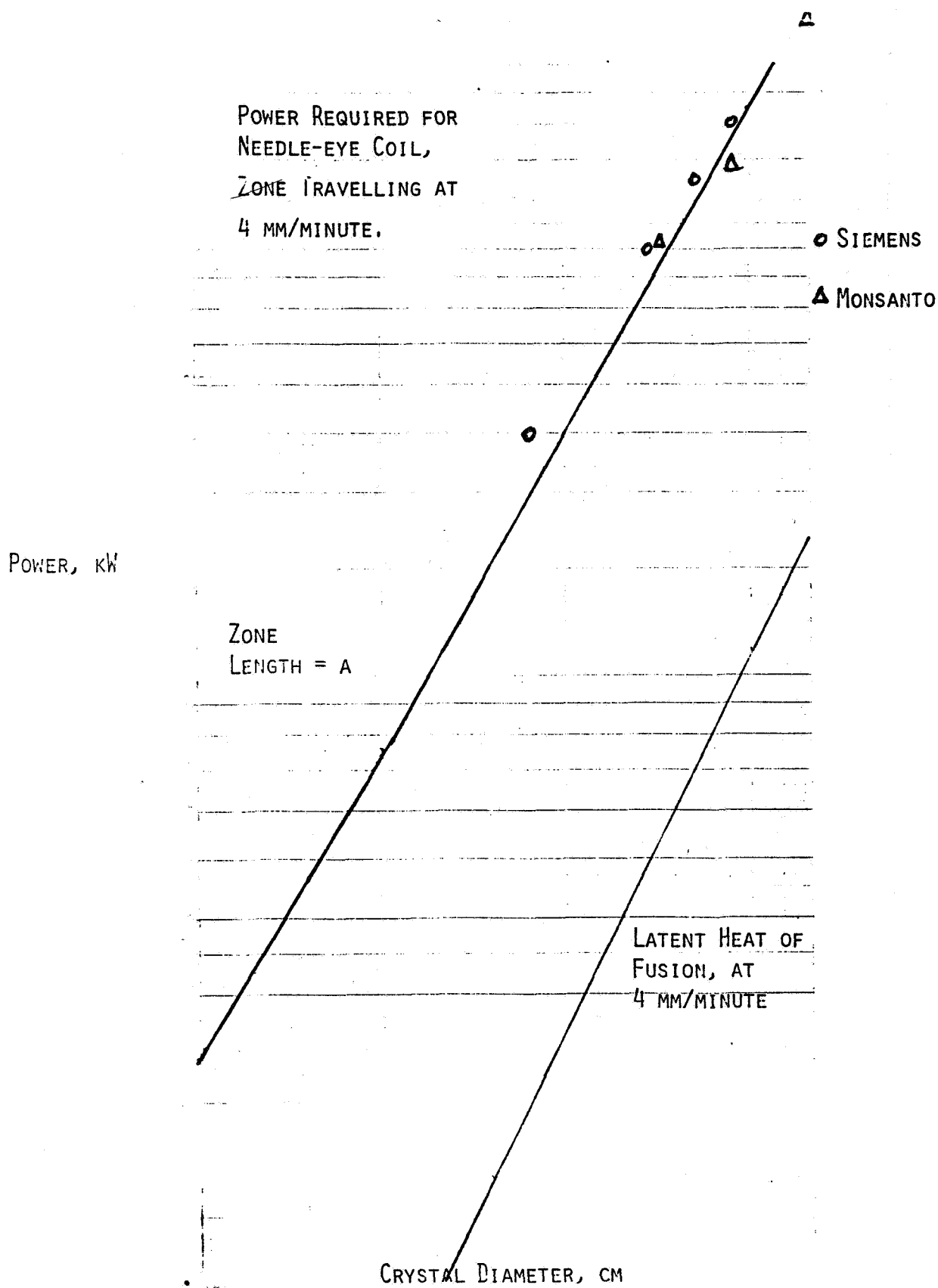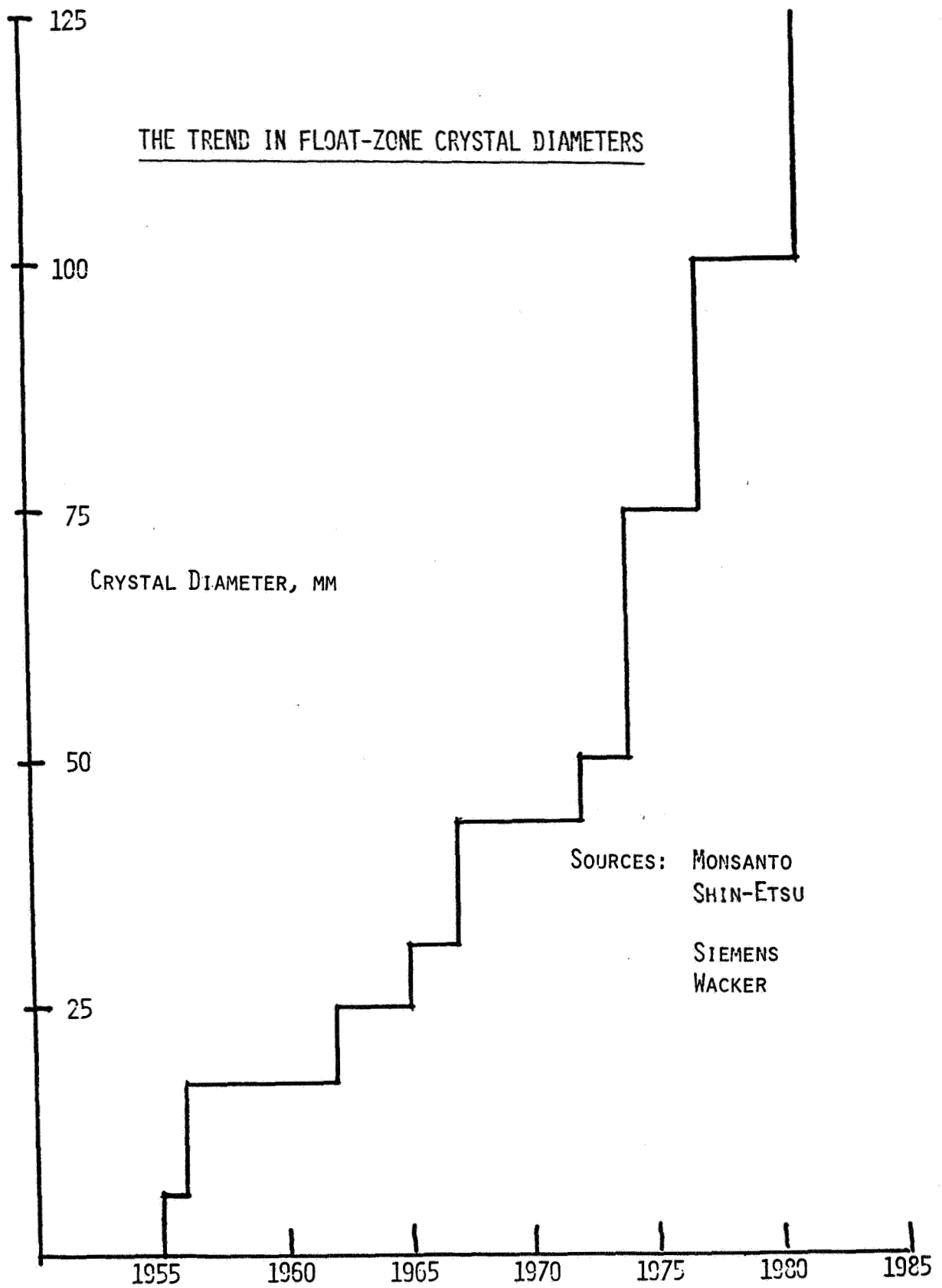
Figure III-20.

IV. GROUND BASED RESEARCH AND MEA
EXPERIMENT SUGGESTIONS

A. SCHEDULE FOR EXPERIMENT PROGRAM DEVELOPMENT

Iva C. Yates
NASA-MSFC
Huntsville, AL

Mr. Yates from the Materials Processing in Space Project Office presented the major phases of the development of facility class experiment hardware. Times typically required for both science working group and project activities are shown in the following figure.

GENERAL SCHEDULE FOR EXPERIMENT PROGRAM DEVELOPMENT

DEFINITION OF OBJECTIVES

WORKING GROUP ACTIVITIES

   REVIEW & ANALYSIS OF OBJECTIVES

   RECOMMEND CONCEPTS/APPROACHES

   DEFINE REQMTS FOR SRT/EXP

   REVIEW STUDY RESULTS/DESIGN CONCEPTS

   REVIEW SRT/EXP PROGRESS & RESULTS

MPS PROJECT ACTIVITIES

SRT/TECHNOLOGY DEVELOPMENT

ADVANCED STUDIES (ØA) FZPS

   DEFINITION OF CONCEPTS

   DEFINITION STUDY (ØB) FZPS

   SELECT SINGLE APPROACH

   PRELIMINARY DESIGN

   DEVELOP PROJECT COST

   REQUEST NEW START

   PROCUREMENT

DESIGN & DEVELOPMENT (Ø C/D) FZPS

INTEGRATION

FLIGHT

PRECURSOR EXPERIMENTS (MEA)

   DESIGN & DEVELOPMENT

   FLIGHT

Figure IV-1.

B.   GROUND BASED SILICON ZONING PROGRAM

E. L. Kern
Consultant
Del Mar, CA

The purpose and goals of the ground-based investigation phase A/B of the experimental float-zoning of silicon is given in the following figures.   The overall program goals, leading to recommending experiments to be done in phase C/D are spelled out.   Figure IV-4 lists the program content of the contract with Westech Systems, Inc., to start shortly (actual start date was November 17, 1981, and runs for 6 months).   Figure IV-7 is a list of thermophysical properties which must be accurately known if thermophysical models can be compared to experimental zoning of silicon.

ORGANIZATION:	MARSHALL SPACE FLIGHT CENTER	NAME:
CONSULTANT		E. KERN
		DATE: 9/23/81 V-1

GROUND-BASED SILICON ZONING PROGRAM

PURPOSE: PROVIDE FULL GROUND-BASED EXPERIMENTS, ANALYSIS AND HARDWARE FEASIBILITY IN PREPARATION OF BUILDING FLIGHT HARDWARE AND CARRYING OUT EXPERIMENTS IN SPACE.

END GOAL: FULLY CHARACTERIZE THE FLOAT ZONE PROPERTIES OF GROWING SILICON AT $G = 1$, WITH ANALYSIS AND PREDICTIONS OF THE CHARACTERISTICS AT $G \approx 0$. SHOW FEASIBILITY OF GROWTH, CONTROL AND ANALYSIS TO BE DONE IN SPACE AND SPECIFY FLIGHT-HARDWARE DESIGN. RECOMMEND EXPERIMENTS TO BE DONE IN SPACE IN PHASE C/D.

Figure IV-2.

CONSULTANT

SILICON ZONING PROGRAM - SPECIFIC GOALS

1. MODEL AND ANALYZE THE THERMOPHYSICAL NATURE (STEADY STATE AND DYNAMIC) OF A SILICON FLOATING ZONE, INCLUDING BOUYANCY DRIVEN MELT CONVECTION, SURFACE TENSION-DRIVEN SURFACE CONVECTION AND HEAT FLOW

2. PREDICT IMPROVEMENTS IN GROWTH CHARACTERISTICS AND PHYSICAL PROPERTIES AND WAYS TO BETTER CONTROL GROWTH CONDITIONS

3. INVESTIGATE THE BEST HEATING METHODS, IN TERMS OF HEATING PROFILE, POWER EFFICIENCY AND CONTROL, AND SHOW WORKABILITY OF THE BEST METHOD

4. DO THE NECESSARY ANALYTICAL MEASUREMENTS ON THE ZONING SYSTEM AND GROWN CRYSTALS, AND INDICATE WHAT MEASUREMENTS ARE NECESSARY IN SPACE AND SHOW WORKABILITY OF HARDWARE

5. DEVELOP HARDWARE TO THE POINT OF SPECIFIYING FLIGHT HARDWARE DESIGN, INCLUDING ALL CONTROLS, AUTOMATION AND PROGRAMMING AND SHOWING THE RELIABILITY OF SUBSYSTEMS UNDER CONDITIONS SIMILAR TO SPACE

Figure IV-3.

ORGANIZATION:	MARSHALL SPACE FLIGHT CENTER	NAME:
CONSULTANT		F. KERN V-3
		DATE: 9/23/81

SILICON ZONING PROGRAM - PERIOD 1

OUTLINE   OCTOBER 1981 - FEBRUARY 1982

1. PROCURE AND INSTALL A VACUUM/GAS R.F. ZONER (BREADBOARD ZONER) TO
    PROVIDE THE ZONING CAPABILITY TO DO ALL GROUND-BASED ZONING,
    PROVIDING AN ENVELOPE FOR IN-ZONE ANALYTICAL MEASUREMENTS AND
    CHECKING FEASIBILITY OF ZONER HARDWARE DEVELOPMENTS

2. DESIGN AND CONSTRUCT CHANGES IN R.F. COIL DESIGN TO MINIMIZE
    ROTATIONAL STRIATION CAUSE

3. RECOMMEND AND PLAN EXPERIMENTS FOR EARLY MEA FLIGHTS

Figure IV-4.

ORGANIZATION:	MARSHALL SPACE FLIGHT CENTER	NAME:
CONSULTANT		E. KERN
		DATE: 9/23/81 V-6

THERMAL FLUCTUATION STUDY

PURPOSE: STUDY THE NATURE OF PERIODIC AND NONPERIODIC THERMAL-MELT
FLUCTUATIONS AND PREDICT WAYS OF CONTROLLING

STUDY: 1. CHANGE COIL DESIGNS TO MINIMIZE MAGNITUDE OF ROTATIONAL
STRIATIONS AND PREDICT EFFECT AS ZONE LENGTH INCREASES TO πD

2. STUDY TRANSIENT THERMAL FLUCTUATIONS AND PREDICT WAYS OF
CONTROLLING: BOUYANCY OR MARANGONI?

F (ROTATIONAL RATE), RAYLEIGH NO.

3. MEASURE BY: STRIATION ETCHING, SPREADING RESISTANCE (I.R.)

Figure IV-5.

ORGANIZATION:

MARSHALL SPACE FLIGHT CENTER

NAME: E. KERN

DATE: 9/23/81   V-8

CONSULTANT

STUDIES OF ZONE STABILITIES

STUDY EFFECT OF INTERFACE SHAPE AND ISOTHERMS TO

A. STABILITY OF ZONE

B. THERMAL STRESS PROFILE AND DEFECT FORMATION

C. SHOW EFFECT OF R.F. FIELD (MIXING AND LEVITATION/PINCHING)

Figure IV-6.

ORGANIZATION: MARSHALL SPACE FLIGHT CENTER	NAME: E. KERN
CONSULTANT	DATE: 9/23/81 V-9

PHYSICAL PROPERTIES OF SILICON SOLID AND MELT

PROPERTY	VALUE	REFERENCE
SOLID		
THERMAL COND.	—	
THERMAL EXPANSION		
EMISSIVITY	~.68	
REFRACTIVE INDEX	3.45 (1.9μ,26°C)	(NEUBURGER)
RESISTIVITY	—	
MELT		
THERMAL CON.		
THERMAL EXPANSION	1.43 x 10^{-4} K^{-1}	CARRUTHERS
EMISSIVITY	~.3	
REFRACTIVE INDEX		
RESISTIVITY		
VISCOSITY	3 x 10^{-3} cm^2s^{-1}	CARRUTHERS
SURFACE TENSION ($F(T)$)		
CRITICAL RAYLEIGH NO.	$F(D,H)$	KOHLER

Figure IV-7.

117

C. PROPOSE MEA EXPERIMENTS FOR ZONING OF SILICON

E. L. Kern
Consultant
Del Mar, CA

Materials Experimental Apparatus (MEA) experiments are outlined in the following figures. This is a precursory set of experiments which will be proposed to NASA, which will result in meaningful investigation at the power levels available in early Shuttle flights.

118

ORGANIZATION:

CONSULTANT

MARSHALL SPACE FLIGHT CENTER

NAME:
F. KERN

DATE:
9/23/81   VI-1

M. E. A. EXPERIMENTS

M. E. A. = MATERIALS EXPERIMENTAL APPARATUS

A PALLET MODULE TO BE FLOWN ON SPACE SHUTTLE WHICH PROVIDES POWER (500 W. TOTAL), COOLING, START COMMANDS & RECORDING TO 3 (OR 4) CANNISTER EXPERIMENTS, ORIGINALLY BASED ON SOUNDING ROCKET EXPERIMENTAL HARDWARE).

SIZE: 30 + " HIGH (DEPENDING ON MEA A OR B) AND ~16" DIA.

ALL EXPERIMENTAL EQUIPMENT, CONTROLS AND DATA RECORDING MUST FIT INTO THIS MODULE

Figure IV-8.

MARSHALL SPACE FLIGHT CENTER

ORGANIZATION: CONSULTANT

NAME: E. KERN

DATE: 9-23-81   VI-3

PURPOSE OF M.E.A. EXPERIMENTS

PURPOSE : PROVIDE EARLY SPACE EXPERIMENTATION ON SMALL, EASY, INEXPENSIVE SYSTEMS TO INDICATE INITIAL ADVANTAGES TO SPACE PROCESSING. FULL GROWTH ANALYSIS, HARDWARE DEVELOPMENT AND USABLE CRYSTAL SIZES ARE NOT EXPECTED.

GOALS: SHOW THAT AN EXPERIMENTAL SYSTEM WILL WORK IN SPACE (SI OR SI ALLOYS IN A SUITABLE HEATER), THAT THE ANALYSIS SHOWS PREDICTED RESULTS (GROWTH OF HARD TO GROW CRYSTALS OR RESULTS OF LACK OF BOUYANCY CONVECTION), AND THAT USEFUL RESULTS ARE OBTAINABLE WHICH WILL BENEFIT INDUSTRY AND GOVERNMENT PROGRAMS.

Figure IV-9.

ORGANIZATION:

MARSHALL SPACE FLIGHT CENTER

NAME:

CONSULTANT

E. KERN

DATE: 9-23-81   VI-4

M. E. A. PROPOSED EXPERIMENTS

GROWTH OF:

                                                          TIMETABLE

1. GE (GE: GA)   1984

2. SI (SI: GA)   1984

3. SI - GE$_X$ ALLOYS OF $.1 \leq 4 \leq .9$ 1985/6

4. SI DOPANTS AT HIGH CONCENTRATION - TL, IN   1985/6

Figure IV-10.

121

Figure IV-11.

ORGANIZATION:

MARSHALL SPACE FLIGHT CENTER

NAME:
E. KERN

CONSULTANT

DATE:
9-23-81   VI-8

OTHER PROSPECTS FOR FUTURE M. E. A.

OTHER SEMICONDUCTOR OR METAL SYSTEMS THAT NEED VERY CAREFULLY CONTROLLED GROWTH CONDITIONS (GROWTH RATE, THERMAL FLOW, LOW CONVECTION) FOR SINGLE CRYSTAL GROWTH.

III-V SYSTEMS

"DIFFICULT COMPATIBLE METALS"

"OTHER DIFFICULT SEMICONDUCTOR, SEMIMETAL, INSULATION OR OPTICAL/ELECTRO-OPTICAL CYRSTALS"

Figure IV-12.

D. FLOAT-ZONE EXPERIMENTS

John Verhoeven
Iowa State University
Ames Laboratory
Ames, OH

MAIN TASK

Can surface tension driven convection in float-zone experiments be eliminated by means of oxide films (several monolayers)?

EXPERIMENTAL APPROACH

1. Select molten Sn as model system because of low vapor pressure and ease of handling.

2. Develop surface analytic techniques to evaluate oxide film thickness on molten tin versus temperature, O_2 pressure, and time.

3. Develop a system for float-zone melting of Sn which

   1) Allows surface oxide to be controlled and monitored

   2) Maximizes Marangoni flow and minimizes buoyancy flow

   3) Somehow allows analysis of effect of film on convection.

QUALITATIVE DATA ON STRENGTH OF THIN OXIDE FILMS

W. B. Pietenpol and H. A. Miley (Phys Rev 1927)
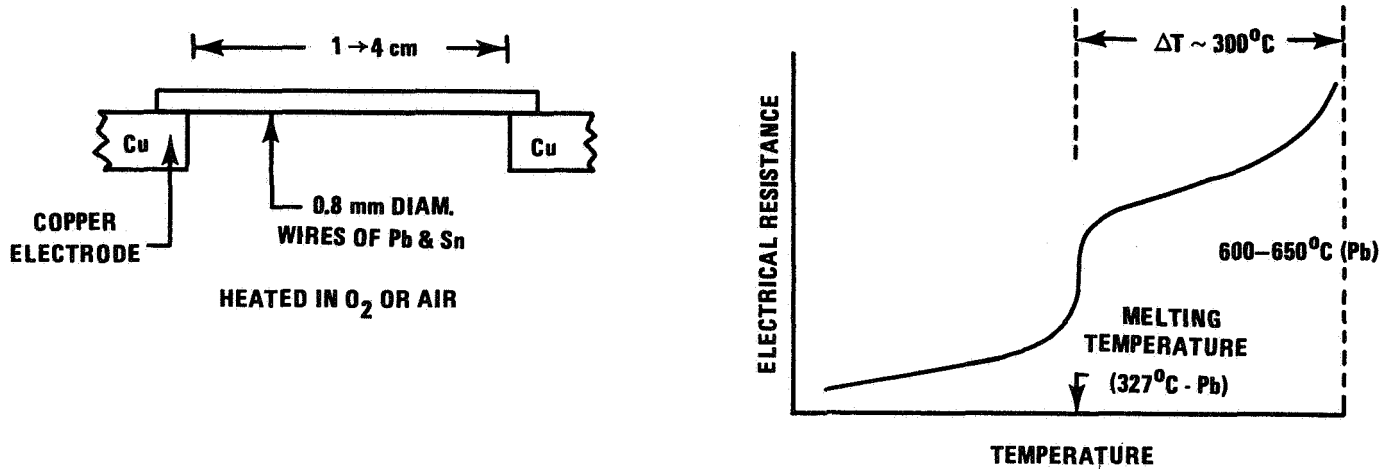
- Strength of oxide sufficient to hold 4 cm of 0.8 mm wire to 600°C

- Ductility of oxide sufficient to withstand thermal expansion encountered by repeated heating and solidification

- Oxide stable - Held at ∿ 250°C above m.p. in air for 1 hour

Our experience:

Uranium chunks of ∿ 3 mm size with native oxide retain their shape after U melts in vacuum of ∿ 10^{-5} Torr.
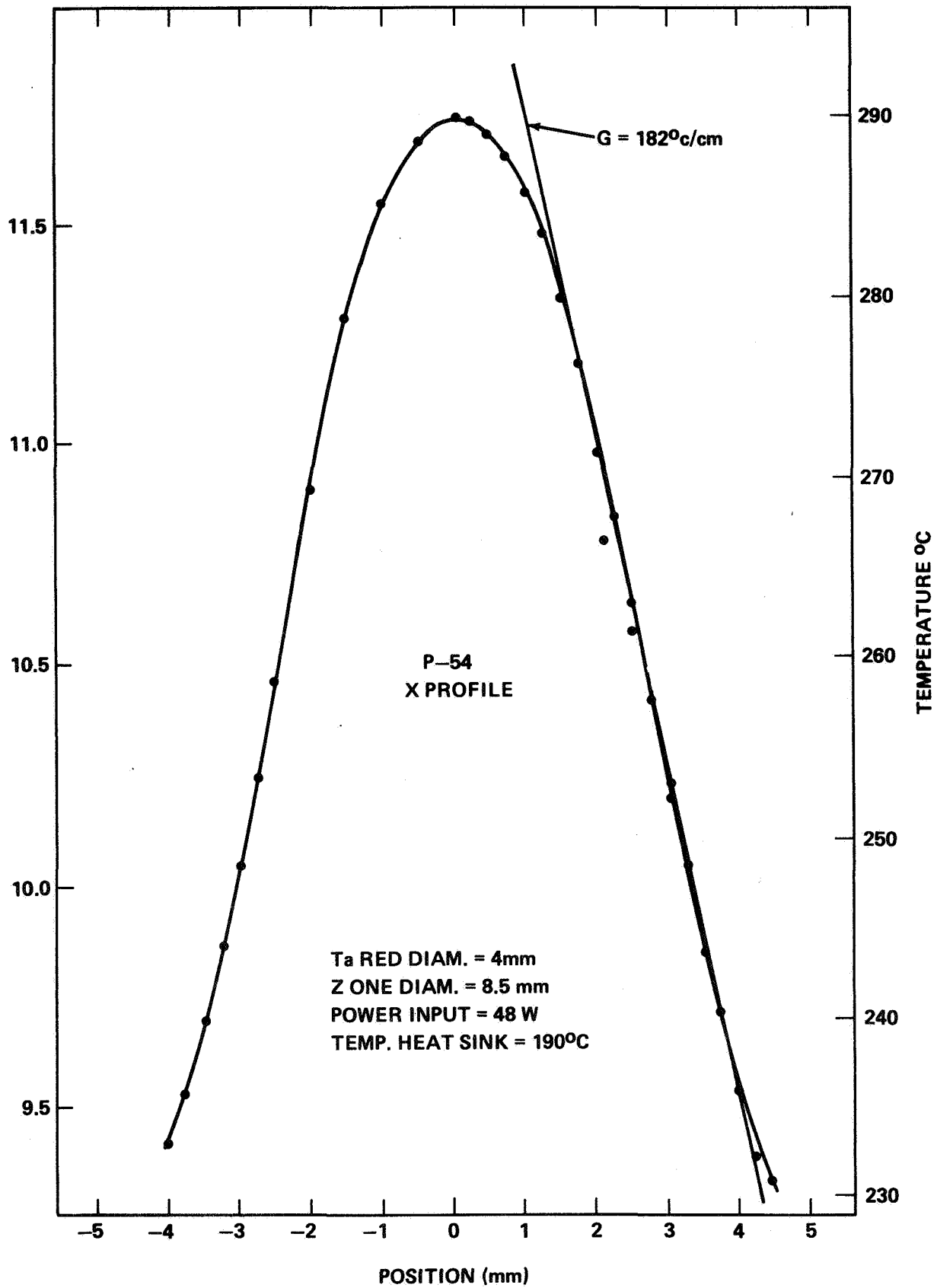
Figure IV-13.
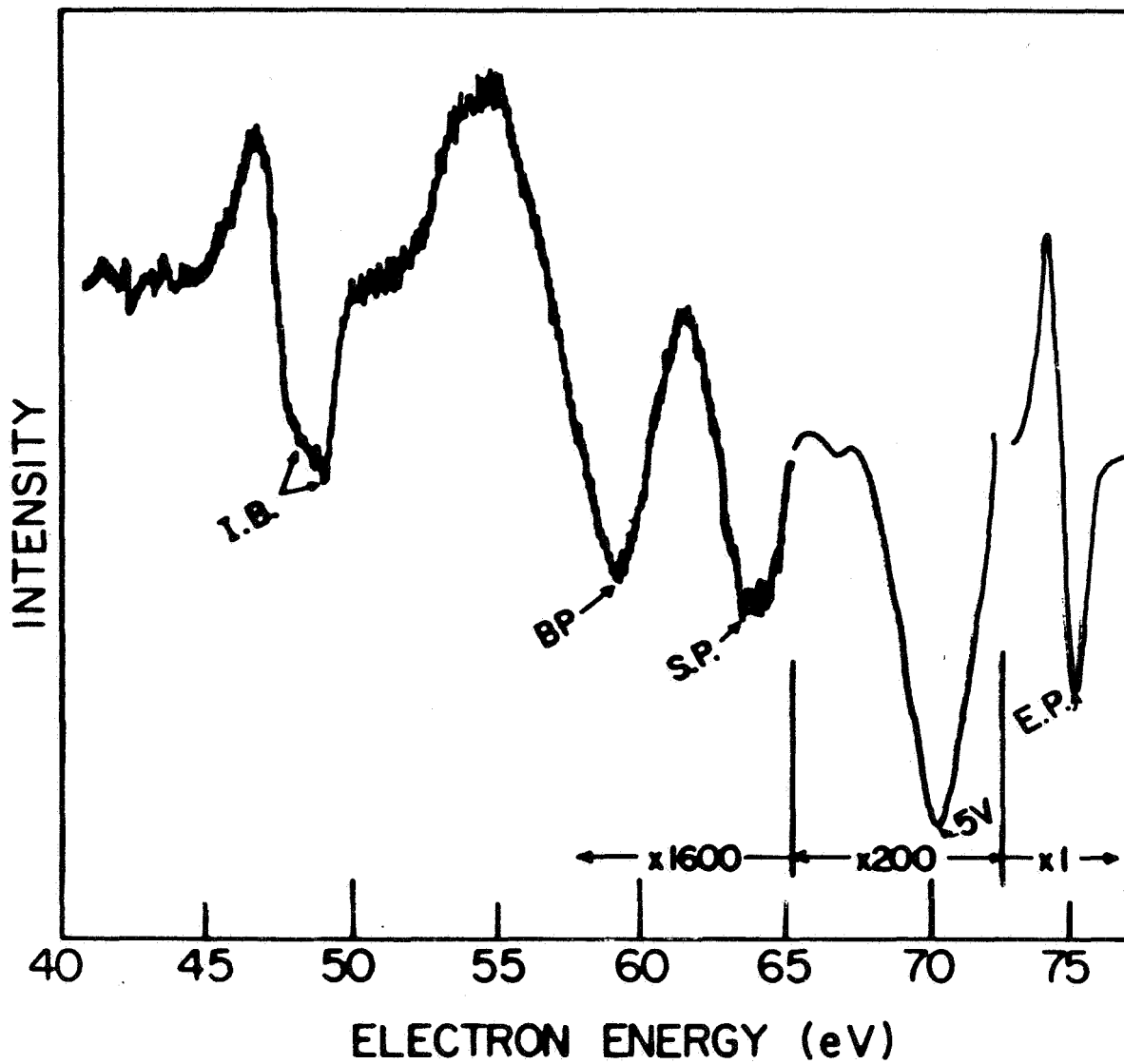
Energy Loss Spectrum (ELS) of SnO_2

	Interband Transition (IB)	Bulk Plasmon (BP)	Surface Plasmon (SP)	5-Volt (5-v)
SnO_2	26.1, 26.8 eV	16.0 eV	10.9 eV	4.8 eV
SnO	26.2, 26.9	11.6	7.3	4.8
Sn	24.0, 25.0	13.5	9.3	(3.8)

Figure IV-14.

14 mm diam. recess milled
into stainless steel plate

Stainless Clad Heater

Silver
rod

Extension
adjustment
screws

Insulated
connectors

Thermocouple
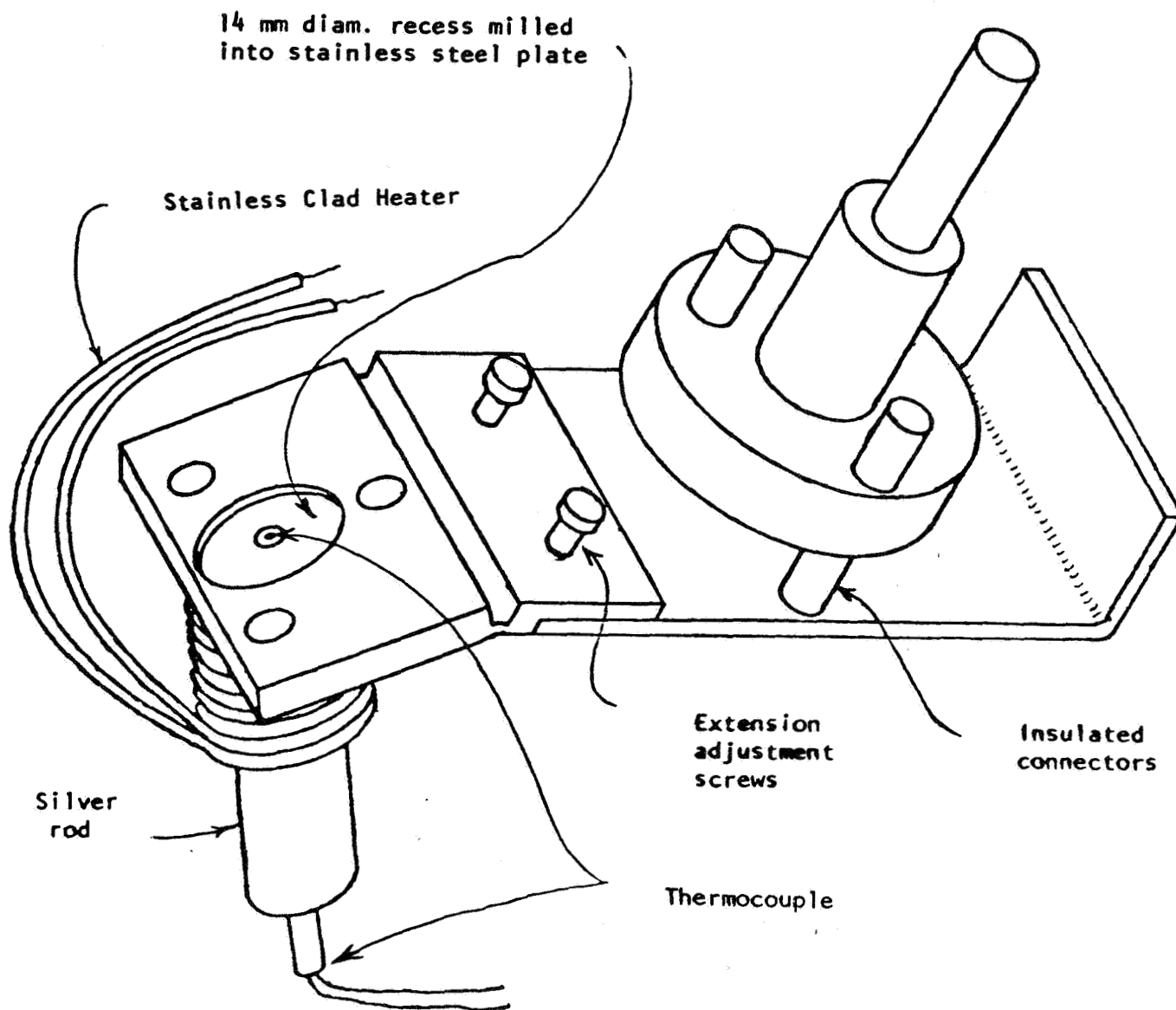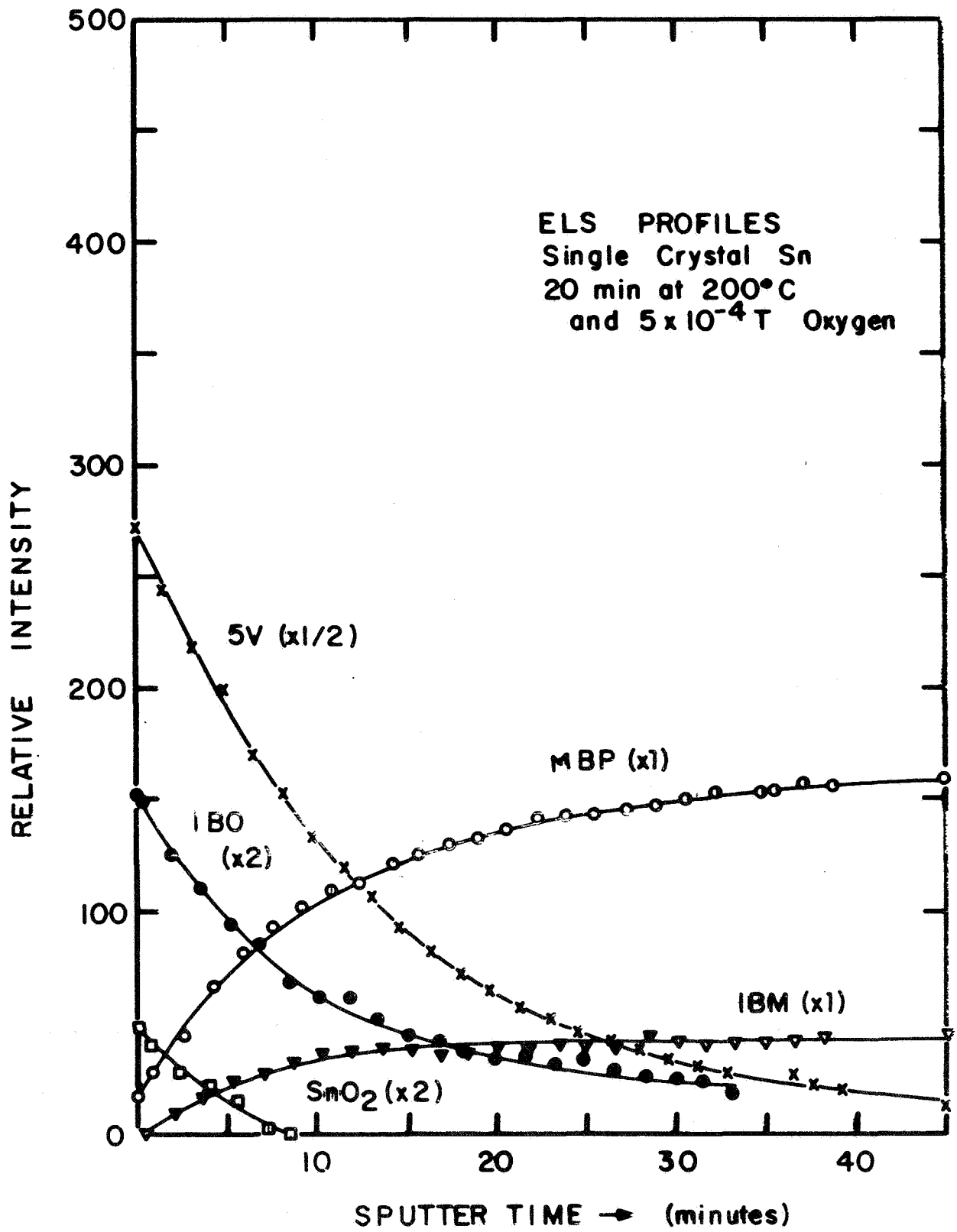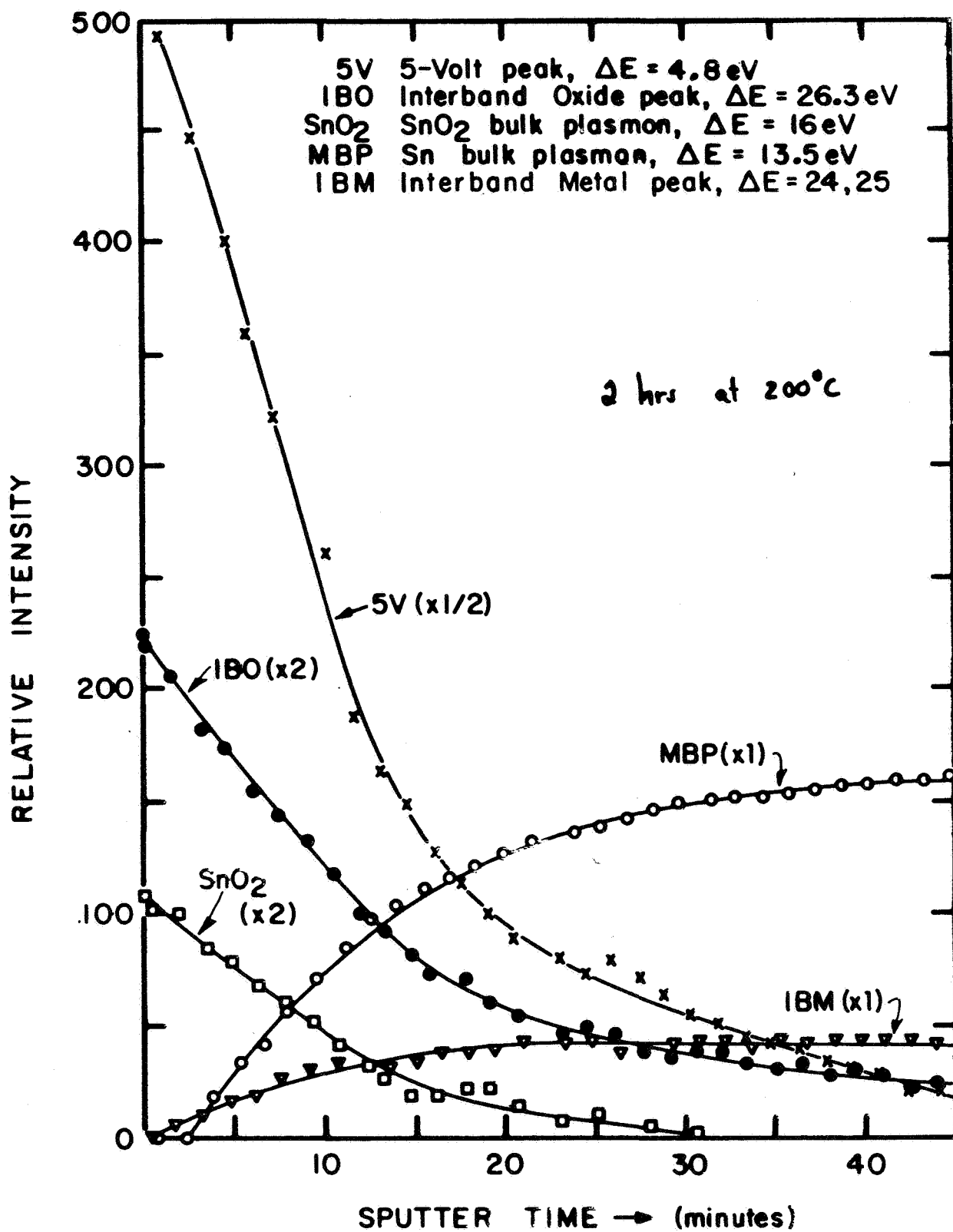
Figure IV-15.

Figure IV-16.

Figure IV-17.
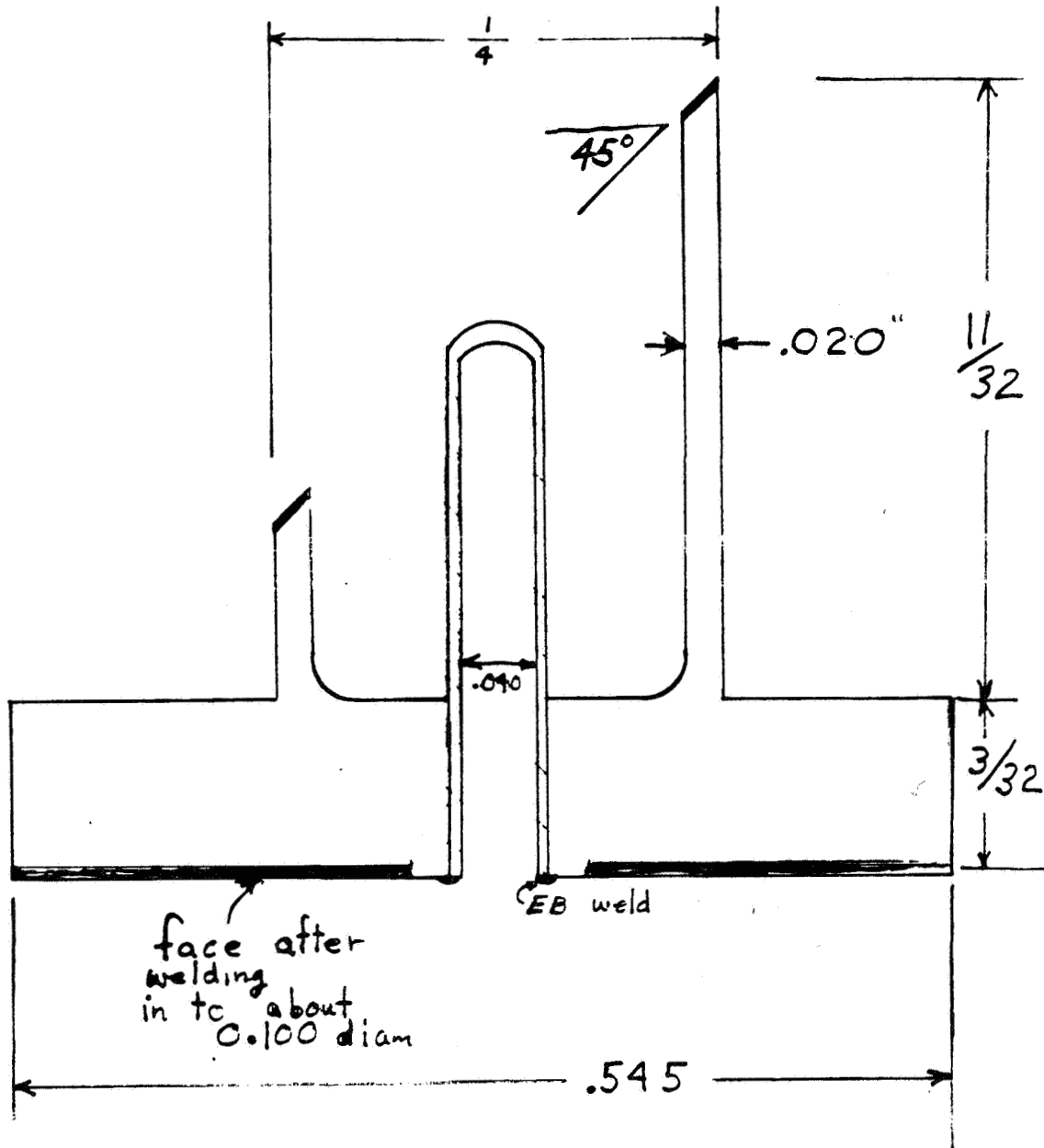
DESIGN OF CUP USED TO HOLD MOLTEN TIN SAMPLE.
ATTACHES TO HEATER ASSEMBLY OF FIGURE 1.

Figure IV-18.

CONCLUSIONS

1. Molten tin surfaces may be readily cleaned by ion bombardment with 2.4 keV argon ions with ion beam current densities of approximately 100 $\mu A/cm^2$.

2. It is very important that the ion bombardment beam is positioned with adequate clearance to avoid striking the CMA shield.

3. Molten tin may be held in Ta containers at temperatures up to at least 240°C without producing contamination detectable at the tin surface.

4. The surface of molten tin at 240°C will remain atomically clean for many hours at total pressures of 4×10^{-9} Torr, and perhaps higher.

INCOMING ELECTRON
BEAM (75eV)

θ

OXIDE

METAL

I_{IBM} = INTENSITY $\begin{cases} \text{REFLECTED ELECTRONS} \\ \text{AFTER EXCITING AN} \\ \text{INTERBAND METAL} \\ \text{TRANSITION} \end{cases}$

$\longleftarrow$ X $\longrightarrow$

$$I_{IBM} = I_o \left[e^{-\frac{X}{\lambda_i \cos\theta}} \right] \left[e^{-\frac{X}{\lambda_o (.74)}} \right]$$

INTENSITY
OF IBM SCATTERED
ELECTRONS WITH NO
OXIDE (X = o)

INELASTIC MEAN FREE PATH OF
INCOMING & OUTGOING ELECTRONS

I_o $\longleftarrow$ FROM SPUTTER CLEANED LIQ Sn

I_{IBM}

OUR RESULTS

$\lambda_i \sim 8.5$ Å (75eV) $\Big\}$ LITER.
$\lambda_o \sim 8.3$ Å (50eV) $\Big\}$ SEAH
$\theta = 45^o$

2 HR OXID.
VALUE

X
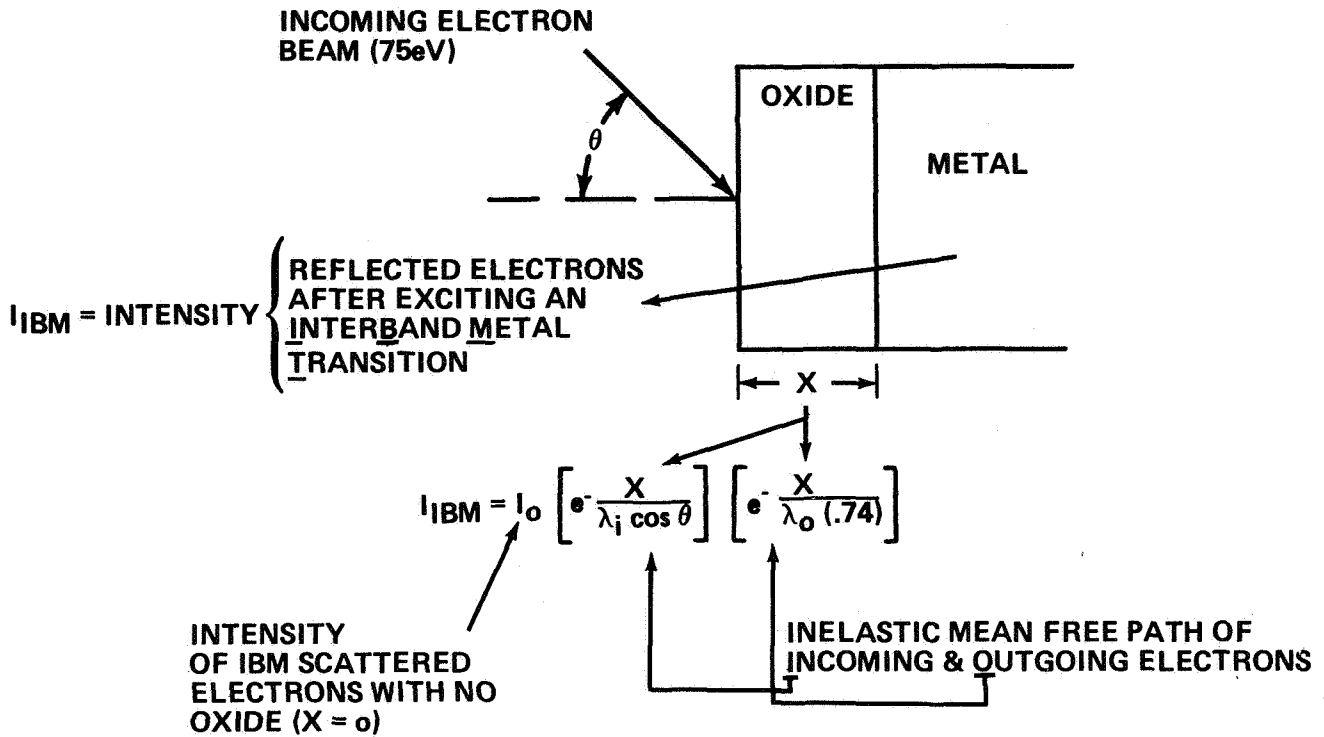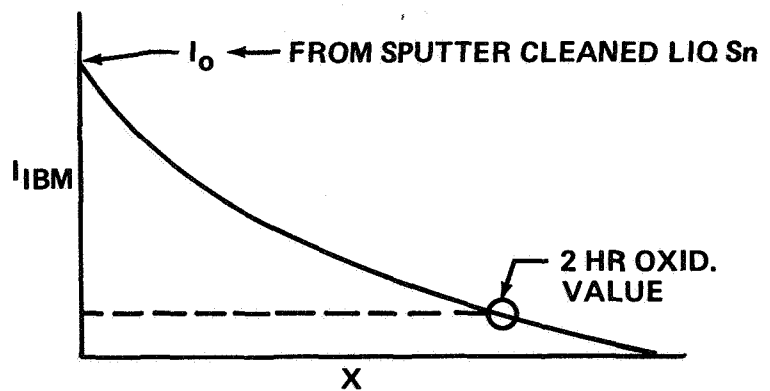
OXIDE THICKNESS X
AFTER 2 HR OXIDATION = $\sim$ 8 Å

Figure IV-19.

5. A two-hour oxidation of molten tin at 240°C produces a compact oxide of at least 8 Å thickness whose surface is predominately SnO_2.
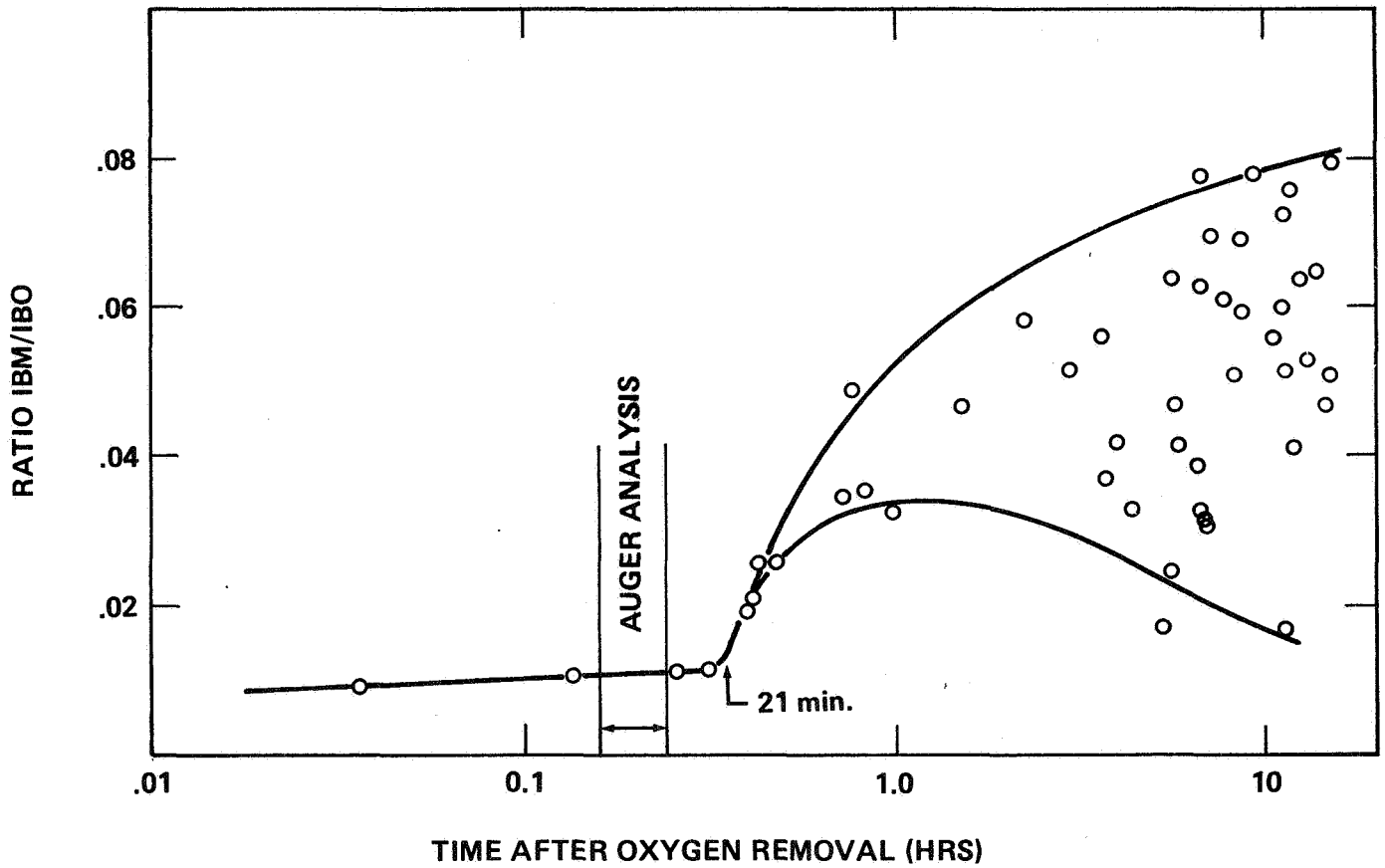
Figure IV-20.

CONCLUSIONS (Concluded)

6. After holding for around 20 to 40 minutes under vacuum this oxide appears to break up into a mobile island structure.

7. Depth profiling of oxidized molten tin does not appear to lend itself to quantitative analysis, apparently due to breakup of the film into a mobile island structure.

IMPLICATIONS FOR OUT STUDY

1. Will be able to produce thin (10 to 15 Å) continuous oxide films on molten tin at O_2 pressure low as 5×10^{-4} T.

2. The films will probably only remain continuous if O_2 pressure is maintained within system to heal cracks.

3. Only moderate vacuum levels required, $\sim 4 \times 10^{-9}$ T.

4. Will be able to make direct contact to molten zone with Ta shielded T.C. — no contamination.

5. Samples may be cleaned over entire molten surface with a stationary ion beam.
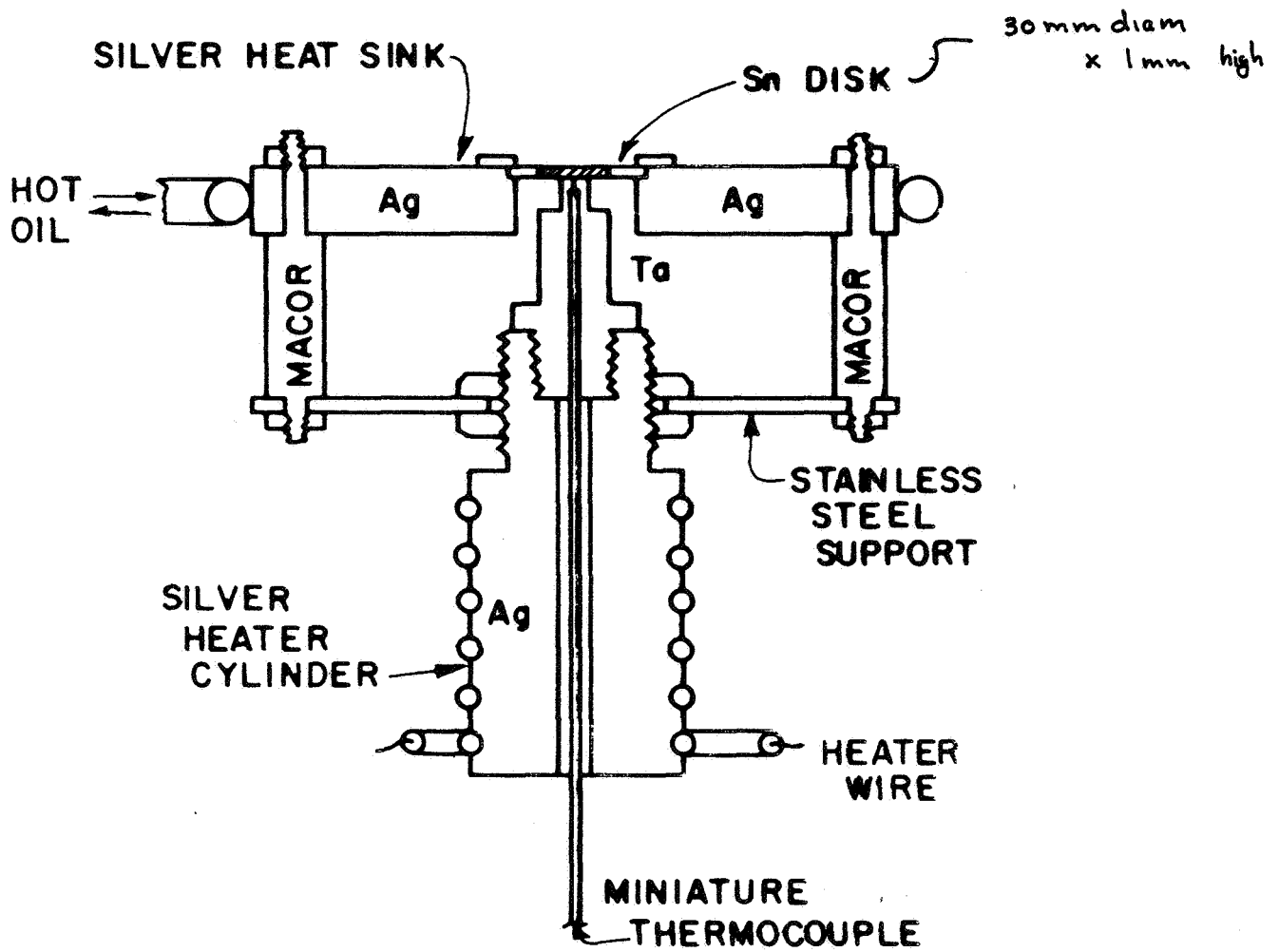
Figure IV-21.

Birikh analysis
(order magnitude)
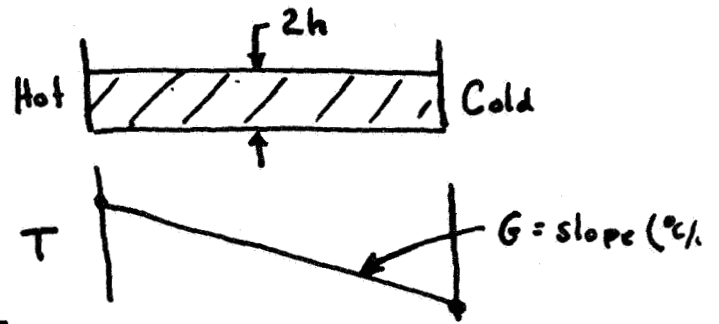
$$U_{top} = \frac{G\,h\,|d\sigma/dT|}{2\mu}\left[\frac{1}{12}\bar{B}_o + 1\right]$$

$$\frac{\rho g \beta (2h)^2}{|d\sigma/dT|} = \text{"modified Bond No" of}$$
$$\text{Si Ostrach}$$

For $2h = 1mm$

$d\sigma/dT$ (Sn) $= .08$ dyne/cm·°c (White)

$$\bar{B}_o = 0.077 \qquad \text{Bouy. contrib:} \frac{.077}{12} \text{ vs } 1$$
$$\sim 0.6\%$$

$$U_{top} \text{ (for } G = 100°C/cm) = \underline{11 \text{ cm/s}}$$

Oscillations

Chun & Schwabe on $\begin{cases} NaNO_3 \\ methyl\ alcohol \end{cases}$

Observe osc for $Ma > \sim 10^4$

$$\frac{|d\sigma/dT|\ \Delta T \cdot L}{\mu\ D_t} \qquad \therefore (Ma)_{cr} \sim 10^4$$

Figure IV-22.

EXPERIMENTAL PLAN

1. Solidify disks with and without oxide films. Measure solute profiles using Bi^{207} and look for effects due to oxide.

   If flow velocities are on order of 1 to 10 cm/s and we solidify at rates ~ 0.001 cm/s (10 μm/s) we should see an effect.

2. Look for oscillatory convection on clean zones utilizing miniature thermocouples for detection. If find, determine whether oxide will suppress temperature oscillations.

PROGRESS

1. Check out disk heater in oil pumped (10^{-6} T) vacuum system.

2. Measure temperature profiles and compare to calculations.

Initial Work with Disk Heater Design

- Trouble with Ta/Sn contact

- Overcome by electropol. Sn disk

Ta heater rod
beneath Sn disk

Boundary between central
electropolished region and
outer masked region

Boundary of molten zone

30 mm
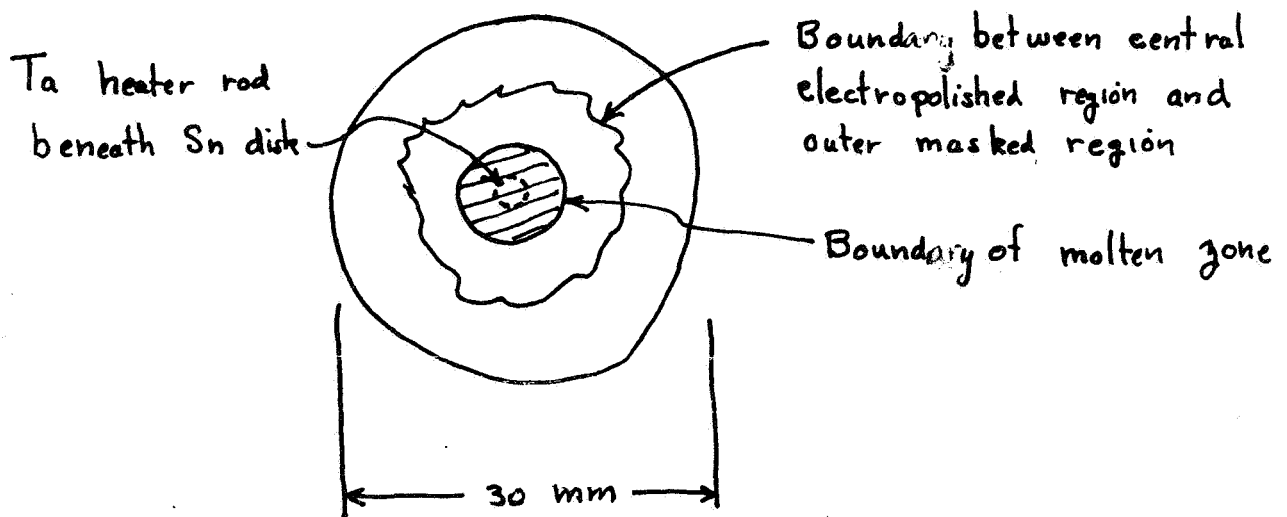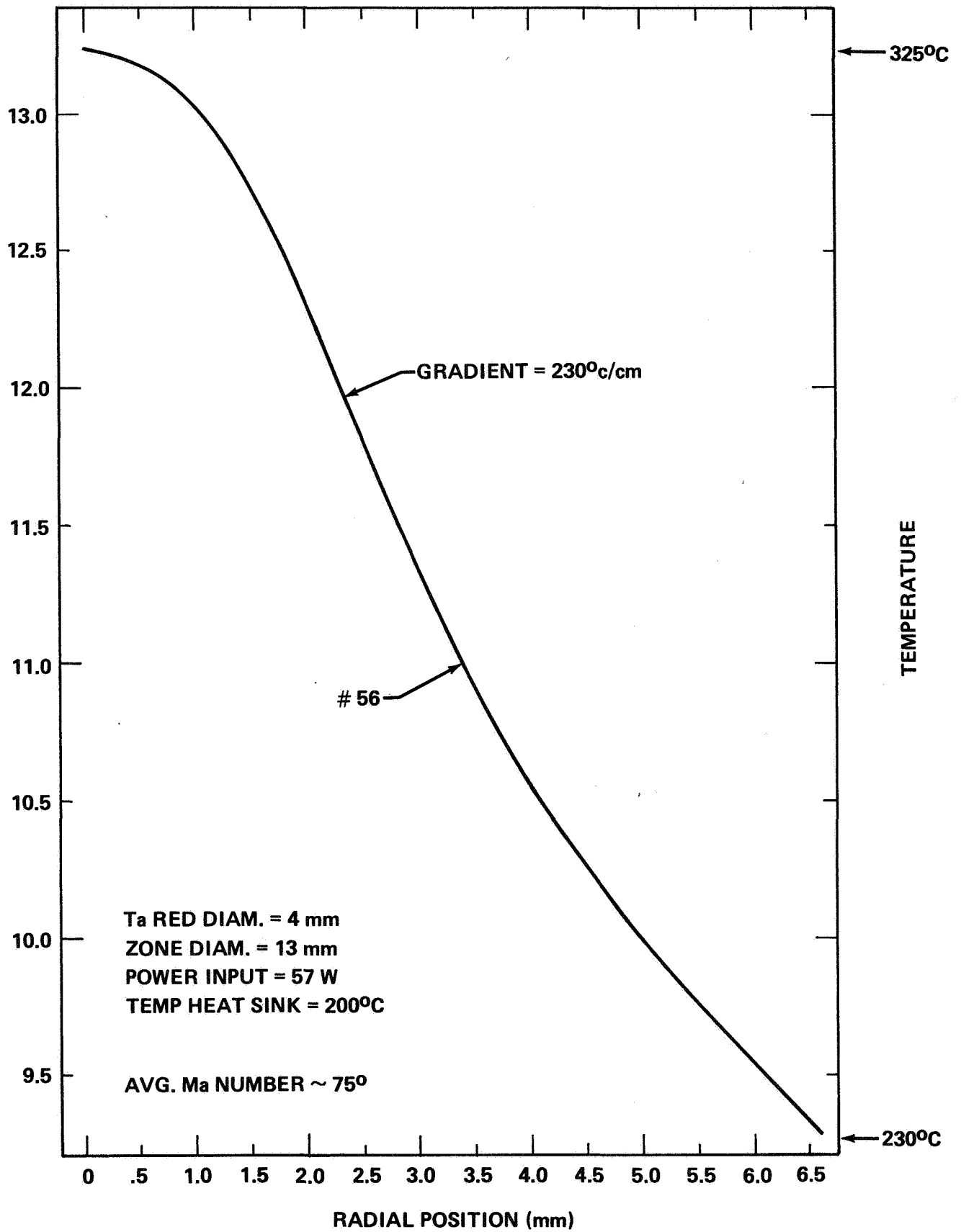
Figure IV-23.

Figure IV-24.

Have started collaborative effort with Bill Gill (Chem Engr. Dept)
and his graduate student, Mr. C.C. Hsu

1. Heat flow analysis (no convection)

$$T = function(\beta, r, z)$$
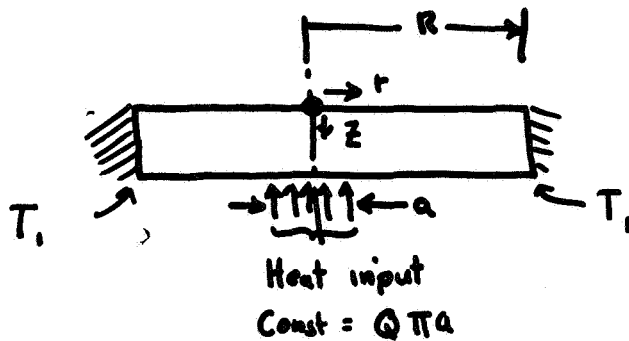
$$\beta \propto \left(\frac{1}{power\ input}\right)$$

Mr. Hsu has obtained the two-dimen. heat flow solution

2. Are working on extending a simple analysis (similar Birikh)
to the disk geometry

Figure IV-25.

5.4   5.2   4.8   4.4   4.0   3.6   3.2 mm

Y

Z

0.2 mm

$$\beta = \frac{Ks\,(Tm - Ti)}{Qa}$$

0.4

= 1.6   1.8   2.0

0.6

0.8

1.0

1.2
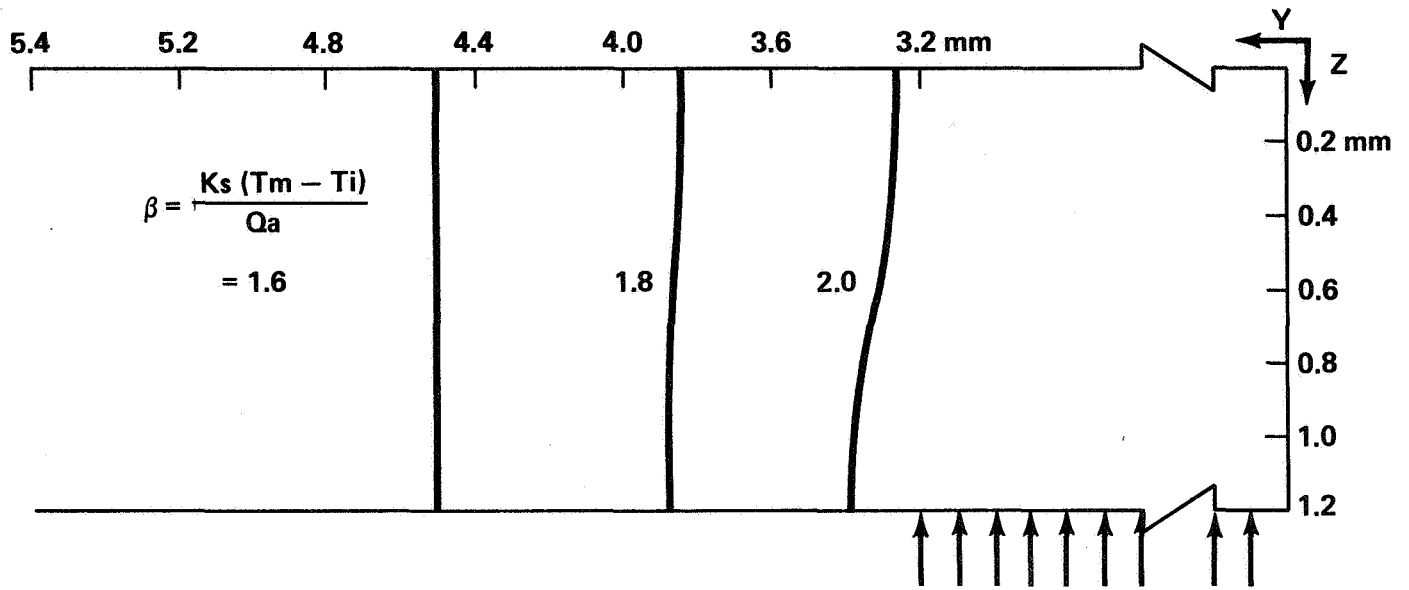
THE SHAPE OF INTERFACE

Figure IV-26,

TEMP. VS DISTANCE

$\beta = 1.5643863$

$$= \frac{Ks\,(Tm - Ti)}{Qa}$$

HEATER

γ (mm)
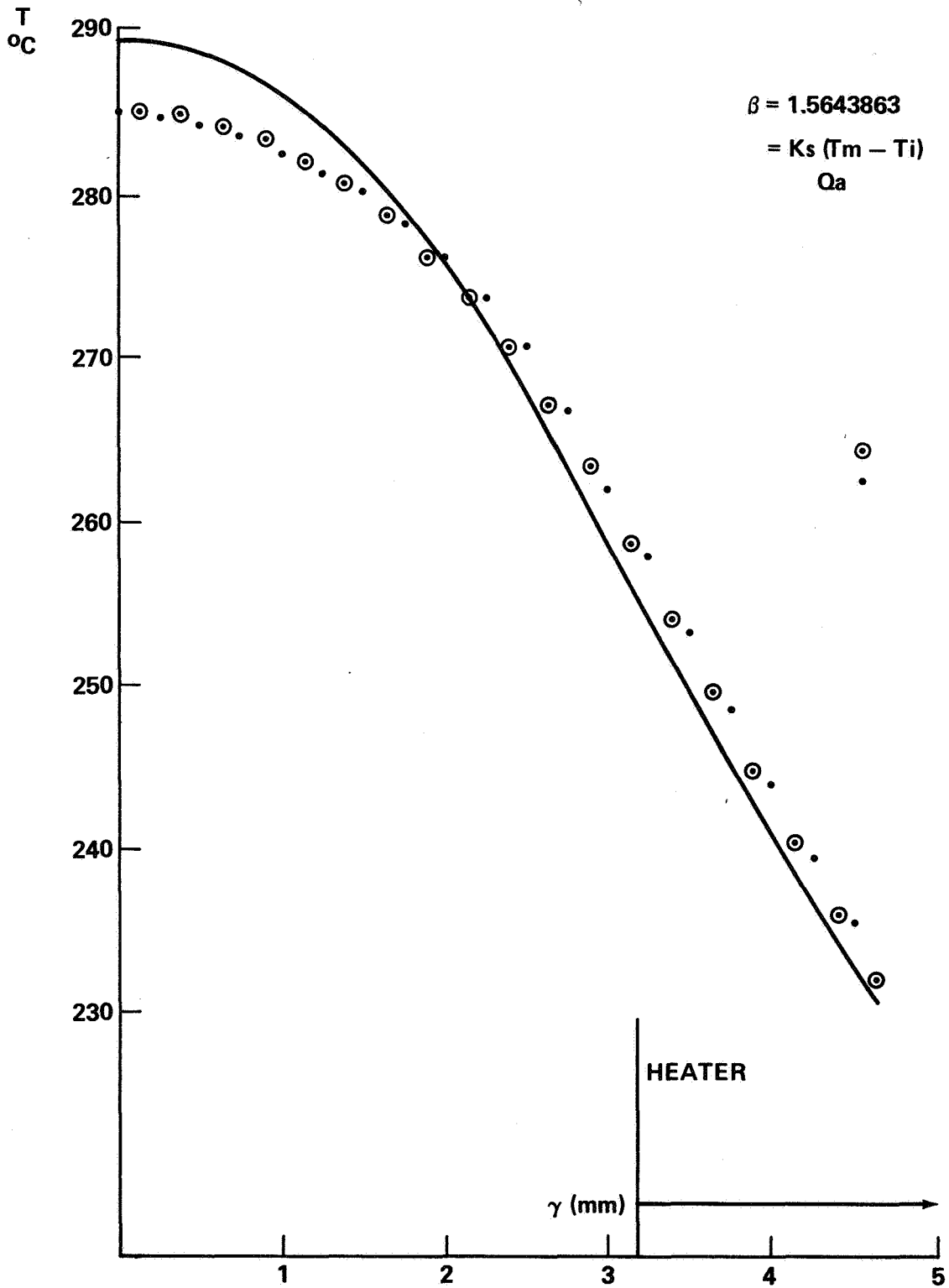
Figure IV-27.

TEMPERATURE VS DISTANCE

$$\beta = \frac{Ks\,(Tm - Ti)}{Qa} = 0.7438077$$
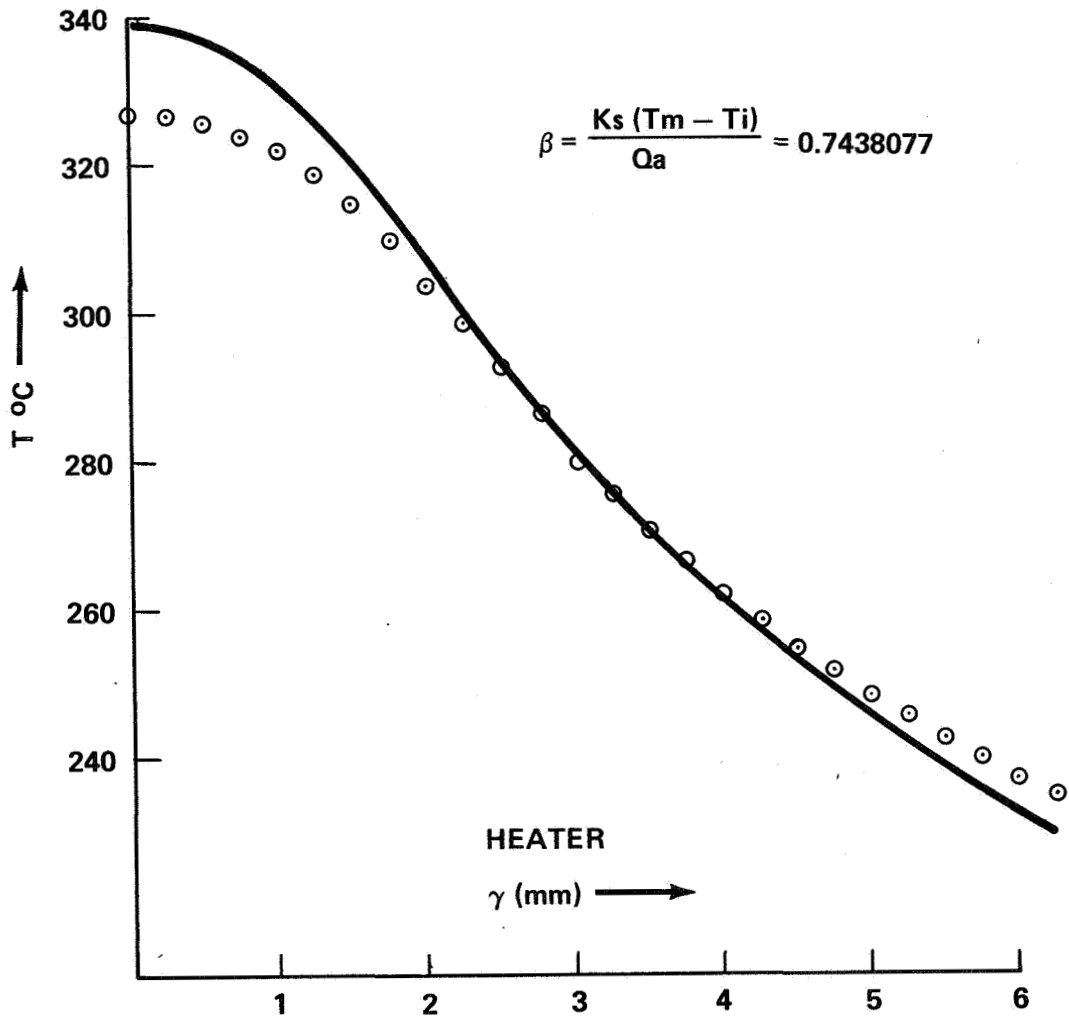
Figure IV-28.

Possible causes of disagreement

1) Convection

2) Meniscus
   disturbance

3) Thermocouple too big
   Extracts heat

.25 mm

1 mm
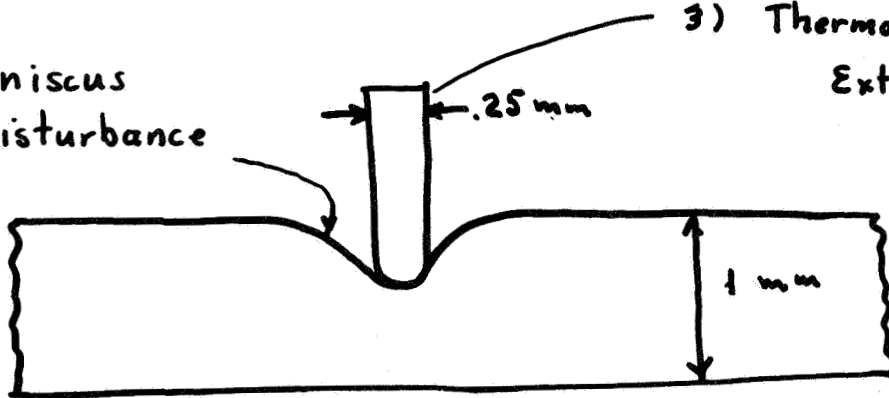
4) Shape does not remain flat (see slide)

Figure IV-29.

Interface shape experiment

CMA
(Auger & ELS)
(Analyser)

Ag
Heater
Block

Ta

liquid Sn

solid Sn

Ag
Cooling
Block

No Film
(Mar. flow)
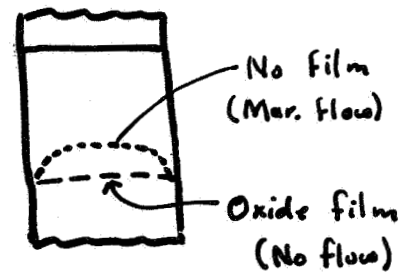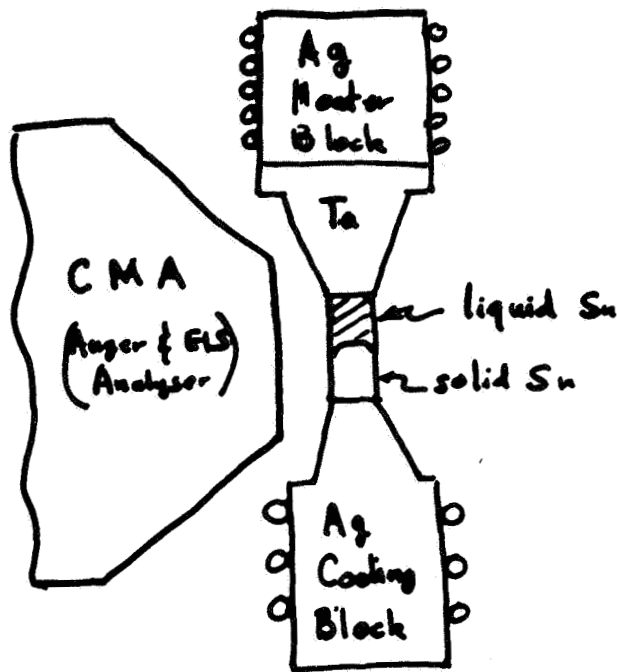
Oxide film
(No flow)

1 - Hold with & without an
       oxide film

2 - Use Pb-Sn eutectic to reveal
       interface shape.

    - no comp. changes expected

3 - Problem with wetting at top

Schwabe :

COLD

Liq

Sol.

KCl

$P_r = .27$

COLD

Liq

Sol

Na NO$_3$

$P_r = 9.3$

Figure IV-30.

146
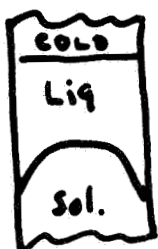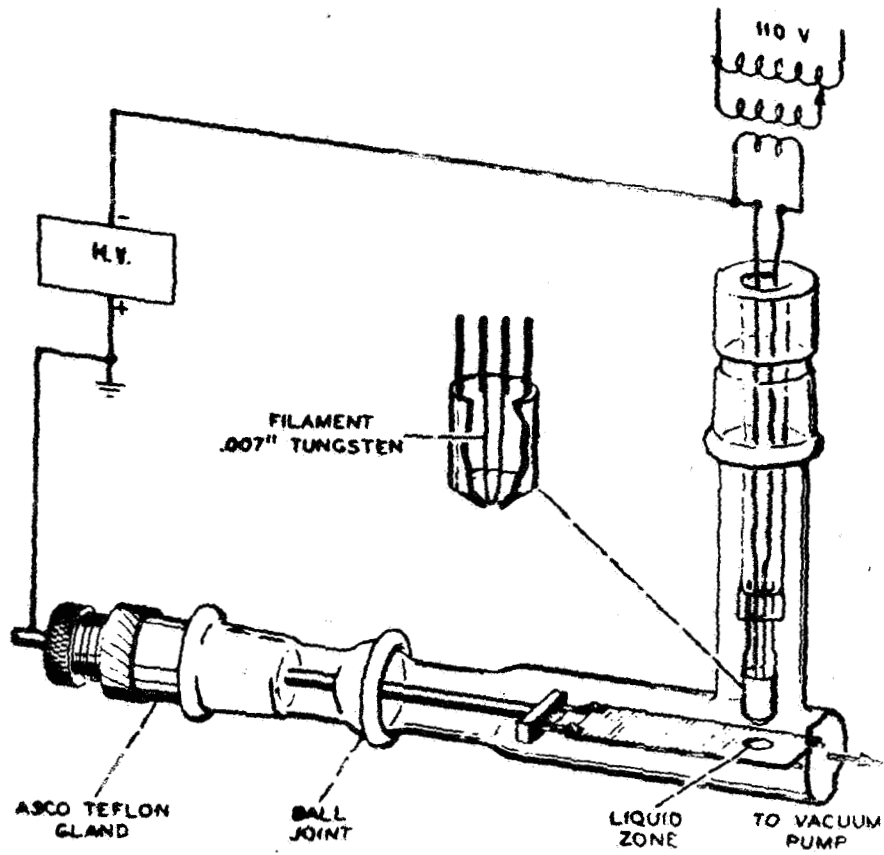
ELECTRON BEAM MELTING APPARATUS

Figure IV-31.
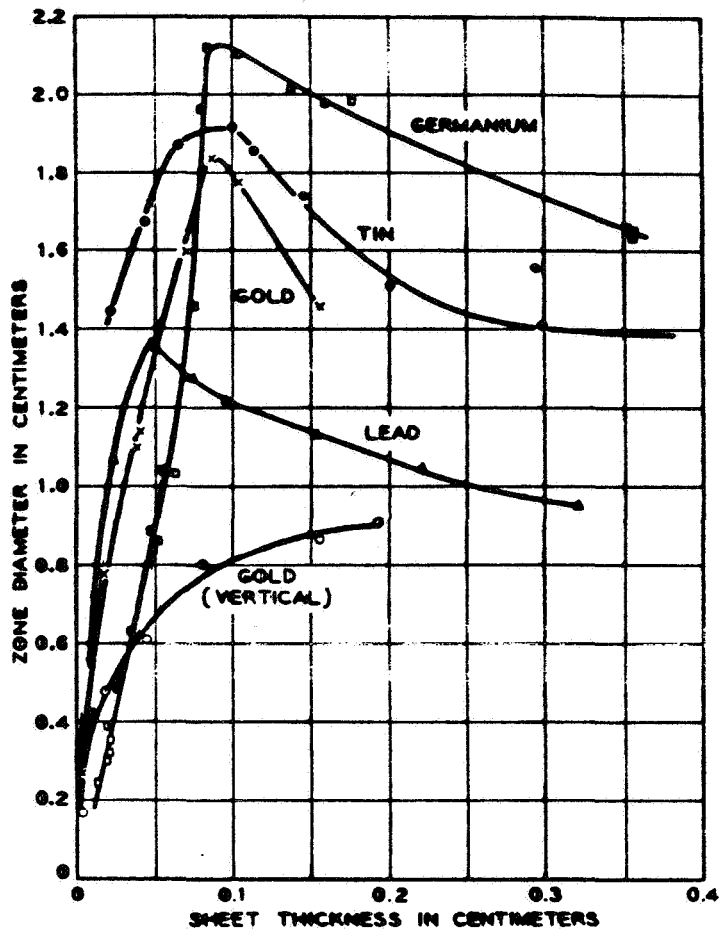
MAXIMUM DISK ZONE DIAMETER VERSUS PLATE THICKNESS

Figure IV-32.

Figure IV-33.

Analysis

Solid

% Solute or Res.

Radial position →

no mixing
($R\delta/_0 \to$ large)

Marangoni flow
$\left(\dfrac{R\delta}{0} \to \text{small}\right)$
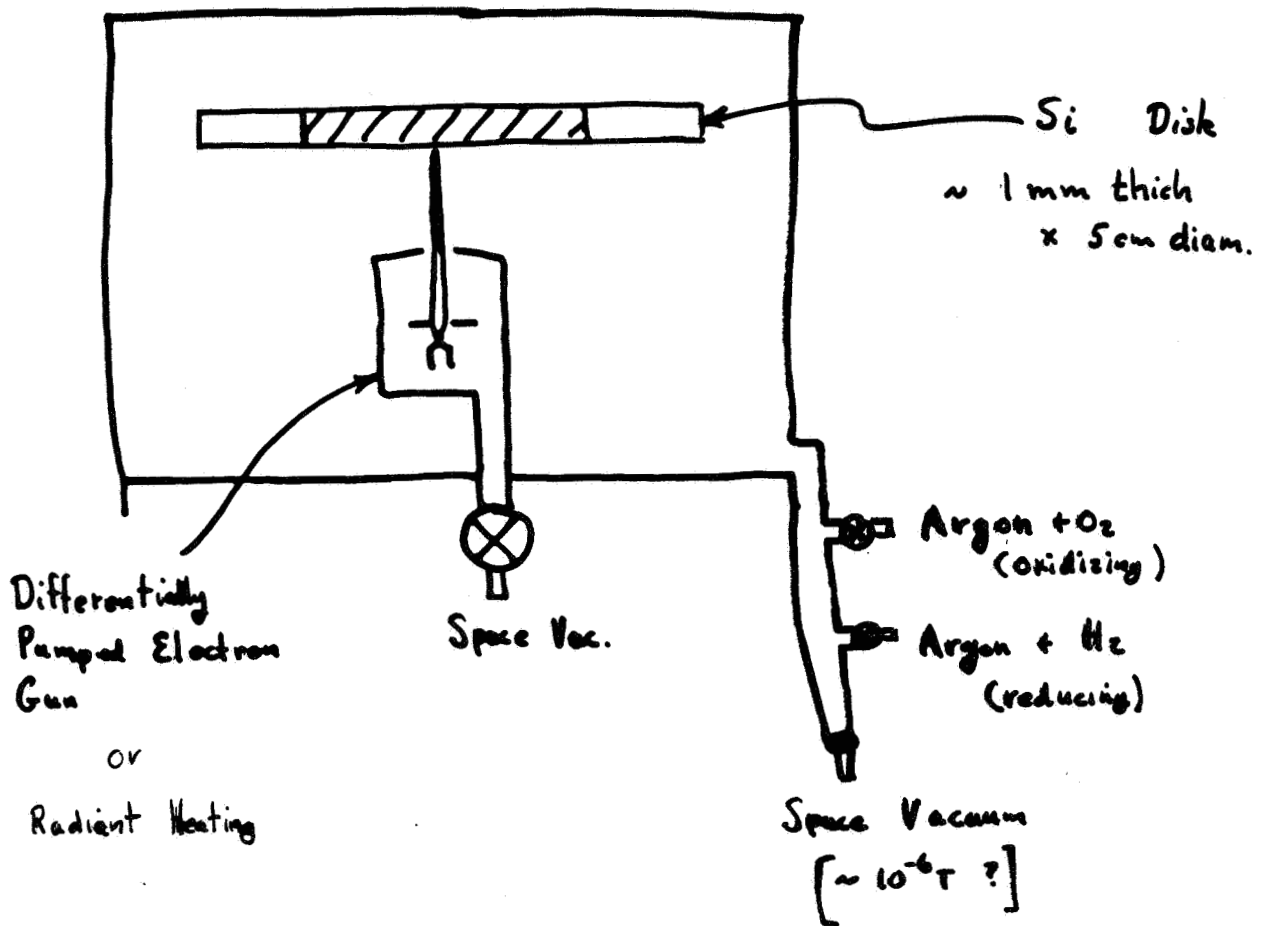
①
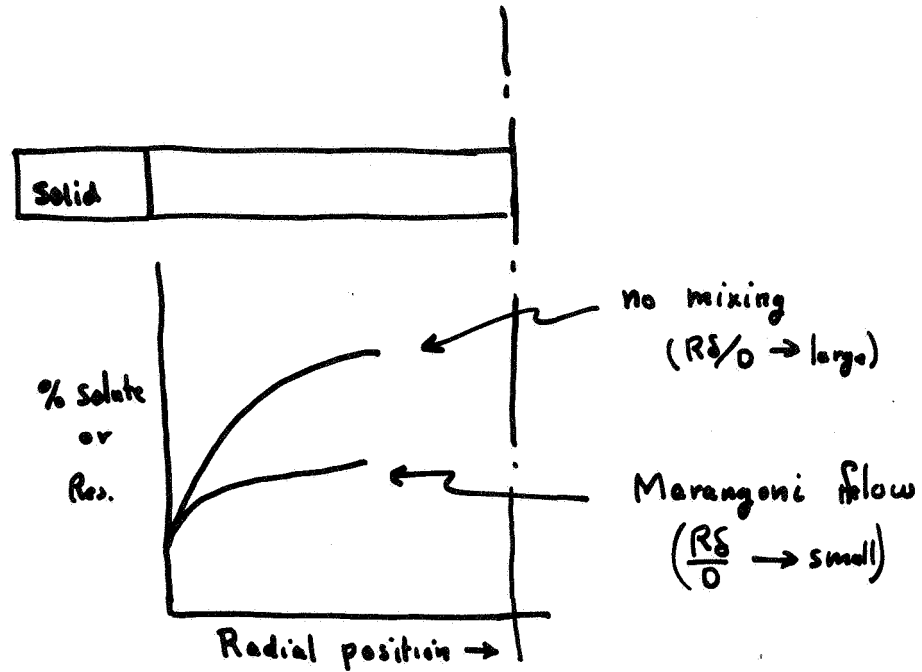
② Look for differences in striation structure under oxidizing and reducing conditions

③ Determine maximum possible molten zone diameter in orbit versus in 1g gravity

Figure IV-34.

E. PRESENT GROWTH TECHNOLOGY OF SILICON-GERMANIUM ALLOYS AND POSSIBLE ADVANTAGES OF MICROGRAVITY GROWTH

Dr. Oscar M. Stafsudd
UCLA
Los Angeles, CA

Dr. Stafsudd, who is Professor of Electrical Engineering at UCLA, reviewed the present growth technology of Silicon-germanium (Si-Ge) alloys and the possible advantages of growth in microgravity. Si-Ge alloys are of interest because they have a continuous variation of bandgap energy from the germanium bandgap (0.65 eV) to the silicon bandgap (1.09 eV) (Fig. IV-35). The unusual two-slope behavior of Eg versus composition is due to the differences in the conduction band structure between Si and Ge. Below 17 percent (atomic), the germanium band structure dominates; and above it, the bands are "silicon like."

One can therefore tune the band structure to produce intrinsic photodetectors at wave lengths of particular importance, such as 1.06 µm for laser detectors and 1.3 to 1.6 µm for fiber optics. The competitive materials in the 1.3 to 1.6 µm range are 3 to 5 ternary and quaternary compounds, for which the microcircuit technologies are not as developed as with silicon materials. Germanium does not possess a native, stable, and protective oxide, such as silicon does, thus providing for each processing and good electrical protection. It will be interesting to study the oxide system of the Si-Ge alloys.

The extrinsic doping levels of dopant ions in Si-Ge alloys varies with alloy composition (Fig. IV-36). While this is of interest for infrared detectors, this development has met with limited success. This may partly be due to reduced mobilities and other degraded electrical properties, due, in part, to low crystal perfection and poor homogenity.

Silicon and germanium form a complete solid solution, since each have the same crystal structures. The phase diagram is shown in Figure IV-37. The crystal system is clearly well behaved, except for the considerable opening of the solidus-liquidis curves. This is somewhat misleading, however, since the alloys are extremely difficult to grow when $0.1 \leq x \leq 0.9$ in $Si_x Ge_{1-x}$.

The problems in crystal growth are similar, in many respects, to several pseudo-binary systems of interest, such as HgTe:CdTe. The Si-Ge system is more tractable in that it is a true binary system and the components have relatively low vapor pressures at the alloy melting point.

One problem in crystal growth arises from the low (and varying) distribution coefficient, as seen for the germanium distribution coefficient as a function of solid alloy content (Fig. IV-38). For $Si_{0.65} Ge_{0.35}$, half of the germanium in the melt is rejected by the solid at the solid-liquid interface. This results in a large variation of the germanium content in the liquid as a function of distance in front of the growth interface. This presents a serious problem in the growth-interface stability, leading to constitutional supercooling. For instance, if one is limited to a temperature gradient at the interface of 100°C/in., the maximum reported stable growth rate is 1/2 mm/hr. Uniform instantaneous growth rates in present crystal growers are hard to control in this range.

The extreme density variation of the alloy with composition leads to further complicate the growth. Figure IV-39 shows the variation of density with alloy composition and Figure IV-40 shows the variation in lattice parameter with density. If one attempts to grow a solid of 50 percent Ge composition, the liquid rejected has a density of 4.8 gm./cc, whereas liquid of 50 percent Ge has a density of 3.6 gm./cc. This provides a large density drive in this system.

The effects of this density segregation is seen in Figures IV-41 and IV-42. Figure IV-41 shows the fraction of Ge in a horizontally grown crystal in three vertical sections taken along the growth direction. Gravitational separation of the heavier Ge leads to a higher concentration at the bottom of each slice. In addition, there is a skin of nearly pure Ge over the entire length of the bottom of the crystal. This shows one of the few undeniable examples of gravitational separation in melt growth at $g = 1$.

Figure IV-42 shows the variation of Ge concentration (vertical scale) as a function of growth rate, R. The variation between top and bottom of an ingot is greater with faster growth rates. Figure IV-43 shows how the top to bottom variation (vertical scale) as a function of the alloy composition.

The thermal expansion data for various alloy compositions is shown in Figure IV-44. Si-Ge alloys make efficient thermoelectric generators at elevated temperatures. Figure IV-45 shows the thermoelectric figure of merit as a function of composition, indicating that the most interesting compositions are also those of high interest to detectors (40 percent Ge corresponds to Eg. = 0.88 or 1.2 to 1.3 µm infrared radiation).

Similar problems in segregation are observed for crystals grown by the Czochralski and float-zone growth methods.

The growth of Si-Ge alloys in microgravity appears very attractive, as pointed out by the $g = 1$ growth experiments and the deleterious role of gravity. In particular, the float-zone method, in which a liquid zone of controlled starting composition (different from the seed and feed rods), can be used to grow a large amount of useful alloy crystal. Large temperature gradients and relatively flat growth interfaces will be necessary in order to obtain homogeneous crystals growth.

152

Eg VS ALLOY COMPOSITION Si - Ge

Figure IV-35.

IMPURITY ENERGY LEVELS IN Si - Ge
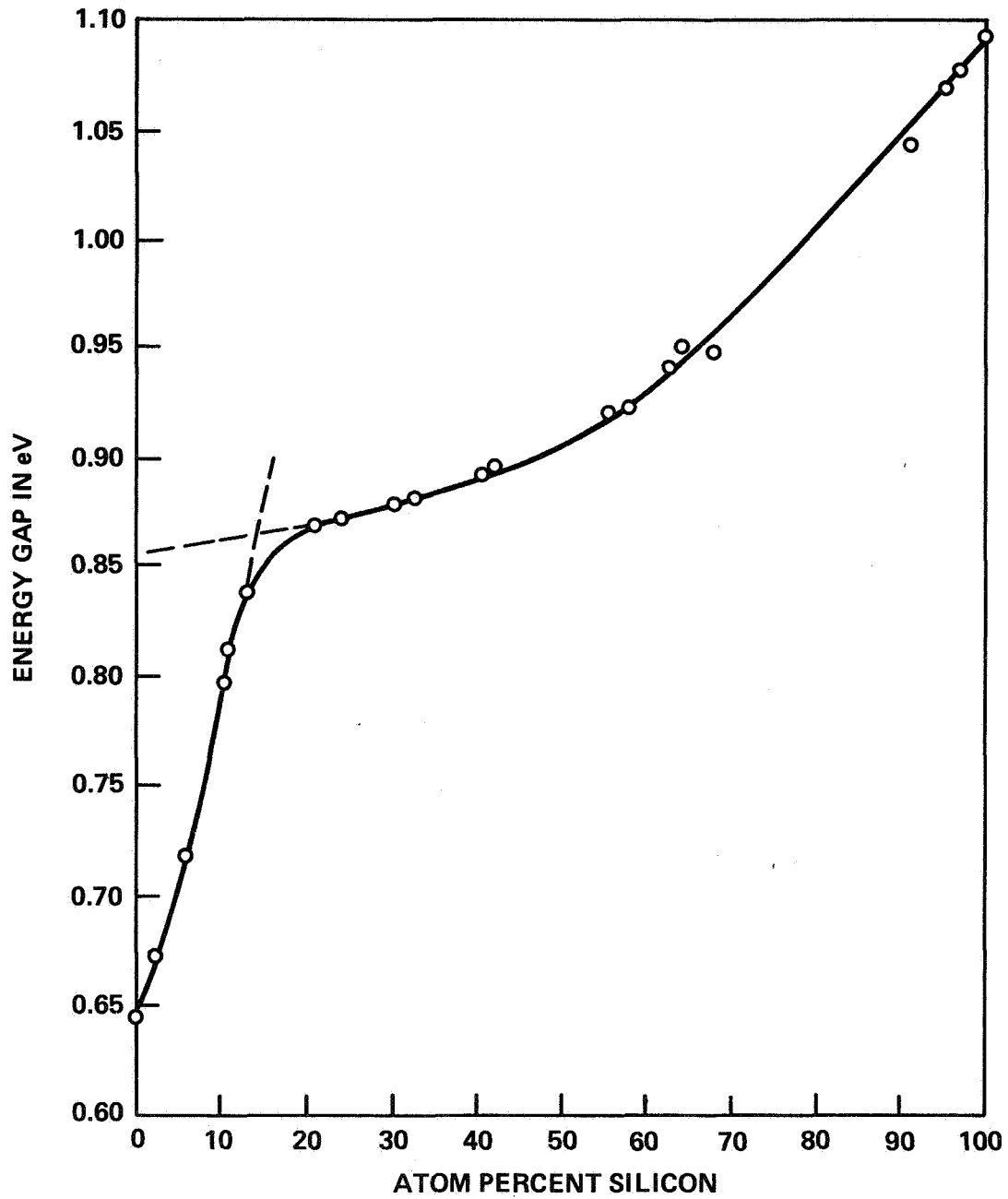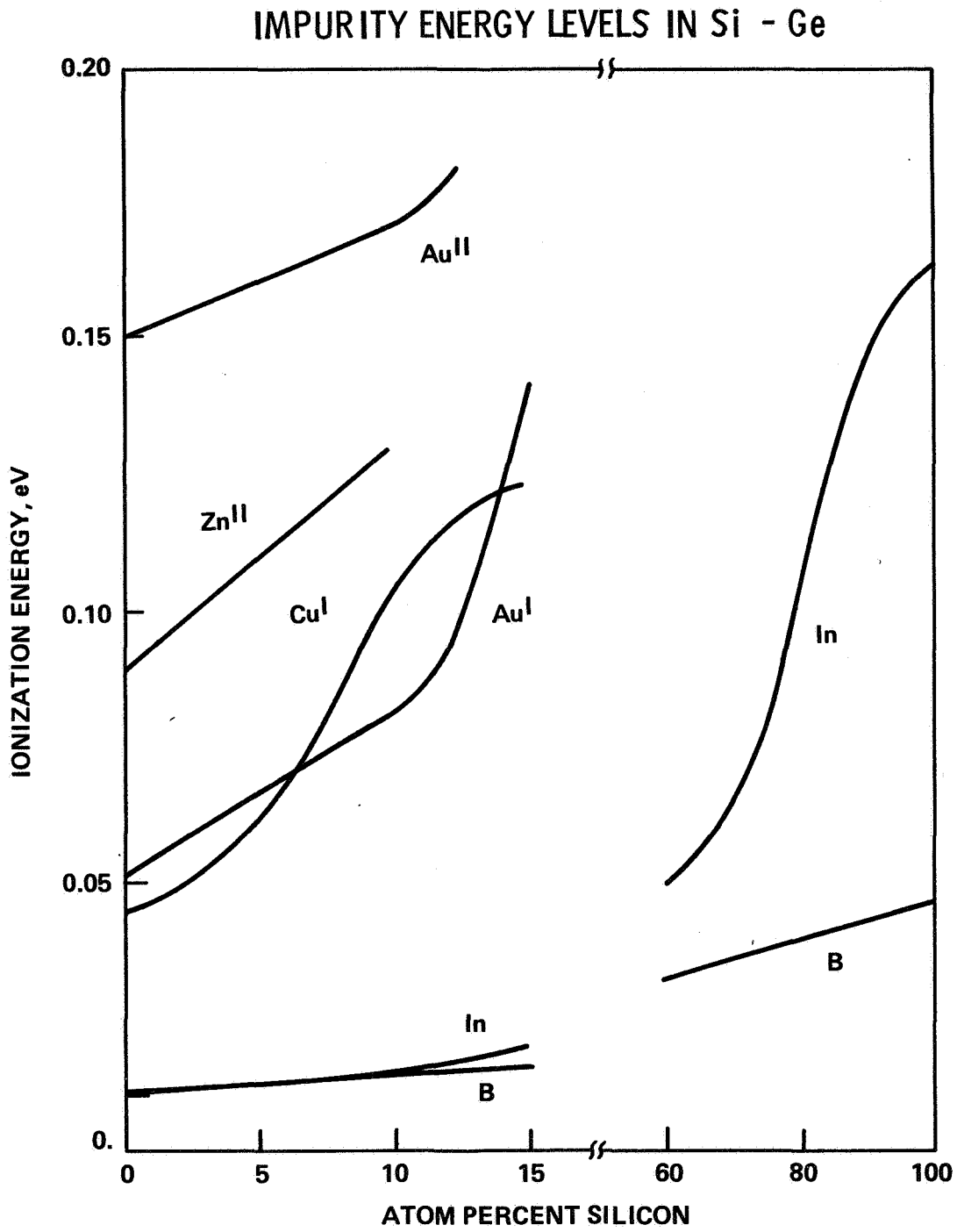
Figure IV-36.

PHASE DIAGRAM Si - Ge
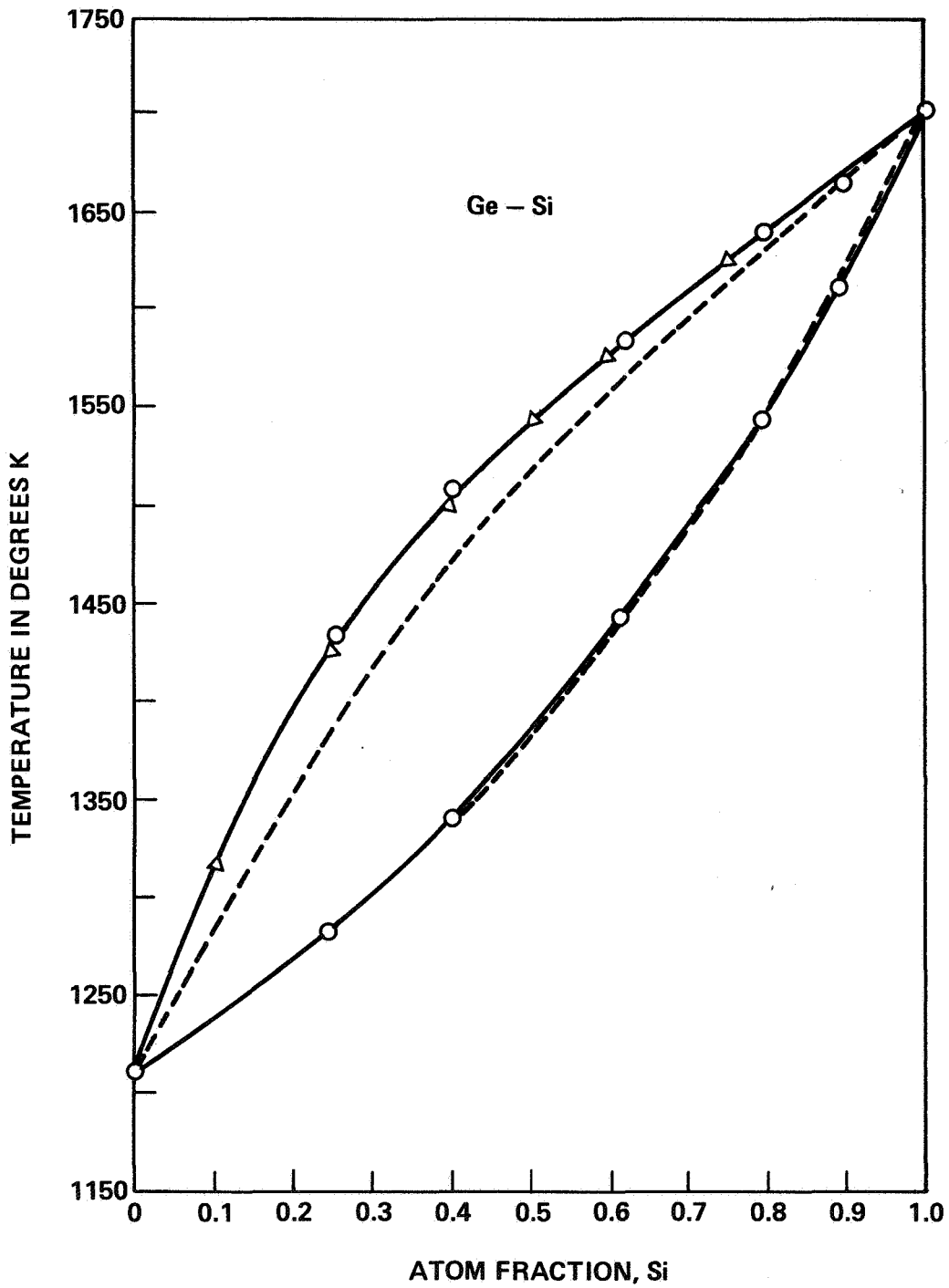
Figure IV-37.

DISTRIBUTION COEFFICIENT
OF Ge IN Si - Ge
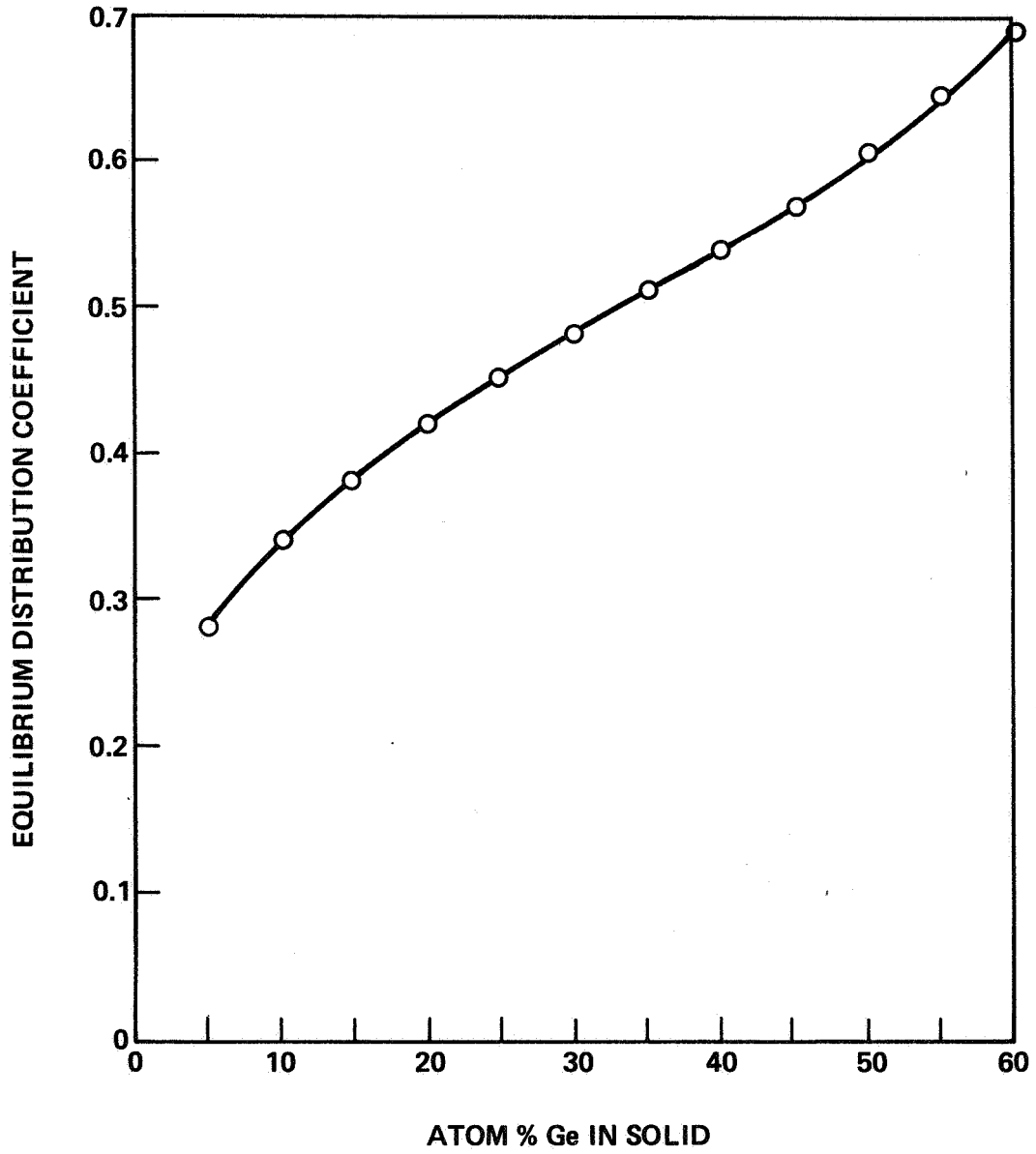
Figure IV-38.

DENSITY OF Si-Ge ALLOYS VS COMPOSITION

○ CHEMICAL ANALYSIS
▲ CALCULATED

d, GM CM⁻³

C(AT % Ge)

Figure IV-39.

157
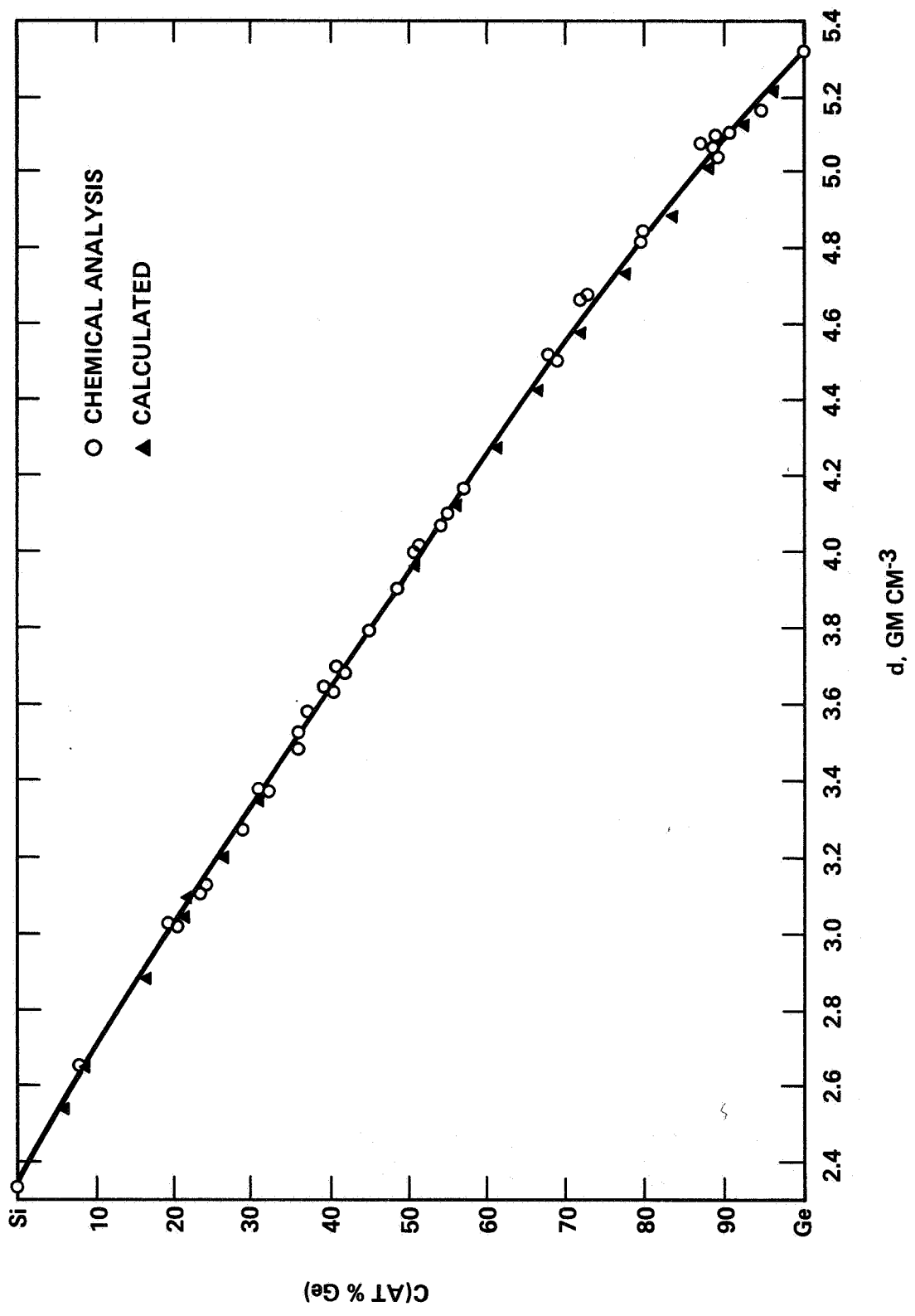
Si – Ge LATTICE PARAMETER AS A FUNCTION OF DENSITY

d (GM CM^{-3})

a(Å)
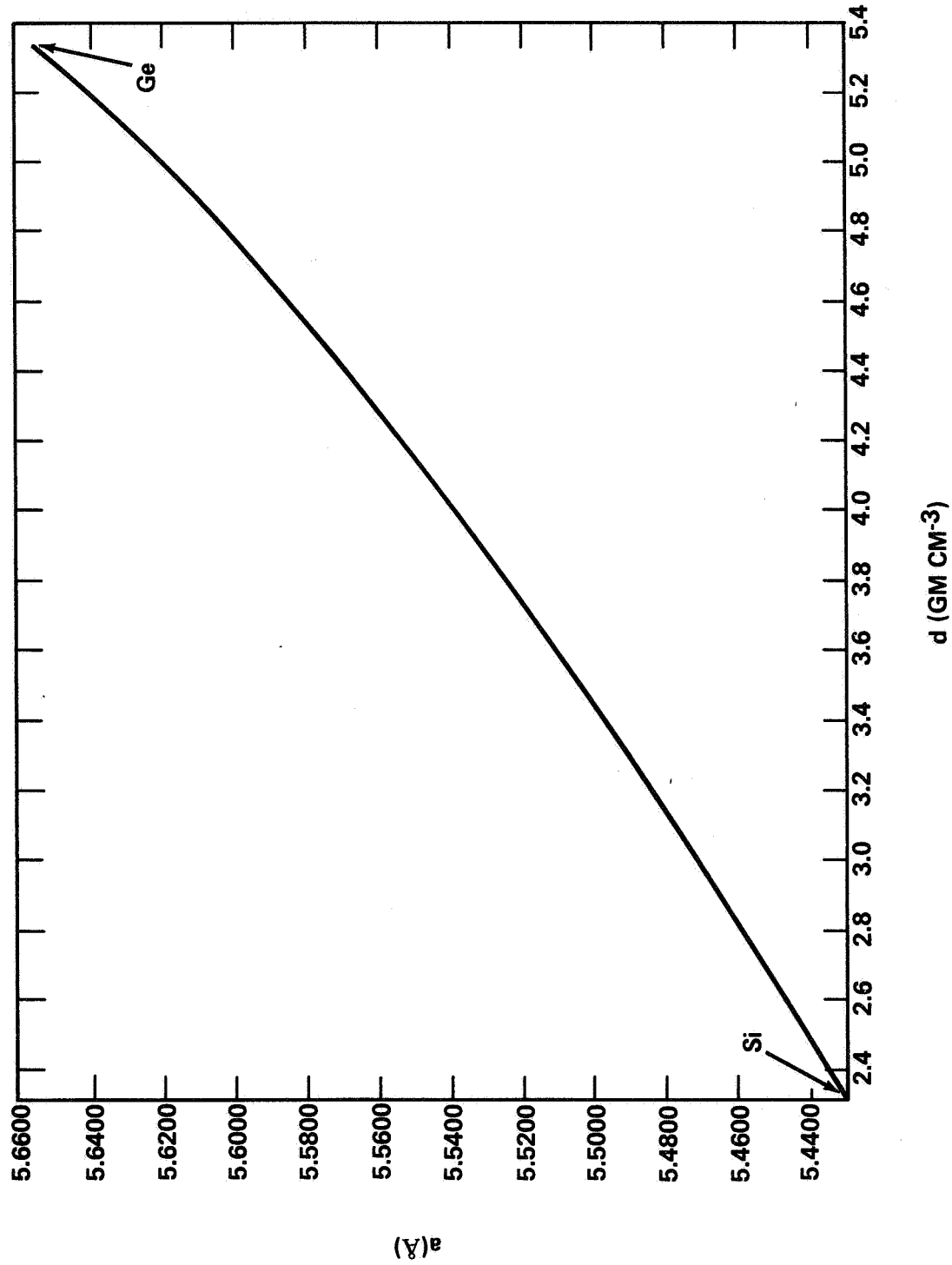
Figure IV–40.

ATOMIC FRACTION Ge VERTICAL SECTION

Figure IV-41.

159
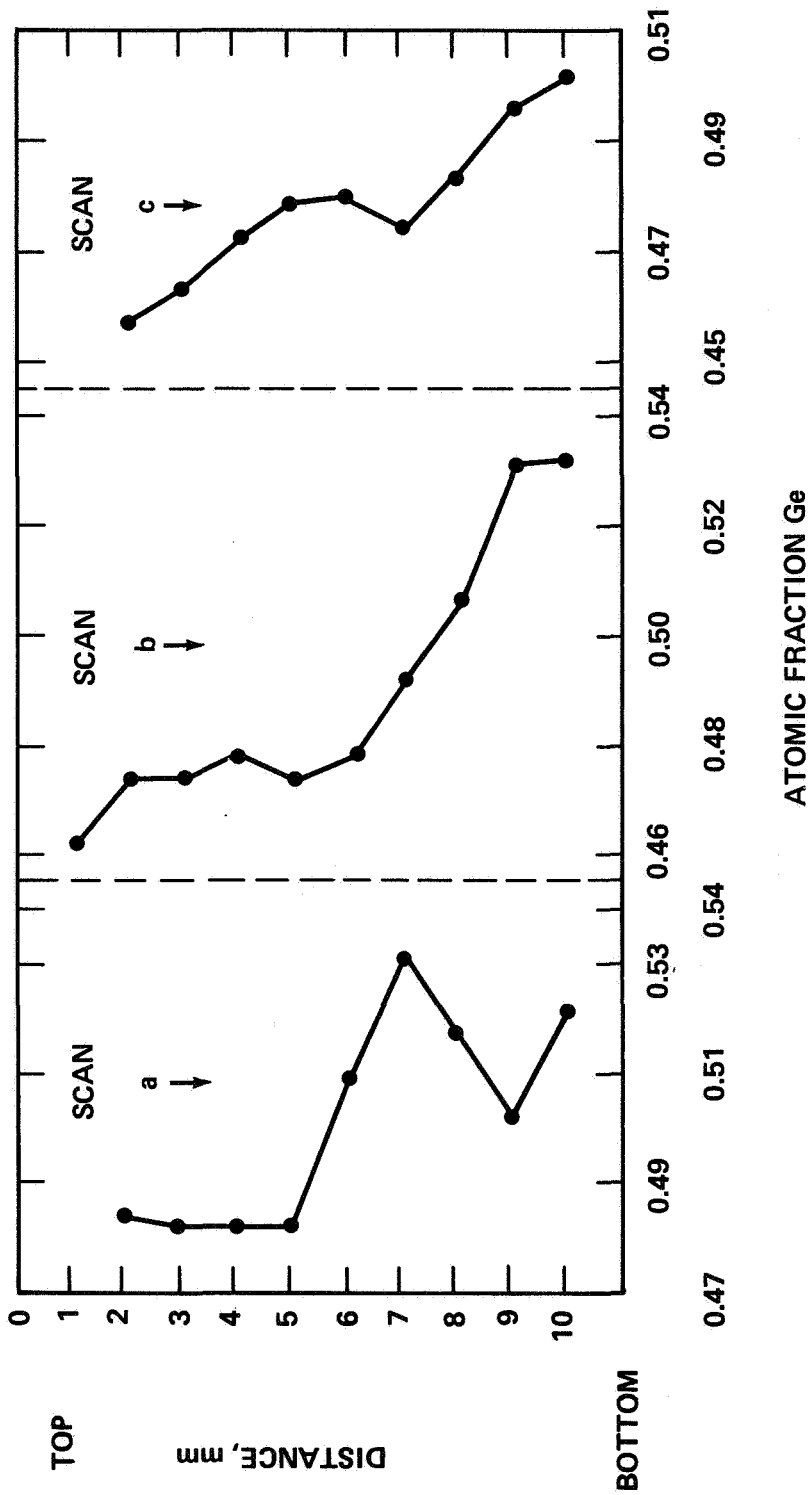
ΔGe CONCENTRATION TOP TO BOTTOM HORIZONTAL FREEZE VS RATE
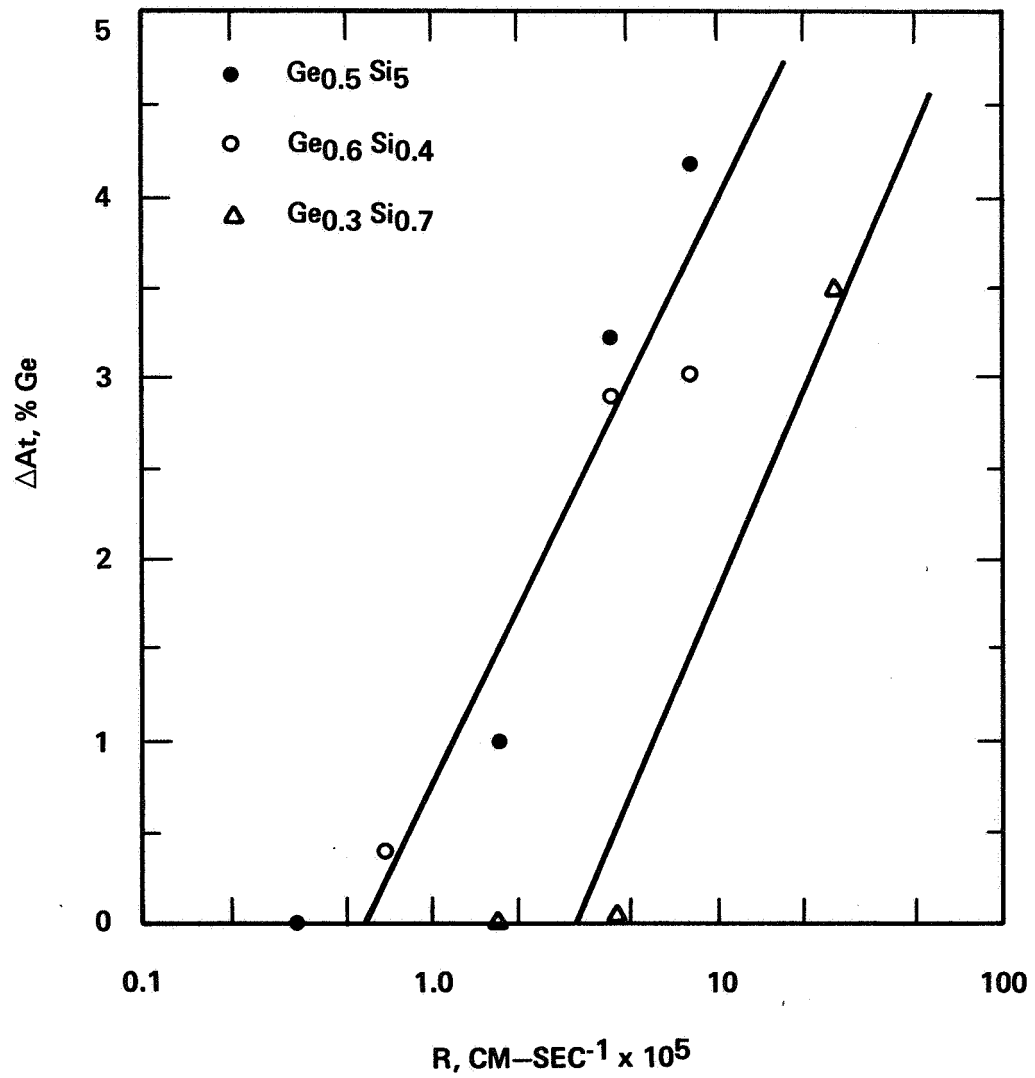
Figure IV-42.

Δ Ge CONCENTRATION TOP TO BOTTOM VS COMPOSITION

$R = 4.4 \times 10^{-5}$ CM–SEC^{-1}

COMPOSITION, ATOMIC FRACTION Ge

ΔAt, % Ge

Figure IV-43.

161
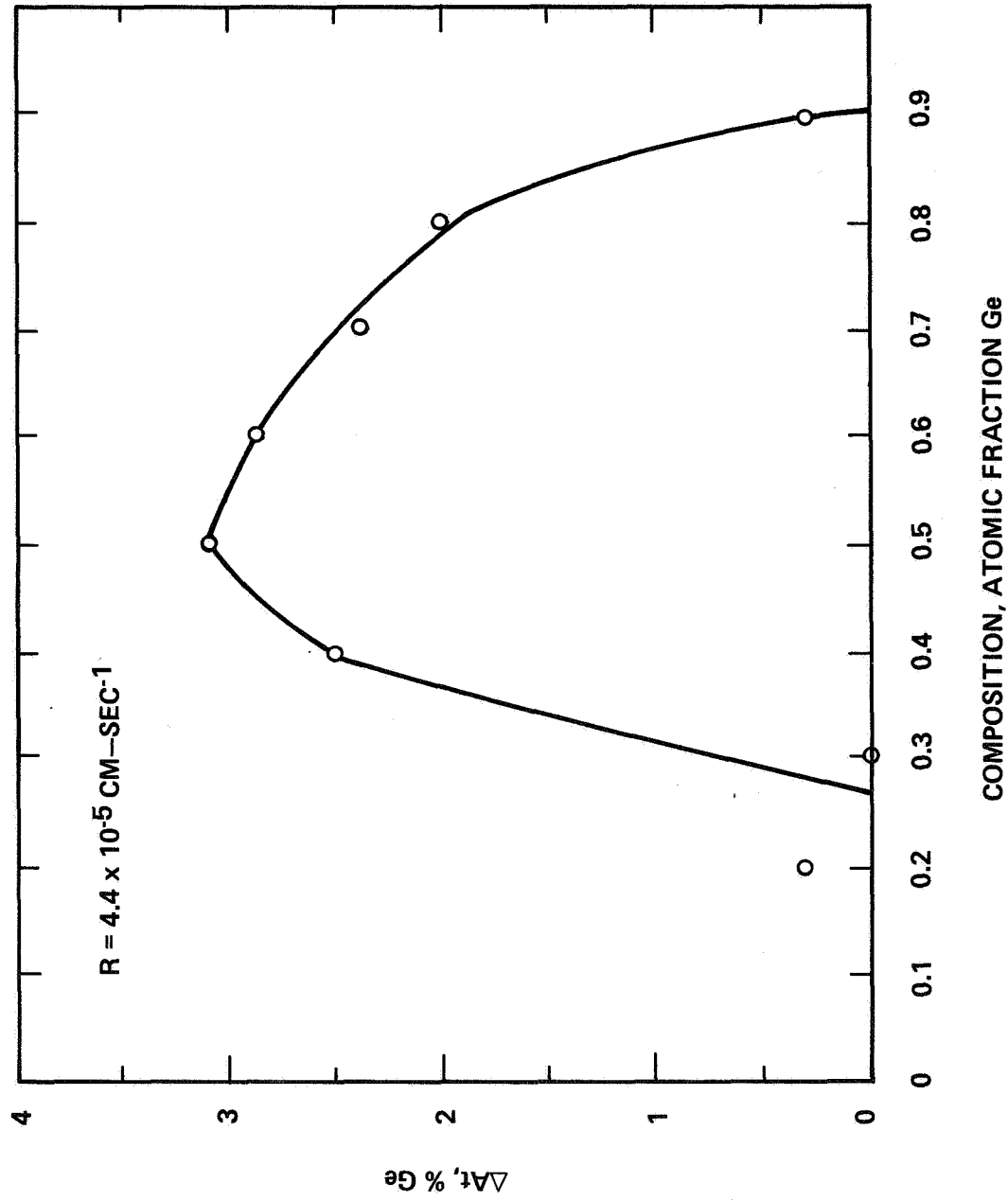
VARIATION OF LATTICE PARAMETER WITH TEMPERATURE OF Si - Ge
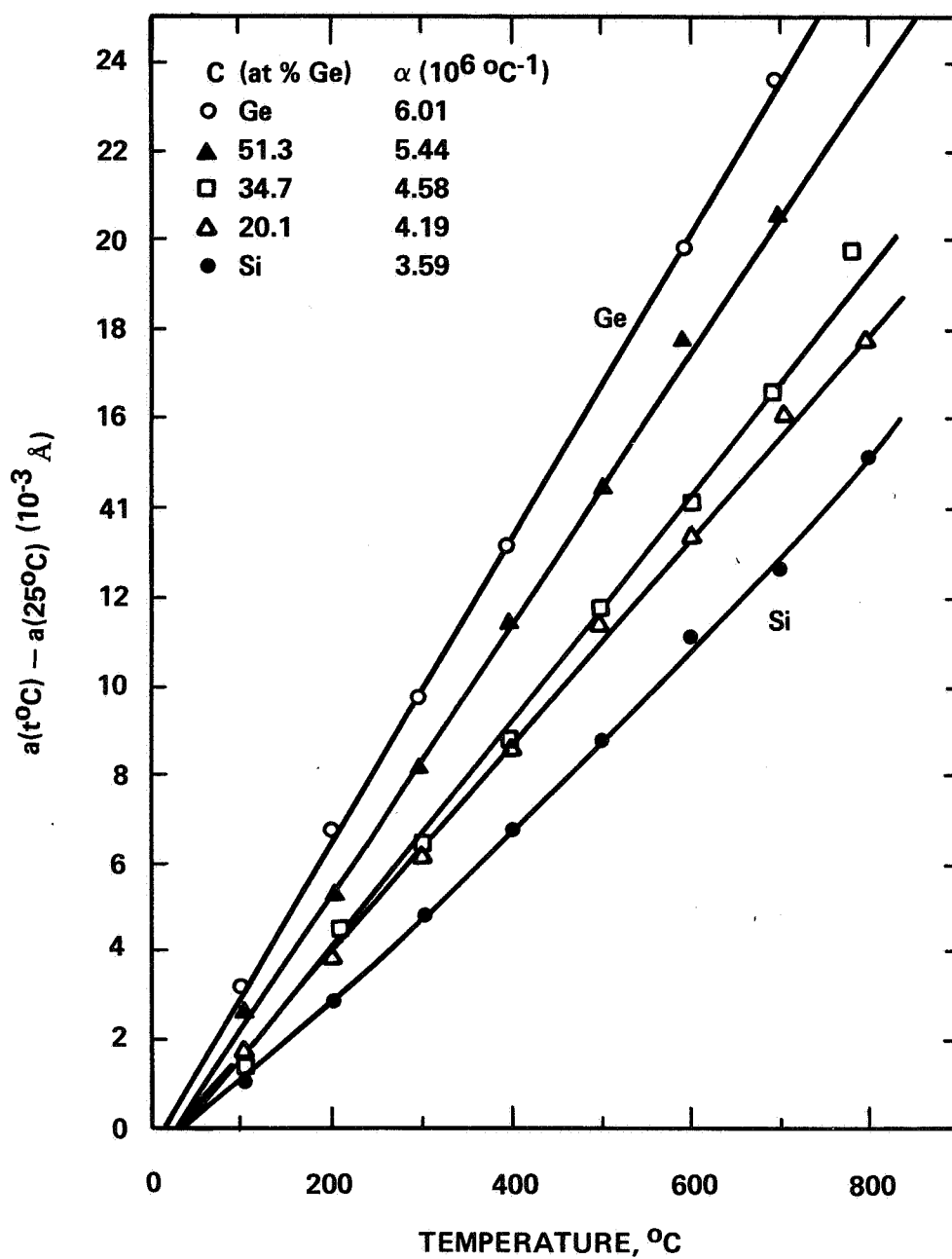
Figure IV-44.

THERMOELECTRIC FIGURE OF MERIT
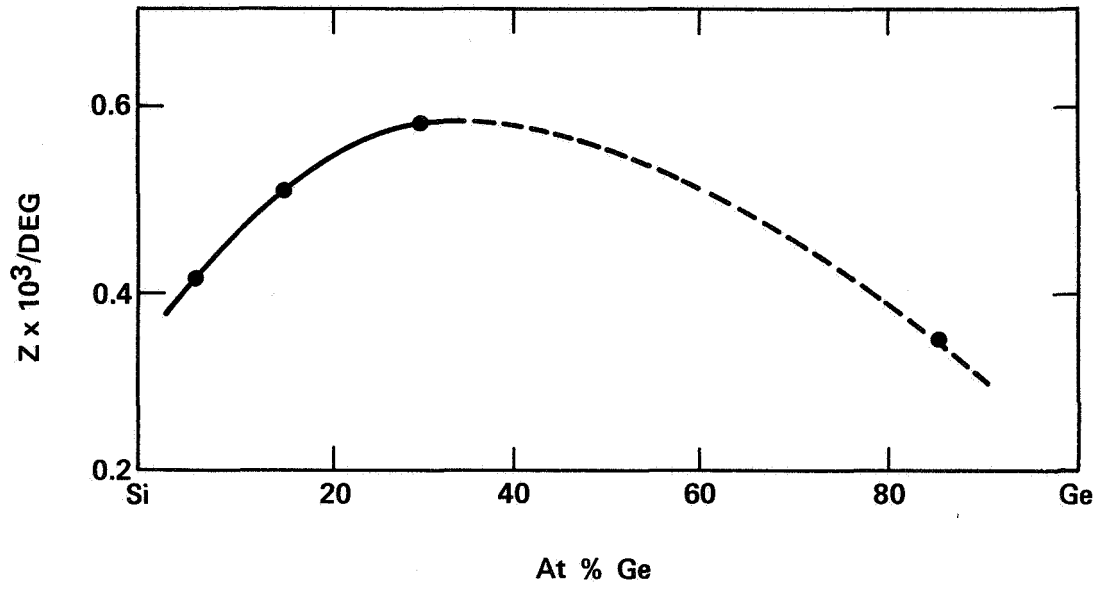
Figure IV-45.

V. DETERMINING THE MARANGONI EFFECT

A. REVIEW OF LITERATURE SURFACE TENSION DATA FOR MOLTEN SILICON

Stephen Hardy
National Bureau of Standards
Washington, DC

Measurements of the surface tension of molten silicon have been attempted by a number of workers over the last thirty years (Table V-1). Although the values cluster around 730 mJ/m^2, there is evidence that the surface tension of clean silicon surfaces is much higher than this. The work of Reference 2 found that the surface tension increased from 730 mJ/m^2 to 860 mJ/m^2 in about 15 min in a hydrogen atmosphere suggesting a reduction in oxygen activity. Thus the 730 mJ/m^2 value commonly found may lie as much as 130 mJ/m^2 below the true value.

For Marangoni flow, the important parameter is the variation of surface tension with temperature, not the absolute value of the surface tension. There have been no measurements of this quantity for silicon. Estimates in the literature are, I believe, no more than guesses. For instance, a recent book gives $d/dT = -0.10$ mJ/m^2 °K and cites References 1A and 2 in the table. Presumably this value was calculated by taking the difference between the surface tension of Reference 1A and that found with ZrO$_2$ substrates in Reference 2. However, the surface tension value of [1A] appears to be a typographical error. The correct value from the original literature is listed as [1B]. Note that the use of the correct data would give a positive temperature coefficient, which is almost certainly wrong for a pure material. It is obvious that other pairs of numbers from the table give widely different temperature coefficients. In general, it is not possible to calculate temperature coefficients using surface tension measurements from different experiments because the systematic errors are usually larger than the changes in surface tension because of temperature variations.

The lack of good surface tension data for liquid silicon is probably due to its extreme chemical reactivity. Extensive efforts have not found a material which resists attack by molten silicon. Thus all of the sessile drip surface tension measurements are probably for silicon which is contaminated by the substrate materials.

TABLE V-1.

Temperature (°C)	Atm	Substrate	γ mJ/m^2	Reference	Method
1410	Ar	-	730	1A	drop weight
1410	Ar	-	720	1B	
1450	He	ZrO_2	725	2	
1450	He	TiO_2	730	2	sessile drop
1450	He	MgO	740	2	
1450	H	MgO	860	2	
1550	Vac.	?	720	3	sessile drop
1550	Vac.	?	750	4	sessile drop
1550	Ar	-	825	5	pendant drop

1A.   Handbook of Physics and Chemistry, Vol. 50, 1969.

1B.   Kek, P. H., Van Horn, W., Phys. Rev. 91, 512, 1953.

2.   Kingery, W. D. and Humenik, M., J. Phys. Chem., 57, 359, 1953.

3.   Geld and Petrushevski, Izv. A. N., OTN, 3, 160, 1961.

4.   Dshemilev, Popel, and Zarevski, Fiz. Met. i Met., 18, 83, 1964.

5.   Eljntin, Kostikov and Levin, Izv. Vys Uch Zav., Tsvetn. Met., 2, 131, 1970.

B. CALCULATIONS OF THE SURFACE TENSIONS OF LIQUID METALS

David G. Stroud
Department of Physics
The Ohio State University
Columbus, OH

A crucial ingredient in understanding the Marangoni effect and predicting its influence in gravity-free environments is a knowledge of the surface tension of liquid metals, particularly as a function of temperature and of impurity concentration. The work described in this presentation is aimed at understanding the surface tension of liquid metals and alloys from as close to first principles as possible. The two ingredients which are combined in these calculations are the electron theory of metals, as developed by many workers over the last twenty years or so, and the classical theory of liquids, as worked out within the framework of statistical mechanics. The results of this work are a new theory of surface properties of liquid metals which permits one to calculate the surface tensions and surface density profiles from knowledge purely of the bulk properties of the coexisting liquid and vapor phases. The method works quite well for those pure liquid metals on which it has been tested; work is now underway to extend it to mixtures of liquid metals, interfaces between immiscible liquid metals, and to the temperature derivative of the surface tension.

The basis of the theory is described in a recent publication by Mon and Stroud [1]. The surface tension is essentially the excess Helmholtz free energy per unit area required to form an interface between the liquid and the vapor. Our theory divides this free energy into two parts (1) a "local" part, arising from the fact that in going from the liquid to the vapor phase the liquid metal must be compressed or expanded away from its preferred equilibrium densities, and (2) a "gradient" term, which comes from the fact that a surface forces the liquid metal to be non-uniform when energetically it is favorable for the liquid to be in a uniform state. The actual surface profile results from a balance between these two competing terms. We find that a high surface tension is correlated with (1) a low compressibility, leading to a high resistance to compression or expansion, and (2) a high coefficient of the gradient term, which is related in a complicated way to the bonding between ions in the liquid metal.

We have tested the theory mentioned above by applying it to a group of ten simple metals, i.e., metals in which the valence electrons are free-electron-like and interact relatively weakly with the ionic cores. The results of this calculation are shown in Figures 1 and 2 of this summary, where the surface tensions (experimental and theoretical) are plotted against r_s. r_s is a linear measure of electron density and is defined by $(\frac{4}{3}\pi r_s^3)^{-1} = n_e$, where n_e is the average density of valence electrons. As may be seen, the theoretical and experimental numbers never differ by more than 30 percent or so, even though the measured surface tension differ among themselves by more than an order of magnitude.

Further tests of the method are described in References 1, 2, and 3, where, in addition to the pure liquid metals, liquid rare gases are considered. These resemble liquid metals in having interatomic forces which are roughly central and two-body, and thus are amenable to treatment by the same methods. In all cases, the agreement with experiment is quite satisfying, as shown in these papers.

Because of this encouraging initial success, we are now in the process of undertaking various extensions of this work in the hope of making close contact with materials directly relevant to the Materials Processing in Space program. Mon and Stroud have extended the theory to treat the interfacial tension between two immiscible liquid metals, and applied the method to treat molten Na-Li alloys. Preliminary calculations yield a surface tension of about 10 dyne/cm at a temperature of 500 K, where the two metals are somewhat but not perfectly soluble in each other. This number is very sensitive to temperature for this particular material. While 10 dyne/cm is rather low compared to the surface tensions of the two pure constituents, (2) is not unreasonable.

Further work is underway to calculate the surface tensions of pure liquid metals as a function of temperature. Initially, Wood and Stroud are concentrating on liquid Na, a metal which is quite well understood in bulk liquid form. It is hoped to understand precisely what bulk parameters affect not only the surface tension but its temperature derivative. If this work is successful, it is intended to consider liquid Ga as a next application, with the intention of making contact with the experimental work of Hardy and Fine [4], and possible also liquid Si, which is a simple metal in its liquid phase and which is potentially of much importance for the gravity-free materials-processing program. Also underway is a calculation in which W. H. Shih and Stroud are trying to use the alloy form of the theory to understand what kinds of impurities will most strongly affect the surface tension of various liquid metals, and which properties of these impurities are most important in this effect. Initially, this work will consider metal-metal mixtures, but it may be possible at some later date to extend the work to such important contaminants as oxide overlays or other nonmetals, most likely only in a semi-empirical way.

REFERENCES

1.   K. K. Mon and D. Stroud, Phys. Rev. Lett. 45, 817, 1980.

2.   C. Ebner, W. F. Saam, and D. Stroud, Phys. Rev. A 14, 2264, 1976.

3.   D. Stroud, proposal to National Aeronautics and Space Administration, March 1981.

4.   S. C. Hardy and J. Fine, NBS report NBS1R 80-202 (July 1980, unpublished).

Calculated and experimental surface tensions of a number of simple liquid metals at their freezing point. The calculated numbers are from Mon and Stroug, Ref. 1. The results are plotted as a function of r_s, a linear measure of conduction electron density n_e. r_s is defined by $(4 \pi r_s^3/3)^{-1} = n_e$.
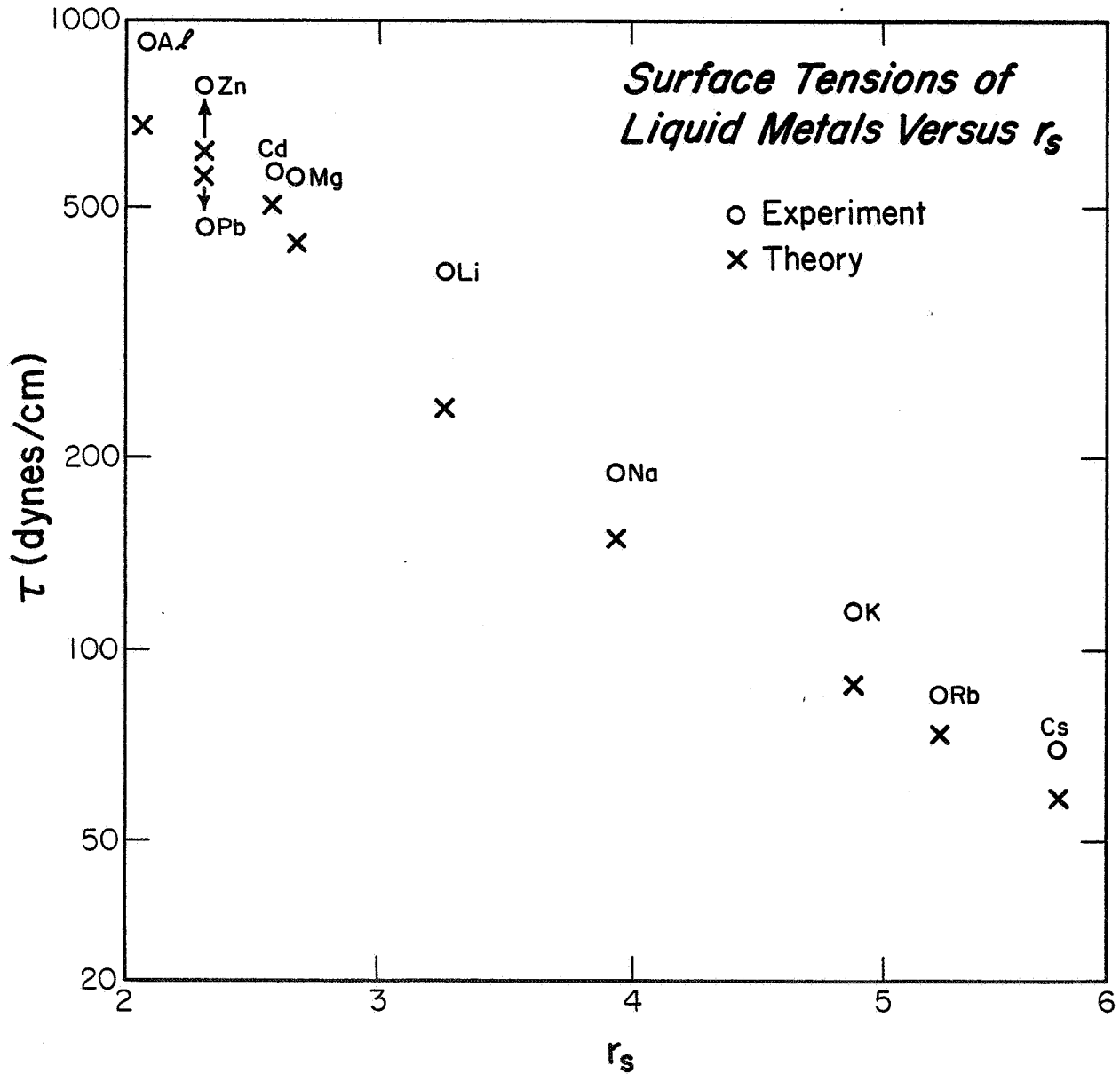
Figure V-1.

Comparison of the theoretical surface tensions with experiment, presented in tabular form. The columns represent the temperature at which the calculation and measurement are carried out, the compressibility of the liquid, the core-radius characterizing the liquid metal pseudopotential, the coefficient of the gradient term in the free energy, the experimental (theoretical) surface tension, and the half-width of the surface density profile. Details are given in Ref. 1.

	Temperature (K)	K_T^a (10^{-12} cm²/dyn)	R_{ec}^b (a_0)	K'/a_0^5 (10^8 K)	τ_{expt}^c [τ_{theor}]^c (a.u.)	w^d (a_0)
Li$^+$	452	9.3	1.40	0.0867	398 [242]	5.11
Na$^+$	371	18.6	1.69	0.228	191 [151.6]	6.39
Na$^+$	452	21.0	1.69	0.242	$\cdots$ [143.8]^e	
K$^+$	337	38.2	2.226	0.579	115 [88]	7.63
Rb$^+$	312	49.3	2.4	0.792	85 [74]	8.28
Cs$^+$	302	68.8	2.62	1.02	70 [57]	8.91
Mg^{+2}	924	4.0	1.38	0.154	559 [436]	3.96
Zn^{+2}	693	2.5	1.27	0.0805	782 [612]	3.47
Cd^{+2}	594	3.2	1.405	0.139	570 [504]	3.66
Al^{+3}	914	2.42	1.117	0.12	914 [666]	3.66
Pb^{+4}	600	3.49	1.48	0.362	468 [563]	4.46

[a] From Ref. 21.
[b] Empty-core radius in atomic units, from Ref. 20.
[c] From Eq. (4).
[d] With use of Eq. (3).
[e] With $(d\tau/d\Gamma)_{expt} = -0.1$ dyn/cm·K and $(d\tau/d\Gamma)_{theor} = -0.09$ dyn/cm·K.

Figure V-2.

172

VI.   MODELING AND CHARACTERIZING THE SILICON FLOAT-ZONE

A. MODELING OF THE FLOAT-ZONE PROCESS

Robert A. Brown
Department of Chemical Engineering
Massachusetts Institute of Technology
Cambridge, MA

SUMMARY

This research is directed towards a fundamental understanding of the inter-action of heat, mass, and momentum transport in the floating-zone method for growing single crystals from the melt. To accomplish this goal we are developing methods for detailed numerical simulation of the transport phenomena in a floating-zone. The results of these calculations can be combined with careful experiments to determine the effects of solidification-induced, surface-tension-driven, and buoyancy-driven convection in establishing dopant redistribution in the melt and the roles of heat transfer in crystal and melt and melt/solid interface shape in determining crystal quality.

To date, state-of-the-art finite-element techniques have been developed for efficiently calculating the influence of natural convection in the melt on the shape of a melt/crystal interface and dopant segregation in the crystal. These techniques are demonstrated here for solidification by the Bridgman technique, another system of NASA interest. Extension of these methods to the floating-zone system has begun. Numerical techniques have been developed that can calculate the shapes of both the melt/solid and melt/gas interfaces simultaneously with the thermal fields in melt and solid.

Models for the fluid flows due to the rotation of the feed and crystal rods have been completed and the effects of these flows on dopant segregation are being studied, especially in the case of zones longer than can be achieved on Earth.

MOTIVATION

1. To provide a theoretical basis for analyzing results of careful experiments where limited output is available from the experiment.

   ● Macro- and Micro-segregation: Radial and Axial

   ● Melt/Solid Interface Shape

   Surface Temperature (?)

```
┌──────────────────────┐              ┌──────────────────────┐
│ FLUID MECHANICS      │ ↘ ↖          │                      │
│ (CRYSTAL-ROTATION)   │              │                      │
└──────────────────────┘              │   MASS TRANSFER/     │
┌──────────────────────┐ → →          │   DOPANT SEGREGATION │
│ HEAT TRANSFER        │ ← ←          │                      │
│ NATURAL CONVECTION   │              │                      │
└──────────────────────┘              └──────────────────────┘
┌──────────────────────┐ ↗ ↙
│ SURFACE-TENSION-DRIVEN│
│       FLOWS          │
└──────────────────────┘
```
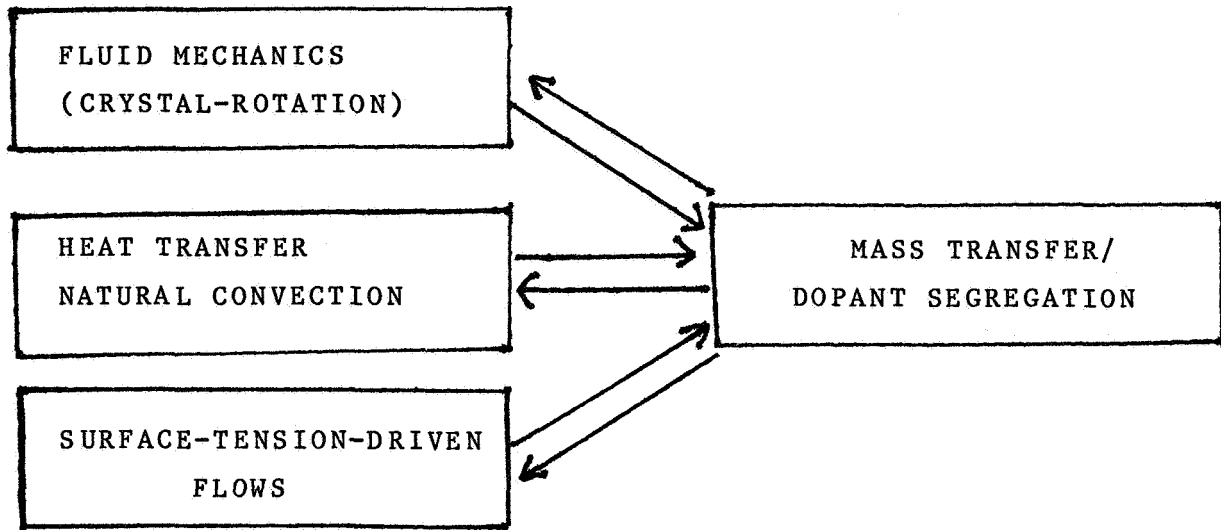
PROCESS CONSIDERED

- Floating-Zone Process: Zero-Gravity Operation
- Capillary Growth and Zone-Refining of Thin Sheets
- Directional Solidification

Figure VI-1.

REGIMES OF CONVECTION IN MELT GROWTH

NO CONVECTION	LAMINAR CONVECTION	OSCILLATORY CONVECTION	TURBULENCE
Only Possible In Idealized Systems	Small Scale Systems	⟷	⟶
Impossible In Floating Zone With Free-Surface		Industrial	Systems
Probably Not Desirable			

INTENSITY OF CONVECTION

PICTURE IS VALID FOR:
- Natural Convection
- Surface-Tension-Driven Flows
- Rotation-Driven Flows

Figure VI-2.

- STUDIES ARE A COMBINATION OF EXACT ANALYSIS AND DETAILED SIMULATION BY FINITE ELEMENT ANALYSIS

- OUR APPROACH HAS BEEN TO DECOUPLE THE PROBLEM. BASED ON
    - Low Prandtl Number
    - High Surface Tension

→BOTH VALID FOR SILICON

STAGES
1. HEAT TRANSFER ANALYSIS WITHOUT CONVECTION, BUT WITH:
       Melt/Solid Interfaces
       Gas/Melt Meniscus
2. CONVECTION AND SEGREGATION

Figure VI-3.

THE "COMPLETE" MODEL OF THE FLOATING ZONE

COMPLICATIONS

- HEAT TRANSFER*
  - Unknown Shapes of Melt/Solid Interfaces
  - Radiation
  - Coupling with Meniscus Shape and Crystal Radius

- CONVECTION

  - Natural Convection*
  - Rotation-Driven Flows*
  - Surface Tension Flows

Figure VI-4.

CONVECTION AND SEGREGATION ANALYSIS FOR DILUTE MELTS

- FINITE ELEMENT CALCULATION OF FLUID FLOW AND TEMPERATURE FIELDS INTERFACE SHAPES

- CALCULATION OF SOLUTE FIELD USING FLUID FLOW RADIAL SEGREGATION
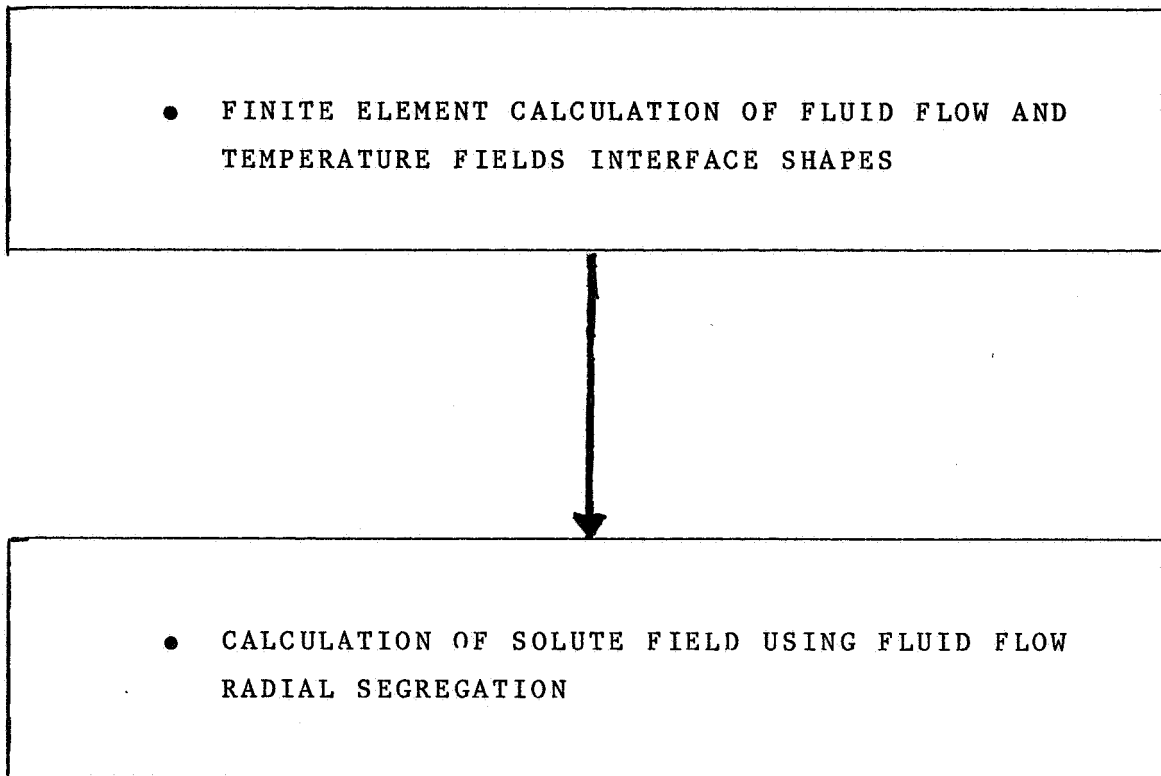
- EXAMPLE FROM DIRECTIONAL SOLIDIFICATION

Figure VI-5.

PROTOTYPE OF VERTICAL BRIDGMAN GROWTH

● STABILIZED AND DESTABILIZED OPERATION
DEPEND ON ORIENTATION OF GRAVITY

● MELT/SOLID INTERFACE SHAPE IS SET BY
HEAT TRANSFER:
  ● CONDUCTION IN MELT AND SOLID
  ● GROWTH INDUCED CONVECTION IN MELT AND SOLID
  ● NATURAL CONVECTION IN MELT

● ADIABATIC ZONE IS DESIGNED TO MAKE INTERFACE PLANAR.
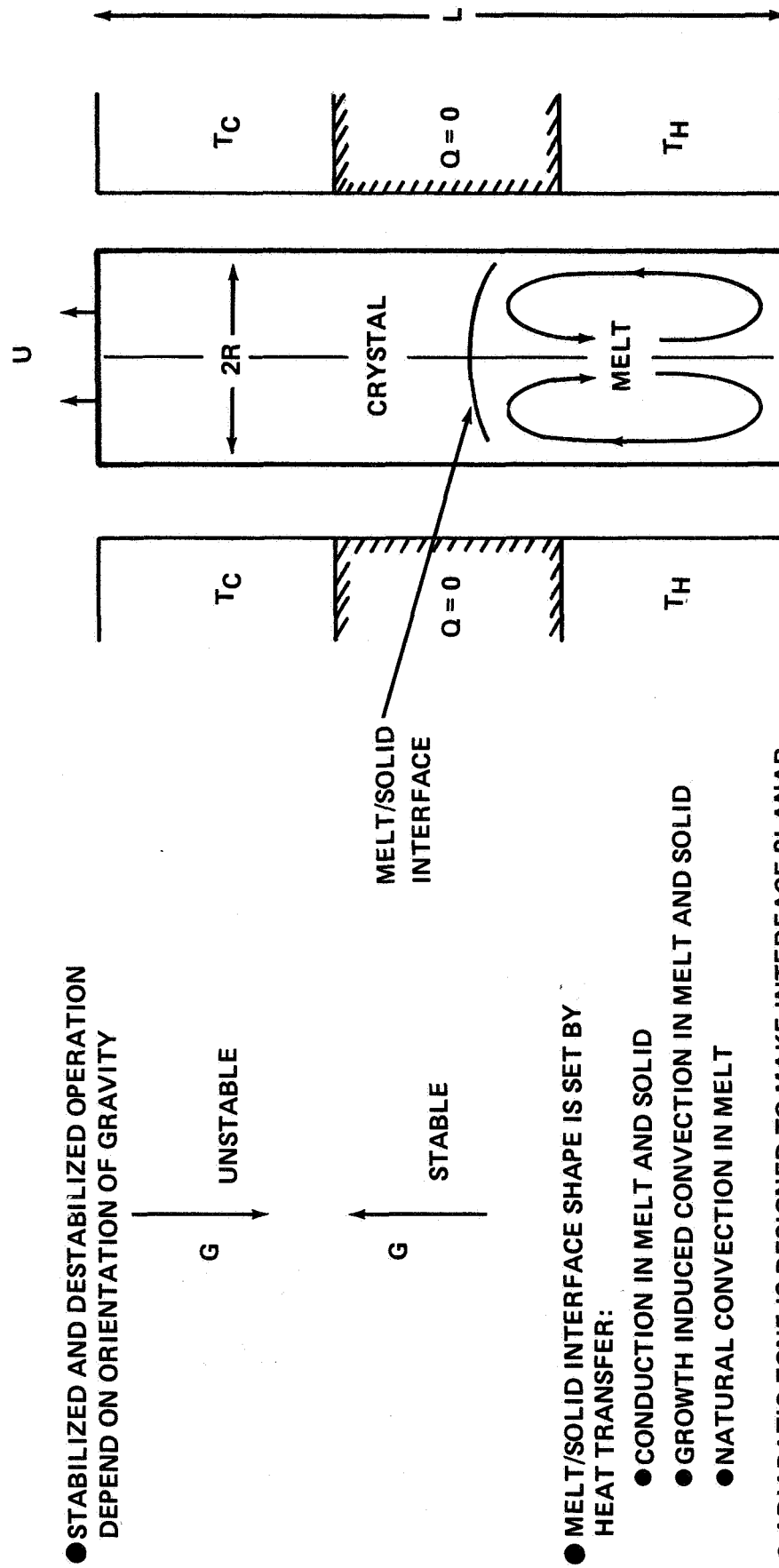
Figure VI-6.

CONVECTIONLESS GROWTH

P_E = 0.01, A = 1/4
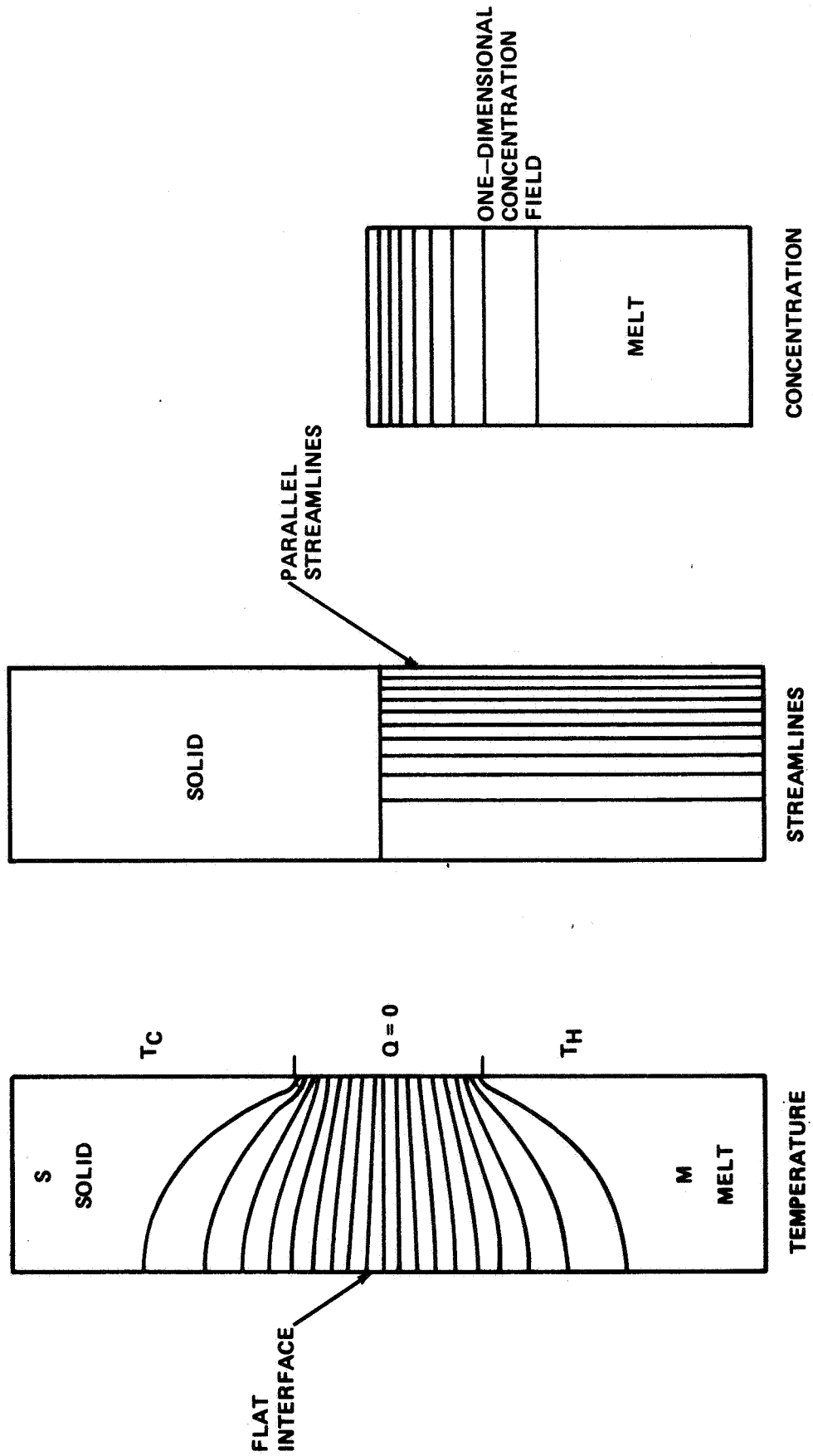
Figure VI-7.

STREAMLINES FOR DESTABILIZING TEMPERATURE GRADIENT

$P_R = 0.01$, $P_E = 0.01$, $A = 1/4$

Figure VI-8.

183
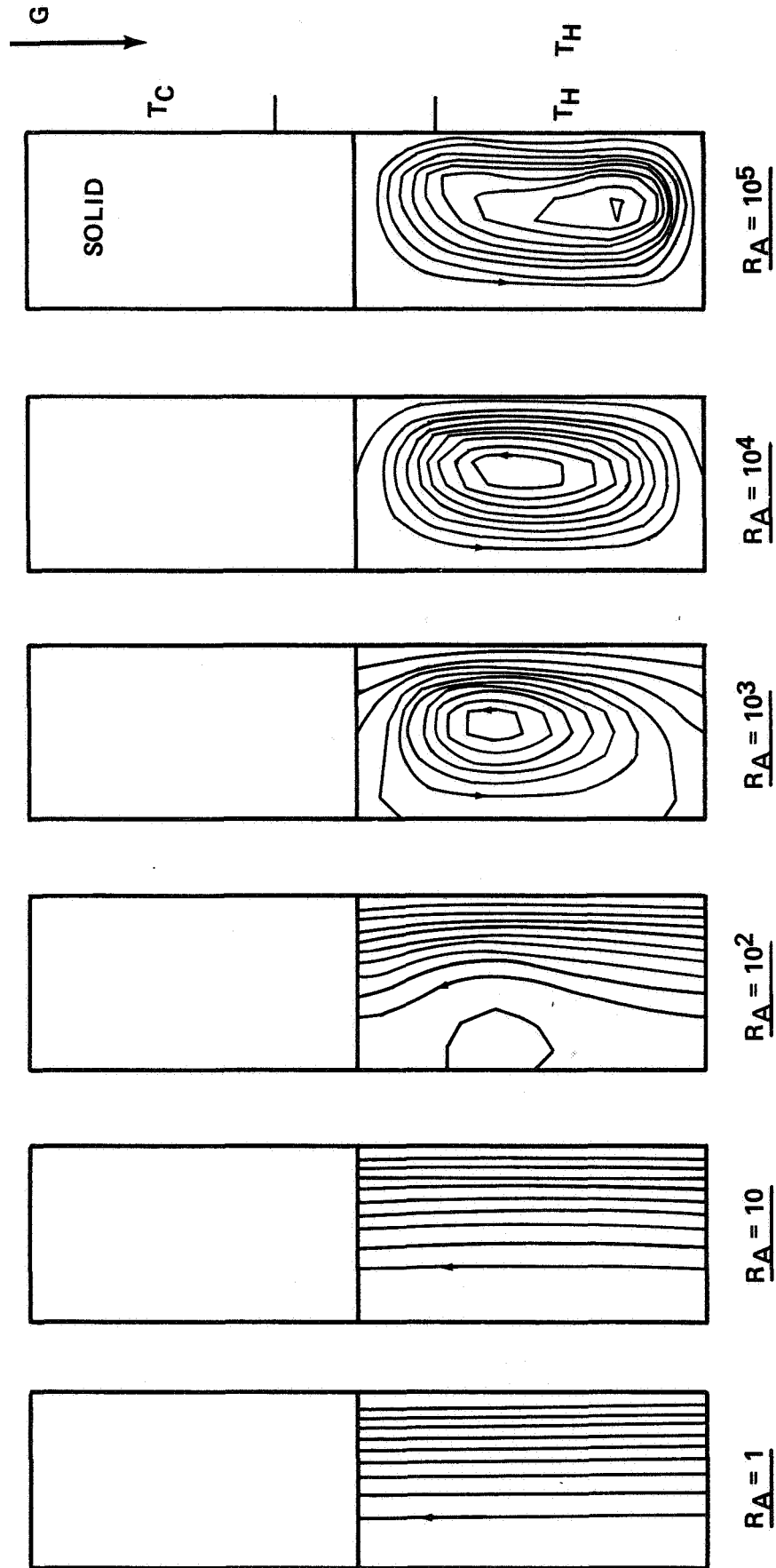
RADIAL SEGREGATION IN
DESTABILIZING TEMPERATURE
GRADIENT

$K = 0.1$

$P_E = 0.01$
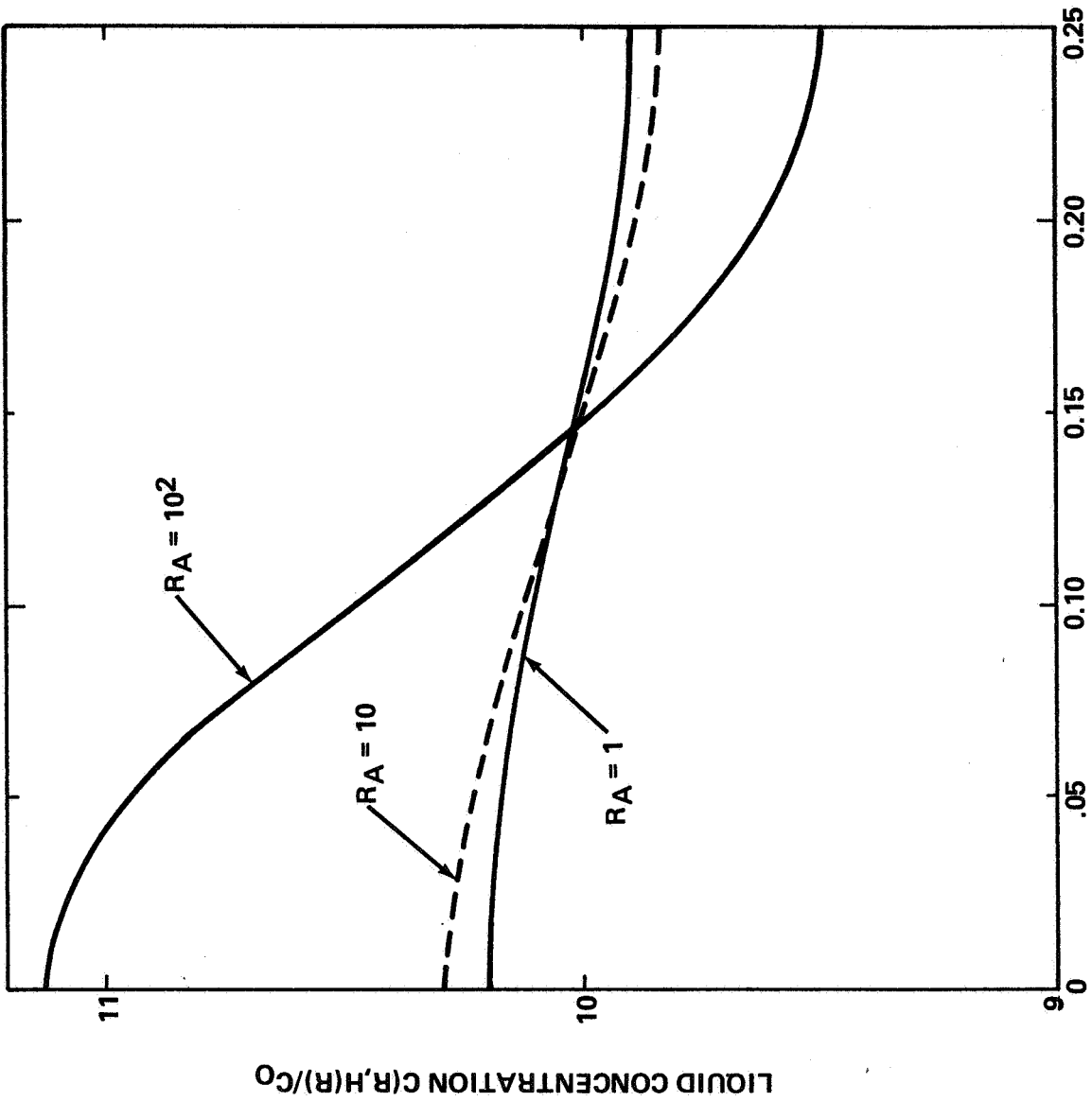
Figure VI-9.

STREAMLINES AND CONCENTRATION FIELDS FOR DESTABILIZING TEMPERATURE GRADIENT

TEMPERATURE GRADIENT

$P_E = 0.01, P_R = 0.01, A = 1/4$

STREAMLINES
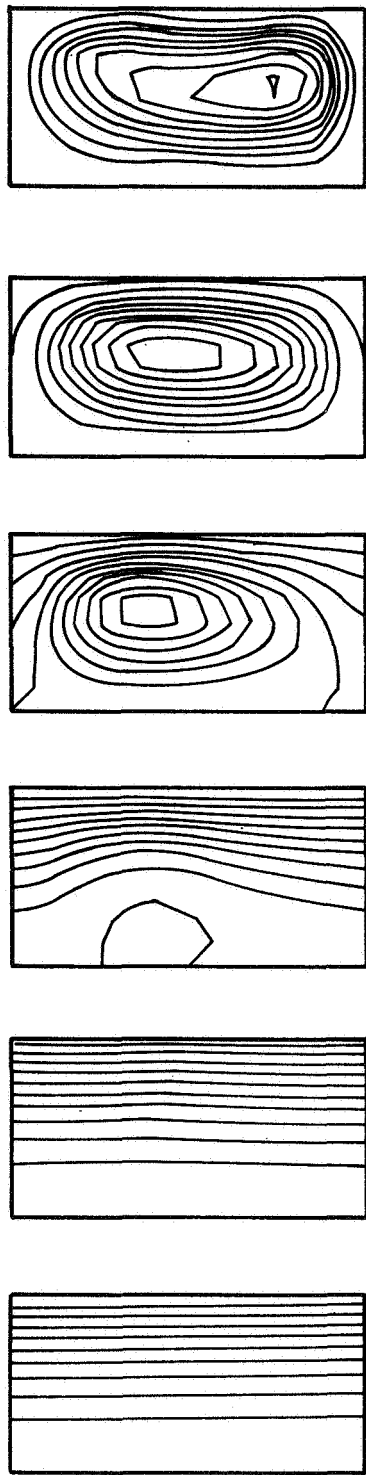
CONCENTRATION FIELDS

$R_A = 1$ $R_A = 10$ $R_A = 10^2$ $R_A = 10^3$ $R_A = 10^4$ $R_A = 10^5$

Figure VI-10.

185
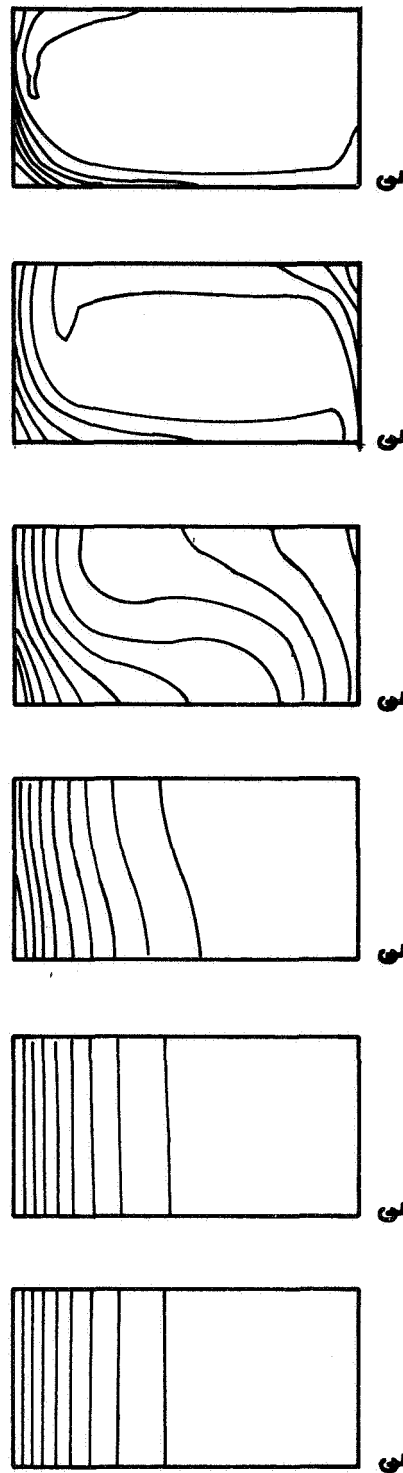
MELT/SOLID INTERFACE SHAPES
FOR DESTABILIZED GROWTH SYSTEM

$$P_R = 0.01 \quad A = 1/4$$
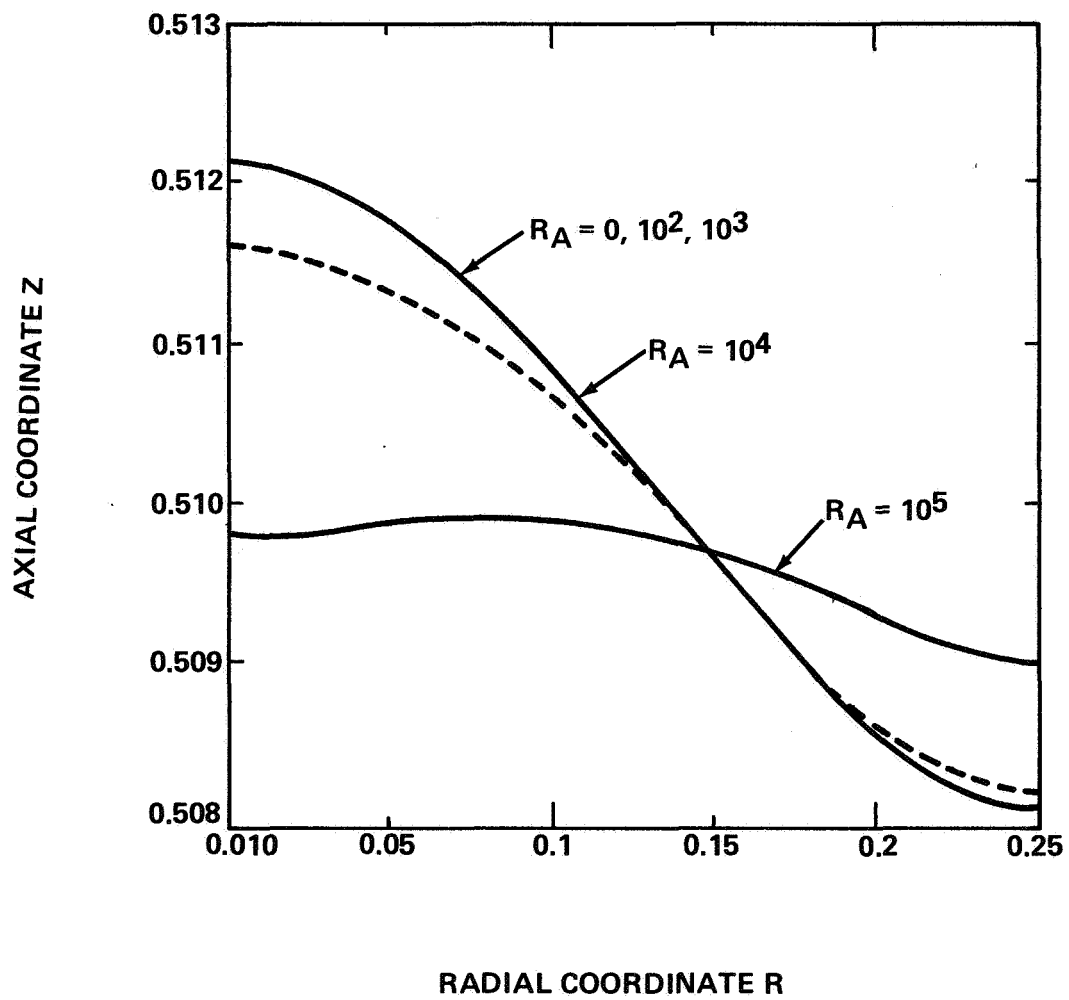
Figure VI-11.

RADIAL SEGREGATION PASSES THROUGH

A MAXIMUM WITH INCREASING CONVECTION
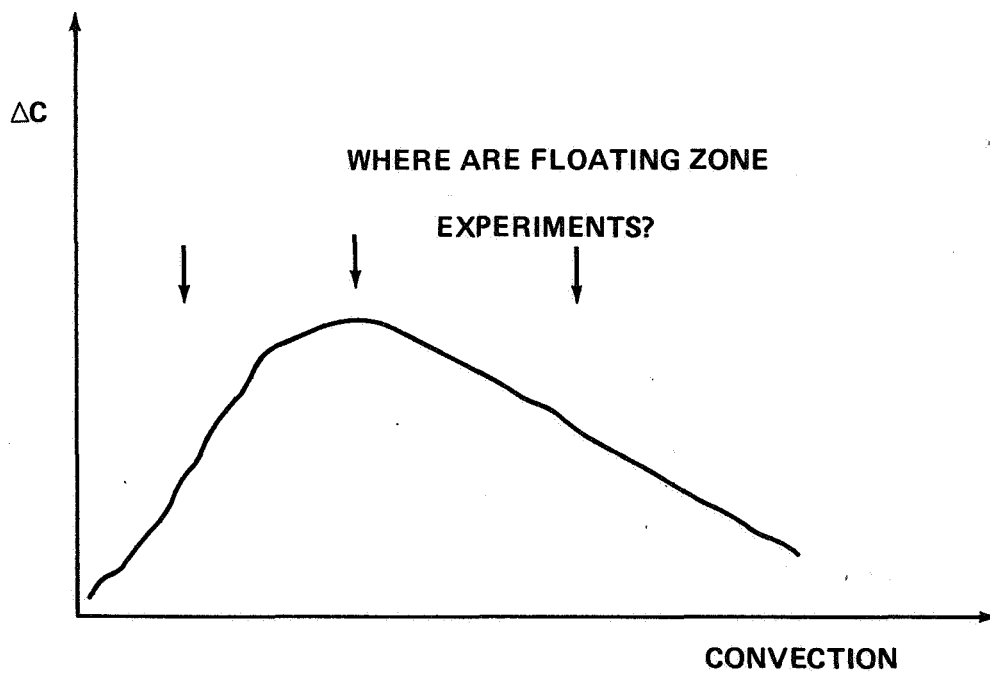
Figure VI-12.

B. FLOAT-ZONE CONTROL SURFACES

Larry M. Foster
Science Applications, Inc.
Huntsville, AL

The equations of state describing a simplified model of the float-zone process are given in Figure VI-13. The process and material parameters in Figure VI-13 are:

P_s	solid Peclet number
P_ℓ	liquid Peclet number
K_S	solid conductivity
K_ℓ	liquid conductivity
h_S	solid heat transfer coefficient
M	material melting temperature
T_1 and T_2	solid regions ambient temperatures
$\mathcal{L}_1$ and $\mathcal{L}_2$	interface parameters, e.g., the product of the crystal growth rate, the liquid density and the latent heat of solidification
T	material temperature
h(x)	liquid surface temperature.

Unfortunately, the abundance of arbitrary boundary conditions in Figure VI-13 over-pose the partial differential equations.

We propose to replace the boundary condition

$$-K_S \frac{\partial T}{\partial r} = h_S (T - T_1) , \quad r = 1 , \quad x < -Q$$

by

$$T(x,1) = f(x)$$

where $f(x)$ is to be computed. The unknown surface control temperature $f(x)$ will be constructed so that the resulting set of boundary conditions do not overpose the partial differential equations.
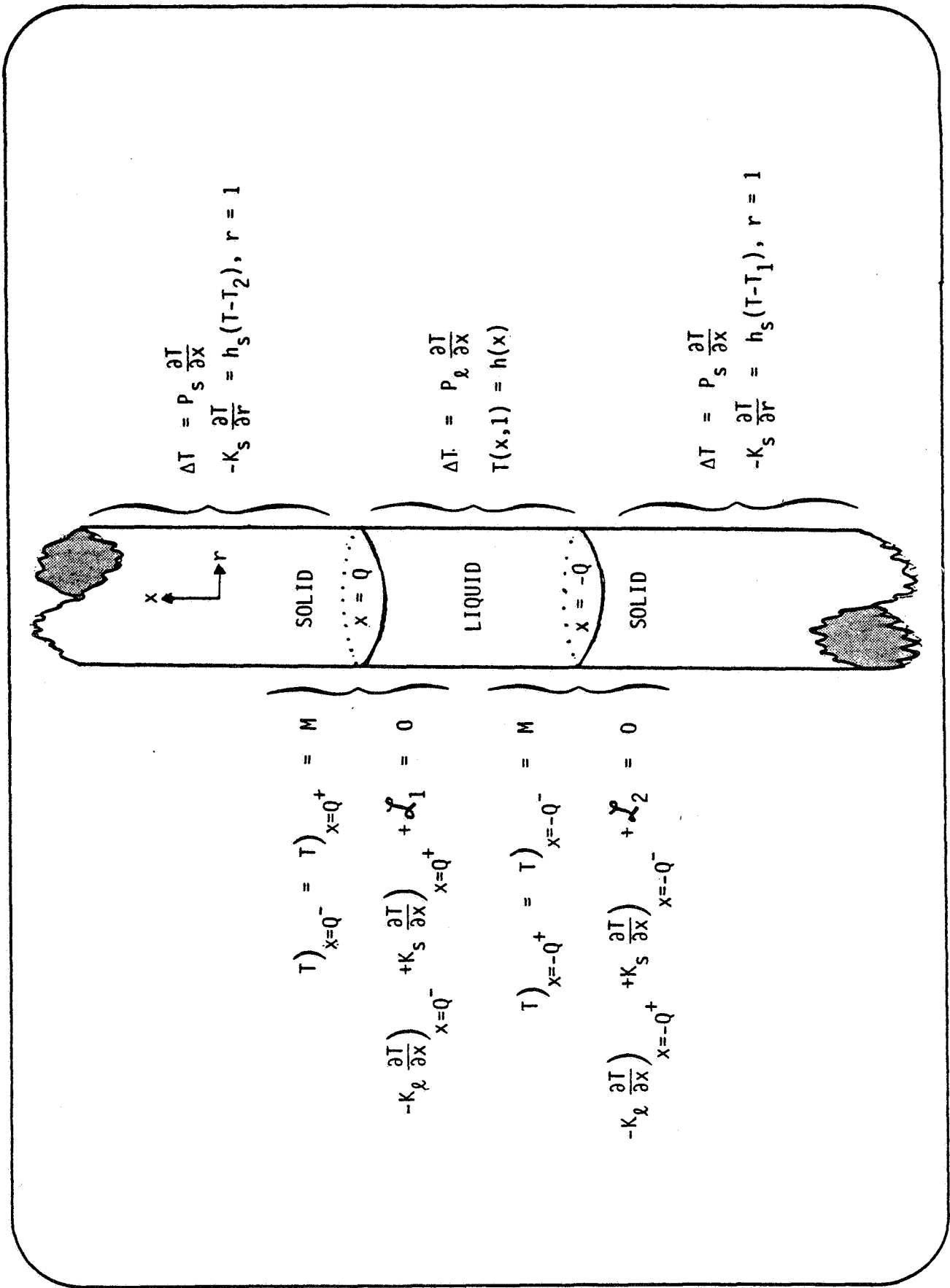
$\Delta T = P_s \dfrac{\partial T}{\partial x}$

$-K_s \dfrac{\partial T}{\partial r} = h_s(T-T_2)$, $r = 1$

$\Delta T = P_\ell \dfrac{\partial T}{\partial x}$

$T(x,1) = h(x)$

$\Delta T = P_s \dfrac{\partial T}{\partial x}$

$-K_s \dfrac{\partial T}{\partial r} = h_s(T-T_1)$, $r = 1$

SOLID

$x = Q$

LIQUID

$x = -Q$

SOLID

x r

$T)_{x=Q^-} = T)_{x=Q^+} = M$

$-K_\ell \dfrac{\partial T}{\partial x}\Big)_{x=Q^-} + K_s \dfrac{\partial T}{\partial x}\Big)_{x=Q^+} + \mathcal{L}_1 = 0$

$T)_{x=-Q^+} = T)_{x=-Q^-} = M$

$-K_\ell \dfrac{\partial T}{\partial x}\Big)_{x=-Q^+} + K_s \dfrac{\partial T}{\partial x}\Big)_{x=-Q^-} + \mathcal{L}_2 = 0$

Figure VI-13.

$\Delta T = P_s \dfrac{\partial T}{\partial X}$

$T(-\alpha, r) = A(r)$
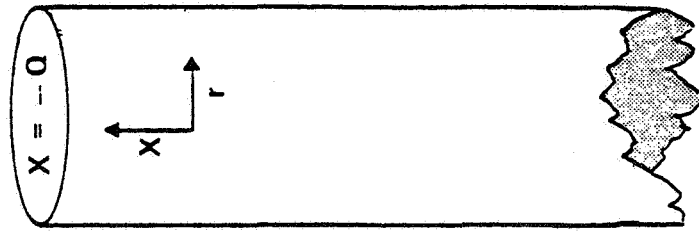
$\dfrac{\partial}{\partial X} T(-\alpha, r) = B(r)$ ⟵ KNOWN

$T(X, 1) = f(X)$ ⟵ UNKNOWN

SAI-12847

Figure VI-14.

190

PROBLEM: COMPUTE f(x) SUCH THAT THE SOLUTION OF

$$
\begin{cases}
\Delta T = P_s \dfrac{\partial T}{\partial x}, & x < -Q, \ 0 < r < 1 \\[2mm]
T(x,1) = f(x) \\[2mm]
T(-Q,r) = A(r)
\end{cases}
$$

(1)

ALSO SATISFIES

(2) $\dfrac{\partial T}{\partial x}(-Q,r) = B(r)$

REMARK:

IF A BOUNDARY CONDITION OF THE FORM

$$K \frac{\partial T}{\partial r} = h(T - g(x))^{\alpha}, \ r = 1$$

IS DESIRED, FIRST SOLVE (1) AND (2) AND THEN SOLVE

$$K \frac{\partial T}{\partial r} = h(f(x) - g(x))^{\alpha}$$

FOR g(x).

Figure VI-15.

191

METHOD OF SOLN:

DEFN: $T(x,r) = \theta(x,r) + f(x)$

$G(x) = P_s f' - f''$

$A(r) - f(-Q) = \mathcal{Q}(r)$

$B(r) - f'(-Q) = \mathcal{B}(r)$

P.D.E.

(3) $\begin{cases} \Delta\theta = P_s\theta_x + G(x) \\ \theta(-Q,r) = \mathcal{Q}(r) \\ \theta_x(-Q,r) = \mathcal{B}(r) \\ \theta(x,1) = 0 \end{cases}$

SOLVE:

$\begin{cases} \Delta\psi(r) + \lambda^2\psi(r) = 0 \\ \psi(1) = 0 \\ \psi'(0) = 0 \end{cases}$

$\psi_n(r) = J_o(\lambda_n r), \quad J_o(\lambda_n) = 0$

Figure VI-16.

DUAL INTEGRAL TRANSFORM PAIR:

(4)
$$
\begin{cases}
\theta(x,r) = \displaystyle\sum_{M=1}^{\infty} \frac{2\,\psi_M(r)}{J_1^{\ 2}(\lambda_M)}\,\overline{\theta}_M(x) \\[3ex]
\overline{\theta}_M(x) = \displaystyle\int_0^1 \theta(x,r)\,\psi_M(r)r\,dr
\end{cases}
$$

LET:
$$
\overline{G}_M(x) = \int_0^1 G(x)\,\psi_M(r)r\,dr
$$

$$
\mathcal{Q}(r) = \sum_{n=1}^{\infty} \mathcal{Q}_n\,J_0(\lambda_n r)
$$

$$
\mathcal{B}(r) = \sum_{n=1}^{\infty} \mathcal{B}_n\,J_0(\lambda_n r)
$$

SOLVE:

(5)
$$
\begin{cases}
-\lambda_M^{\,2}\,\overline{\theta}_M + \overline{\theta}_M^{\,\prime\prime} = P_s\,\overline{\theta}_M^{\,\prime} + \overline{G}_M \\[3ex]
\overline{\theta}_M(-Q) = \mathcal{Q}_M\,\dfrac{J_1^{\ 2}(\lambda_M)}{2} \\[3ex]
\overline{\theta}_M^{\,\prime}(-Q) = \mathcal{B}_M\,\dfrac{J_1^{\ 2}(\lambda_M)}{2}
\end{cases}
$$

Figure VI-17.

<u>SOLN</u>:   LET $S_n = \sqrt{P_s^2 + 4\lambda_n^2}$ ·THEN

$$\overline{G}_M(x) = \frac{J_1{}^2(\lambda_M)}{2\,S_M}\left(\mathcal{B}_M - \frac{P_s - S_M}{2}\,\mathcal{a}_M\right)\,\mathrm{Exp}\left(\frac{P_s + S_M}{2}\,(x+Q)\right)$$

$$+\,e^{\frac{P_s + S_M}{2}\,x}\int_{-Q}^{x}\frac{\overline{G}_M(t)}{S_M}\,e^{-\frac{P_s + S_M}{2}\,t}\,dt$$

$$+\,\frac{J_1{}^2(\lambda_M)}{2\,S_M}\left(\frac{P_s + S_M}{2}\,\mathcal{a}_M - \mathcal{B}_M\right)e^{\frac{P_s - S_M}{2}\,(x+Q)}$$

$$-\,\mathrm{Exp}\left(\frac{P_s - S_M}{2}\,x\right)\int_{-Q}^{x}\frac{\overline{G}_M(t)}{S_M}\,e^{-\frac{P_s - S_M}{2}\,t}\,dt$$

<u>REQUIRE</u>:

(6)
$$\lim_{x \to -\infty}\left[\frac{J_1{}^2(\lambda_M)}{2\,S_M}\left(\frac{P_s + S_M}{2}\,\mathcal{a}_M - \mathcal{B}_M\right)\mathrm{Exp}\left(\frac{P_s - S_M}{2}\,Q\right)\right.$$

$$\left.-\int_{-Q}^{x}\frac{\overline{G}_M(t)}{S_M}\,e^{-\frac{P_s - S_M}{2}\,t}\,dt\right]e^{\frac{P_s - S_M}{2}\,x} = 0$$

<u>FOR CONVENIENCE</u>:

$$G(x - Q) = E(-x),\quad x < 0$$

Figure VI-18.

194

CONTROL EQ:

$$\frac{\lambda_M \ J_1(\lambda_M)}{2} \left(\mathcal{B}_M - \frac{P_s + S_M}{2} \mathcal{Q}_M \right)$$

$$= \int_0^\infty E(t) \ e^{-\frac{S_M - P_s}{2}} \ dt$$

APPROXIMATE E(t):   LET $E(t) \approx \sum_{k=1}^{N} a_k \ e^{-kt}$

SOLVE:

$$\frac{\lambda_M \ J_1(\lambda_M)}{2} \left(\mathcal{B}_M - \frac{P_s + S_M}{2} \mathcal{Q}_M \right)$$

$$= \int_0^\infty \sum_{k=1}^{N} a_k \ e^{-\left(\frac{S_M - P_s}{2} + k \right)t} \ dt$$

FOR $a_1, a_2, \dots, a_N$

Figure VI-19.

$$\sum_{k=1}^{N} a_k \, e^{-kt} = -P_s \, g'(t) - g''(t), \quad t > 0$$

$$g(o) = \mathcal{A}(1), \quad g'(o) = -\mathcal{B}(1)$$

LET:

$$f(t) = g(-Q - t), \quad t < Q$$

Figure VI-20.

196

SOLVE:

$$\sum_{k=1}^{N} a_k\, e^{-kt} \;=\; -P_s\, g'(t) - g''(t), \quad t > 0$$

$$g(0) = A(1), \quad g'(0) = -B(1)$$

LET:

$$f(t) \;=\; g(-Q - t), \quad t < Q$$

Figure VI-21.

Figure 3

SAI-12646

$T_1 = T_2$

AND $\quad \dfrac{\partial T_1}{\partial X} = \dfrac{\partial T_2}{\partial X}$

$T_2 = M = T_3$

$-K_\ell \dfrac{\partial T_3}{\partial X} + K_s \dfrac{\partial T_2}{\partial X} + L = 0$

$T_3 = T$

AND $\quad \dfrac{\partial T}{\partial X} = \dfrac{\partial T_3}{\partial X}$

X

r

X = L

X = 0

X = −Q

$\Delta T_1 = P_s \dfrac{\partial T_1}{\partial X}$ $\quad$ AND

$-K_s \dfrac{\partial T_1}{\partial r} = h_s T_1, r = 1$

$\Delta T_2 = P_s \dfrac{\partial T_2}{\partial X}$ $\quad$ AND

$\dfrac{\partial T_2}{\partial r} = 0, r = 1$

$\Delta T_3 = P_\ell \dfrac{\partial T_3}{\partial X}$ $\quad$ AND

$\dfrac{\partial T_3}{\partial r} = 0, r = 1$

$\Delta T = P_\ell \dfrac{\partial T}{\partial X}$ $\quad$ AND

$T = f(X), r = 1$
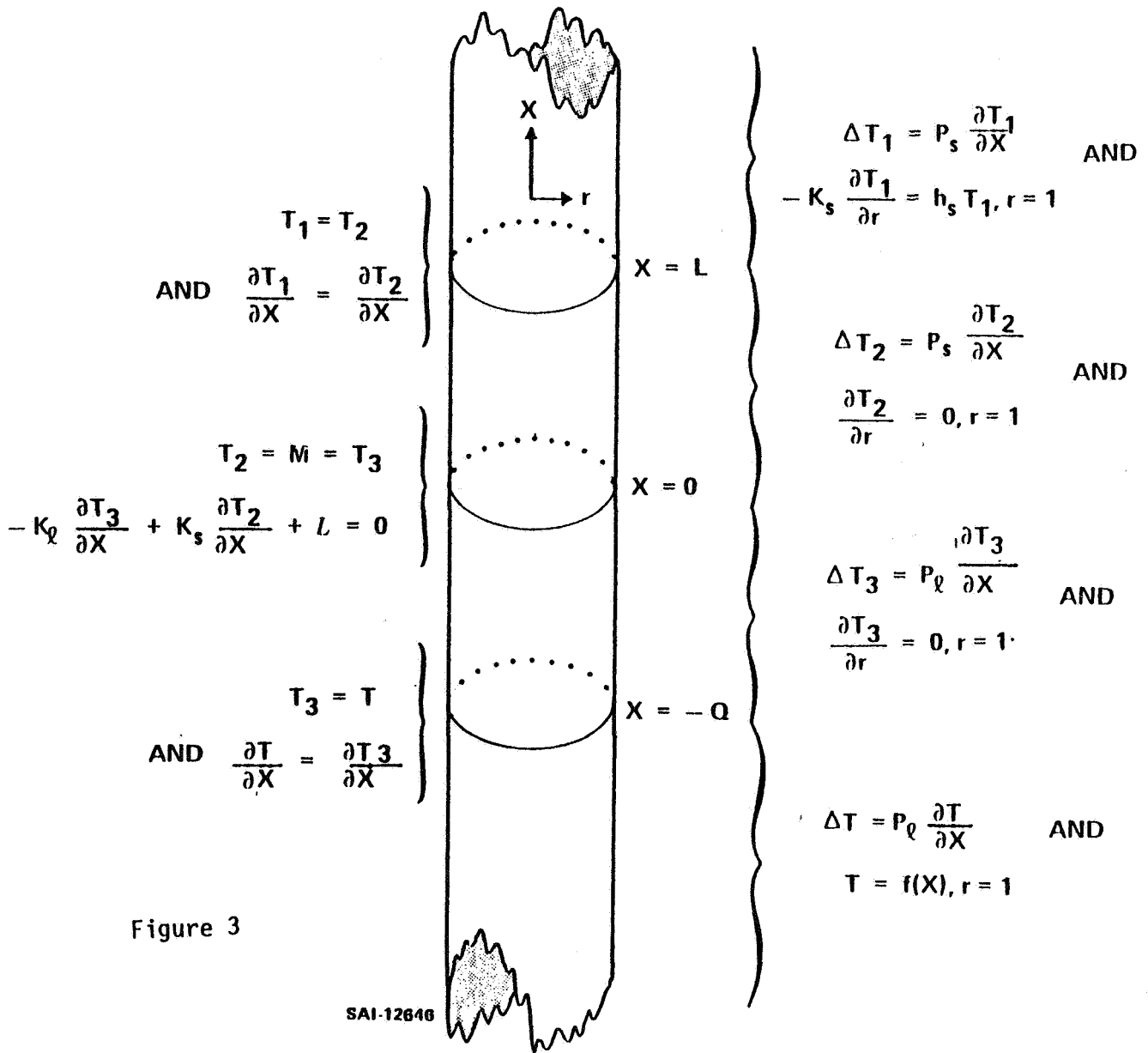
NUMERICAL CASE STUDY: (BRIDGMAN–STOCKBARGER)

Figure VI-22.

198

PARAMETERS:

P_ℓ = .1

P_s = .2

h_ℓ = h_s = K_s = K_ℓ = L = Q = L = 1.0

M = 10.0

CONTROL f(x):

x	f(x)	x	f(x)
—1	14.055	— 6.5	107.70
—1.5	14.967	— 7.0	118.57
—2.0	13.405	— 7.5	128.55
—2.5	14.701	— 8.0	137.65
—3.0	20.701	— 8.5	145.94
—3.5	30.600	— 9.0	153.47
—4.0	42.918	— 9.5	160.31
—4.5	56.359	—10.0	166.5
—5.0	70.012	—10.5	172.11
—5.5	83.307	—11.0	177.19
—6.0	95.922		

RMK: lim   f(x) = 225.57
$x \to -\infty$

SAI-12645

Figure VI-23.

199

VII. SUMMARY

SUMMARY OF THE SEPTEMBER 1981 FLOAT-ZONE WORKSHOP

Edward L. Kern
Chairman, FZWG
Del Mar, CA

Improvements, recommended in the December 1980 Float Zone Workshop, have been made in orienting the research of this program toward technologically important materials. Silicon, the most important semiconductor crystal, will be the primary material under investigation. It does create some problems. Because of its high melting point and high reactivity with almost all other materials, crucial measurements are difficult. Solutions to these problems were discussed and investigators are already working on them.

Industry participation, as recommended in the 1980 Workshop, was the key ingredient in developing the rationale for space float-zone experimentation. Device related material scientists from several leading U.S. semiconductor companies and from U.S. government labs stressed the importance of understanding and making improvements in undesired material characteristics which lead to limited performance or degradation of devices. The most troublesome, which are largely unsolved, are:

1) Resistivity striations

2) Vacancies, which complex with other impurities.

The 1980 Workshop had indicated that the direction of the NASA program should be to study and control these and radial segregation. Programs which will address all of these areas are now beginning. They include eliminating the RF coil slot, studying the nature of thermal oscillations, and modeling the heat flows to make the interface and isotherms flatter, reducing vacancy formation. Equipment to breadboard technology drivers, recommended in the 1980 Workshop, is also being set up.

SILICON

The first objective of the float-zone ground and space research program will be to understand the growth of silicon single crystals. Silicon will be used as the model for all semiconductors. The understanding should be sufficient to lead to growth improvements here on Earth (g = 1), where the bulk of silicon crystals will always be grown.

Why silicon? First, it is the most important semiconductor material to both industry and government. Second, there are problems that need to be solved to get better important devices such as visible light detectors and imagers, infrared imagers and radiation hard space solar cells. Third, one cannot adequately model silicon problems with lower temperature crystals. The magnitude of important phenomena effecting growth (i.e., Marangoni driven convection, radiation and buoyancy driven convection) are very different at this high growth temperature.

A secondary payoff, which evolves naturally from the planned program, is the growth of uniform crystals hich are needed for standards. The Chairman of the ASTM Semiconductor committee indicated the industry/government-wide need for silicon measurement standards for:

1) 4 point probe resistivity

2) Spreading resistance

3) Oxygen determination

4) Carbon determination.

Where do we stand on modeling the float-zone system? We have a good, across the board, start. Analytical modeling in the axisymmetric geometry should provide a good understanding of the Marangoni convection. Since inaccurate values, such as surface tension, can lead to erroneous predictions, a number of thermophysical properties may need to be critiqued and remeasured. The entire complex zone is being modeled and will be compared with experimentally zoned crystals. For the first time, we are asking the analysts to tell us what heat profiles are needed to get a desired growth configuration. Usually we empirically develop a heating method, and then explain what it gives us. In this case, a lot of nonuniformity!

SILICON DIAMETERS

Why do we need large diameter silicon? First, you cannot model a large diameter growing crystal (with large molten zone volume) with a small geometry. The modeler cannot predict all of the effects accurately. Financial support and the very large computer programs have not been provided to model the real shape of a molten zone.

The second reason for large diameter is to test the improvement that uniform silicon has on a specific device. Modern processing lines and photolithography masks are at 2-in. diameter, at the smallest. That will be for proving the material superiority. If devices are to be made in production, 3 in. is standard for float-zone crystals and 4 in. will be the "workhorse" from 1983 to 1990. Diameters of Czochralski crystals are now 4 and 5 in.

POWER REQUIREMENTS

Analyses (3 papers) were in good agreement on the power needed to grow silicon at various diameters. These took into account the heat processes in the growth system (heat of fusion, specific heat, conduction, and radiation) and the power conversion efficiencies of different heating methods. All heating methods were reviewed. Two-inch diameter silicon can be fabricated with the power available to a pallet experiment in the space shuttle bay (5 to 8 kW), but only if power generation and coupling efficiencies are raised from the present 20 to 33 percent efficiencies to 50 percent (for 8 kW available) or 80 percent (for 5 kW available). Fifty percent efficiency will take development effort, but meeting the goal seems probable. Seventy to eighty percent would require extensive development. If space produced crystals make significant improvements and are wanted for critical devices, then the power for 3 in. (15 kW at 50 percent efficiency) and 4 in. (25 kW at 52 percent efficiency) would need the power of the extended Materials Experiment Carrier (MEC) attached to the Space Platform (SP). The 12.5 kW version is now scheduled for 1988 launch. The extended 25 kW version could be in the same time frame as a Silicon MEC unit could be developed (1991).

SEMICONDUCTOR ALLOYS

A second semiconductor type which would greatly benefit from microgravity processing is semiconductor alloys, such as Si:Ge, InP, As and Hg, CdTe. Si:Ge is of interest for military devices, such as designators and imaging systems, in the 1.0 to 1.5 µm range. Si:Ge and InP, As are of interest in the 1.3 to 1.5 µm fiber optics telecommunication area, for the high-band width and low-loss wavelength range. These crystals are very hard to grow on Earth because of heavy component segregation and constitutional supercooling. $Si_x:Ge_{1-x}$ cannot be grown at $g = 1$ when $0.1 \leq x \leq 0.9$.

Extremely slow and uniform growth rates are needed in microgravity. These are also conditions to grow Si:X, where X is a heavy dopant (T1) needed in high concentrations for higher operating temperature infrared imagers. These are of interest to the Air Force.

PRECURSORY EXPERIMENTS

The rationale for experimentally growing silicon in space, at larger diameters, is being developed. Is there a reason to do early experiments in space? Yes. In a complex growth system, one cannot always predict what will take place. For instance, the cooling or insulating effect of an inert zoning gas (argon) cannot be predicted well, and slow growth rates in microgravity for Si:Ge cannot be modeled.

Possible Materials Experiment Apparatus (MEA) experiments were proposed and the scientific background surveyed. The workshop reviewed and discussed these areas. The doped silicon and Si:Ge alloys will be proposed shortly. This would provide an early trial for testing conditions for zoning silicon.

Discussion led to a suggested experiment for a self-contained cannister configuration, probably on a sounding rocket or a Get-Away-Special. It involves a simple experiment of melting the center of a silicon slice and observing (1) the shape of the solid-gas-liquid trijunction and (2) the magnitude of Marangoni flows.

CONCLUSION

It is now probable that a well-planned ground based investigation can provide the needed modeling to predict the effect process changes will have on crystal growth, including the change of gravity. Modeling and corresponding experimentation can be complemented by precursory experiments in space. This program should provide the rationale for proceeding with a major space experiment. Definition of a major space experiment should be possible in 1984.

APPROVAL

FLOAT ZONE WORKSHOP

Edited by E. L. Kern and E. K. Cothran

The information in this report has been reviewed for security classification. Review of any information concerning Department of Defense or nuclear energy activities or programs has been made by the MSFC Security Classification Officer. This report, in its entirety, has been determined to be unclassified.

C. R. O'Dell
Acting Director, Space Sciences Laboratory